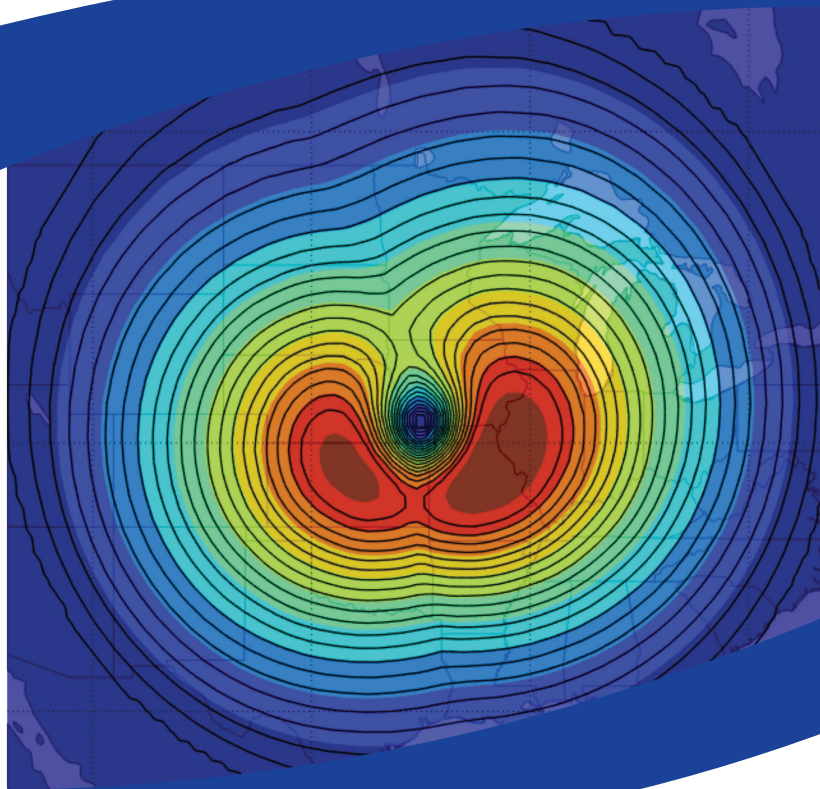


High-Altitude Electromagnetic Pulse and the Bulk Power System

Potential Impacts and Mitigation Strategies



High-Altitude Electromagnetic Pulse and the Bulk Power System

Potential Impacts and Mitigation Strategies

3002014979

Final Report, April 2019

EPRI Project Manager
R. Horton

DISCLAIMER OF WARRANTIES AND LIMITATION OF LIABILITIES

THIS DOCUMENT WAS PREPARED BY THE ORGANIZATION NAMED BELOW AS AN ACCOUNT OF WORK SPONSORED OR COSPONSORED BY THE ELECTRIC POWER RESEARCH INSTITUTE, INC. (EPRI). NEITHER EPRI, ANY MEMBER OF EPRI, ANY COSPONSOR, THE ORGANIZATION BELOW, NOR ANY PERSON ACTING ON BEHALF OF ANY OF THEM:

(A) MAKES ANY WARRANTY OR REPRESENTATION WHATSOEVER, EXPRESS OR IMPLIED, (I) WITH RESPECT TO THE USE OF ANY INFORMATION, APPARATUS, METHOD, PROCESS, OR SIMILAR ITEM DISCLOSED IN THIS DOCUMENT, INCLUDING MERCHANTABILITY AND FITNESS FOR A PARTICULAR PURPOSE, OR (II) THAT SUCH USE DOES NOT INFRINGE ON OR INTERFERE WITH PRIVATELY OWNED RIGHTS, INCLUDING ANY PARTY'S INTELLECTUAL PROPERTY, OR (III) THAT THIS DOCUMENT IS SUITABLE TO ANY PARTICULAR USER'S CIRCUMSTANCE; OR

(B) ASSUMES RESPONSIBILITY FOR ANY DAMAGES OR OTHER LIABILITY WHATSOEVER (INCLUDING ANY CONSEQUENTIAL DAMAGES, EVEN IF EPRI OR ANY EPRI REPRESENTATIVE HAS BEEN ADVISED OF THE POSSIBILITY OF SUCH DAMAGES) RESULTING FROM YOUR SELECTION OR USE OF THIS DOCUMENT OR ANY INFORMATION, APPARATUS, METHOD, PROCESS, OR SIMILAR ITEM DISCLOSED IN THIS DOCUMENT.

REFERENCE HEREIN TO ANY SPECIFIC COMMERCIAL PRODUCT, PROCESS, OR SERVICE BY ITS TRADE NAME, TRADEMARK, MANUFACTURER, OR OTHERWISE, DOES NOT NECESSARILY CONSTITUTE OR IMPLY ITS ENDORSEMENT, RECOMMENDATION, OR FAVORING BY EPRI.

THE ELECTRIC POWER RESEARCH INSTITUTE (EPRI) PREPARED THIS REPORT.

NOTE

For further information about EPRI, call the EPRI Customer Assistance Center at 800.313.3774 or e-mail askepri@epri.com.

Electric Power Research Institute, EPRI, and TOGETHER...SHAPING THE FUTURE OF ELECTRICITY are registered service marks of the Electric Power Research Institute, Inc.

Copyright © 2019 Electric Power Research Institute, Inc. All rights reserved.

ACKNOWLEDGMENTS

The Electric Power Research Institute (EPRI) prepared this report.

Principal Investigators

R. Horton
C. Perry
B. Leonardi
B. Philips
J. Snider
J. Butterfield
N. Bhatt
B. Arritt

This report describes research sponsored by EPRI.

EPRI would like to thank the following individuals for their detailed technical review and feedback on this report.

J. Ostrich
W. Tedeschi
U.S. Department of Energy
Washington, D.C.

M. Rivera
J. Cooley
Los Alamos National Laboratory
Los Alamos, NM

J. Rogers
A. Kelic
Sandia National Laboratories
Albuquerque, NM

B. Kirkendall
Lawrence Livermore National Laboratory
Livermore, CA

This publication is a corporate document that should be cited in the literature in the following manner:

High-Altitude Electromagnetic Pulse and the Bulk Power System: Potential Impacts and Mitigation Strategies. EPRI, Palo Alto, CA: 2019. 3002014979.

ABSTRACT

The detonation of a nuclear weapon at high altitude or in space (~ 30 km or more above the earth's surface) can generate an intense electromagnetic pulse (EMP) referred to as a high-altitude EMP or HEMP. HEMP can propagate to the earth and impact various land-based technological systems such as the electric power grid. Because of the extreme differences in views among experts regarding the potential impacts of HEMP on the electric power grid and the potential societal implications, the Electric Power Research Institute (EPRI) launched a three-year research project in April 2016 to investigate the potential impacts of a HEMP attack on the electric transmission system and to identify possible options for mitigating impacts. This report summarizes the research and findings of this three-year research effort.

Keywords

E1 EMP assessment

E3 EMP assessment

Electromagnetic pulse (EMP)

High-altitude electromagnetic pulse (HEMP)

Transformer thermal assessment

Voltage stability assessment

Deliverable Number: 3002014979

Product Type: Technical Report

**Product Title: High-Altitude Electromagnetic Pulse and the Bulk Power System:
Potential Impacts and Mitigation Strategies**

PRIMARY AUDIENCE: Asset owners and operators of the United States bulk power system

SECONDARY AUDIENCE: Regulators, state and federal entities

KEY RESEARCH QUESTIONS

This research sought to answer two key research questions:

1. What are the potential impacts of a high-altitude electromagnetic pulse (HEMP) attack on the modern electric transmission system?
2. If impacts are of significant concern, what are possible mitigation options and potential costs and benefits of each?

RESEARCH OVERVIEW

Background

The detonation of a nuclear weapon at high altitude or in space (~ 30 km or more above the earth's surface) can generate an intense electromagnetic pulse (EMP) referred to as a high-altitude EMP or HEMP. HEMP can propagate to the earth and impact various ground-based technological systems such as the electric power grid. Depending on the height of the explosion above the earth's surface and the yield of the weapon, the resulting HEMP can be characterized by three hazard fields, denoted as E1 EMP, E2 EMP, and E3 EMP.

The International Electrotechnical Commission (IEC) defines the three HEMP hazard fields based on their distinct characteristics and time scales:

- The early time component (E1 EMP) consists of an intense, short-duration electromagnetic pulse characterized by a rise time of 2.5 nanoseconds and amplitude on the order of tens of kV/m (up to 50 kV/m at the most severe location on the ground).
- The intermediate time component (E2 EMP) is considered an extension of E1 EMP and has an electric field pulse amplitude on the order of 0.1 kV/m and duration of one microsecond to approximately ten milliseconds.
- The late time component (E3 EMP) is a very low frequency (below 1 Hz) pulse with amplitude on the order of tens of V/km with duration of one second to hundreds of seconds. E3 EMP is often compared with severe geomagnetic disturbance (GMD) events; however, the intensity of E3 EMP can be orders of magnitude more severe, and E3 EMP is much shorter in duration than GMD events, which can last for several days.

Potential impacts of HEMP vary depending on the component (E1 EMP, E2 EMP, or E3 EMP) that is responsible for the resulting disruption or damage.

The geographic area exposed to varying levels of E1 EMP fields can be quite large, as the area of coverage is characterized by the line of sight from where the weapon is exploded to the horizon. For example, a detonation at 200 km can affect a circular area of on the order of 3 million square miles. However, not all areas included within the circular region experience the maximum electric field, and strength of the field falls off with distance from the ground zero location. The incident E1 EMP can couple to overhead lines and cables, exposing connected equipment to voltage and current surges (referred to as the conducted threat). The resulting E1 EMP can also radiate equipment directly (referred to as the radiated threat). Potential impacts from E1 EMP on the electric transmission system include disruption or damage of electronics such as digital protective relays (DPRs), communication systems, and supervisory control and data acquisition (SCADA) systems.

The characteristics of E2 EMP are often compared with nearby lightning strikes. However, it is important to understand that E2 EMP does not couple to overhead lines or cables in the more traditional sense of how lightning strikes a transmission tower or a conductor. Rather, E2 EMP couples to conductors through the air, like E1 EMP. This coupling mechanism is similar to how the field created by a nearby lightning strike couples to an overhead transmission line. Because the amplitude of the incident E2 EMP field is quite low (0.1 kV/m), impacts to the transmission system are not expected to occur.

E3 EMP induces low-frequency (quasi-dc) currents in transmission lines and transformers. The flow of these geomagnetically induced currents (GICs) in transformer windings can cause magnetic saturation of transformer cores, which causes transformers to generate harmonic currents, absorb significant quantities of reactive power, and experience additional hotspot heating in windings and structural parts. Potential impacts of E3 EMP on the bulk power system can include voltage collapse (regional blackout) and transformer damage due to additional hotspot heating.

When the EPRI EMP research project was launched, publicly available data on the HEMP threat, potential impacts of HEMP on the electric transmission system, and field-tested E1 EMP mitigation options specific to substations were limited. Additionally, there were differences between the findings of EMP research conducted during the 1980s through the early 1990s by the Department of Energy (DOE) and others and more recent findings communicated by the former Commission to Assess the Threat to the United States from Electromagnetic Pulse Attack (former EMP Commission). Because of these differences and the potential impacts that a HEMP attack could have on society, EPRI launched a three-year research project in April 2016 to provide electric utilities and other stakeholders with a technical basis for making more-informed decisions regarding the potential impacts of HEMP on the electric transmission system and potential options for mitigating possible impacts. By the conclusion of the project, the research was financially supported by more than 60 U.S. utilities.

Research Scope and Approach

The main goal of this research effort was to provide the electric utility industry and other stakeholders with an unclassified, technical basis for 1) assessing the potential impacts of a HEMP attack on the transmission system, and 2) hardening the system against those impacts, should any be found to be of significant concern. The research specifically focused on the electric transmission system (overhead transmission lines, substations, and switchyards), and did not consider the potential effects of HEMP on generation facilities, nuclear reactors, distribution systems, loads, or other key elements or infrastructure sectors.

An important aspect of this project was the close collaboration with various government entities that have extensive expertise and knowledge of the HEMP threat. Key collaborators included DOE, Lawrence Livermore National Laboratory (LLNL), Sandia National Laboratories (SNL), Los Alamos National Laboratory (LANL), and the Defense Threat Reduction Agency (DTRA). EPRI, in close collaboration with the DOE, also developed a Joint Electromagnetic Pulse Resiliency Strategy¹ that was published in July 2016.

To address the two fundamental research questions that were identified, the project was broken up into five research areas:

- *Environment and Modeling* – Several conservative (bounding) unclassified HEMP environments for use in assessments were identified and/or obtained from the DOE and national labs, and software tools and methods for performing assessments were developed. All three hazard fields—E1 EMP, E2 EMP, and E3 EMP—were included in the environment and modeling research effort.
- *Testing* – Extensive laboratory testing of DPRs was conducted to provide data on the levels of E1 EMP stress that could cause operational disruption of or damage to these devices. Testing included free field illumination testing per MIL-STD-461G/RS 105 to assess performance when subjected to radiated threats, and direct injection testing using a voltage impulse with waveform defined in MIL-STD-188-125-1 to assess performance when subjected to conducted voltage surges. Direct injection testing of instrument transformers such as a potential transformer and a capacitor coupled voltage transformers was also conducted to investigate propagation of voltage surges through these devices. Additionally, testing to evaluate potential mitigation options and shielding effectiveness of substation control houses was performed. Testing focused on E1 EMP impacts.
- *Assessment* – Assessments using bounding HEMP environments were conducted to improve understanding of the potential impacts of a HEMP attack on the bulk power system. These assessments included E1 EMP, E2 EMP, E3 EMP, and the combined effects from E1 EMP and E3 EMP.
- *Mitigation, Hardening, and Recovery* – Various mitigation and hardening approaches that could be employed to reduce the potential impacts of E1 EMP on DPRs were evaluated. Potential unintended consequences of various mitigation and hardening strategies were considered, and system recovery following a HEMP-induced blackout was explored.
- *Decision Support* – A framework for supporting risk-informed decisions regarding the implementation of HEMP hardening and mitigation measures was developed.

¹ https://www.energy.gov/sites/prod/files/2016/07/f33/DOE_EMPStrategy_July2016_0.pdf

KEY FINDINGS

Key findings from this research were as follows.

E1 EMP

- Assessments using bounding E1 EMP environments showed that this hazard field has the potential to cause disruption or damage to DPRs over large areas such as an electrical interconnection. Potential damage to DPRs, assuming the nominal E1 EMP environment provided by LANL (up to 25 kV/m at the most severe location on the ground) was found to be moderate, whereas damage from the same environment but scaled so that the maximum peak field at the most severe location on the ground was 50 kV/m was found to be more severe. Based on the assumptions made in the assessments, it was estimated that approximately 5% of the transmission line terminals in a given interconnection could have a DPR that is disrupted or damaged by the nominal E1 EMP environment that was simulated, whereas approximately 15% could be impacted by the scaled (up to 50 kV/m at the most severe location on the ground) E1 EMP environment.
- E1 EMP impacts alone were not found to cause immediate, interconnection-scale disruption or blackout of the power grid, but this finding is not conclusive due to uncertainties regarding how damaged DPRs might respond during an actual event (refer to Combined Effects of E1 EMP and E3 EMP below) or how potential E1 EMP damage to generator controls and other systems such as automatic generation control (AGC), not included as a part of this study, might affect the long-term operation of the grid. Additional research is needed to quantify and understand these uncertainties and how they might, in combination, affect the stability of the bulk power system.
- Results from extensive modeling and laboratory testing of DPRs indicated that the following design options, when used in concert, could provide adequate mitigation of E1 EMP impacts up to the full IEC 61000-2-9 threat level of 50 kV/m:
 - Shielded control/signal cables with proper grounding
 - Low-voltage surge protection devices and/or filters
 - Use of fiber optics based protection and control systems
 - Modifications to substation control houses to enhance electromagnetic shielding properties
 - Grounding/bonding enhancements

Additional supplies of DPRs and other critical assets could also be included as part of a mitigation strategy.

E2 EMP

- Assessments evaluating the potential impacts of E2 EMP alone using the maximum threat level of 0.1 kV/m defined in IEC 61000-2-9 indicated that damage to the transmission system is not expected to occur. Thus, no specific mitigation options were identified as a part of this research.

E3 EMP

- E3 EMP alone was found to pose a threat to the operation and performance of the bulk power system. Assessment results indicated that a regional blackout (multiple states) is possible, but immediate, widespread transformer damage due to hotspot heating from part-cycle saturation is not expected to occur.

- Options for mitigating E3 EMP impacts were found to be like those that can be employed to protect against the effects of GMD events and include the following:
 - Avoiding protection system misoperations by modifying protection and control schemes to be resilient to harmonics and system imbalance
 - Blocking or reducing the flow of GICs
 - Automatic removal of some shunt reactive power compensation devices, for example shunt reactors, and/or employing under-voltage load shedding (UVLS)
 - Sparring of large power transformers and high-voltage circuit breakers

Combined Effects of E1 EMP and E3 EMP

- Assessment of the combined effects of E1 EMP and E3 EMP showed that widespread E1 EMP impacts to DPRs, as they were modeled, did not significantly affect the outcome of the E3 EMP assessment results. This finding was based on testing and analysis that indicated that DPRs that are damaged by surges that propagate into the voltage inputs of the device would not result in the immediate disconnection of transmission lines, but rather would disable the DPRs such that they would no longer be able to perform their intended protection and control function. There is uncertainty with this assumption, as not all DPRs that are currently in use were tested, and testing of some DPRs indicated that control outputs could be damaged by voltage surges induced in unshielded control cables and could potentially result in circuit breaker tripping. Additionally, it is unknown how various DPRs across an interconnection would respond during an actual event. However, significant damage to DPRs and other controls from E1 EMP would be expected to degrade recovery efforts and longer-term viability of controlling system frequency due to potential damage to automatic generation control (AGC) and other ancillary functions. These latter effects could impact the long-term stability (voltage and/or frequency) of an area affected by the HEMP attack.

Recovery and Restoration

- Until the transmission system is appropriately hardened against the potential impacts of E1 EMP, recovering from a HEMP-induced blackout may present operators with challenges that have not been experienced following previous blackouts from more traditional causes. These potential challenges are primarily related to unavailable, inoperable, or damaged equipment and impaired situational awareness capability that could occur as the result of E1 EMP related damage.
- Predefined Transmission Operator step-by-step facility energization procedures currently in place may not be practical to implement following a HEMP event, due to the possibility of widespread unavailable, inoperable, or damaged equipment and impaired situational awareness. Thus, developing alternative plans that consider the potential impacts that HEMP, and in particular E1 EMP, can have on the transmission system may be worthwhile. Training on the differences between system recovery following a HEMP-induced blackout and one from a more traditional cause may also prove beneficial.
- Because damage to large power transformers is expected to be minimal, recovery times following a HEMP-induced blackout would be expected to be commensurate with historical large-scale blackouts *if robust E1 EMP protections are deployed such that E1 EMP impacts to equipment, situational awareness, SCADA, and other infrastructures that support power system restoration are minimal.*

WHY THIS MATTERS

A properly functioning electric grid is critical to national security and society, and its potential loss for an extended period (months or longer) could severely impact both. The findings of this research, which evaluated the potential effects on the electric transmission system only, indicate that if a HEMP attack occurred and the resulting fields were like the bounding E1 EMP, E2 EMP, and E3 EMP environments that were evaluated, impacts such as regional disruption or damage to DPRs and regional voltage collapse could be experienced. Research findings do not support the notion of blackouts encompassing the contiguous United States (CONUS) and lasting for many months to years. The technical basis for these findings and options for mitigating the potential impacts that were identified have been made available in this report so that the electric utility industry and other stakeholders can have the data necessary to make more informed decisions regarding the threat of a HEMP attack on the U.S. electric grid.

HOW TO APPLY RESULTS

Through this research, options for hardening the electric transmission system against the potential impacts of E1 EMP have been identified, but additional research is needed to improve mitigation designs and understanding of the potential unintended consequences of E1 EMP hardening so that system reliability is not adversely affected. A collaborative research effort between EPRI and multiple utilities is currently underway to perform field evaluations of the various E1 EMP hardening options that were identified as part of this effort.

Several options exist for mitigating E3 EMP impacts, and the industry has some limited experience with these since they can also be used to mitigate the potential impacts of severe GMD events.

Although E3 EMP is not expected to cause immediate, widespread damage to large power transformers, it may be prudent to evaluate the number of transformer spares that are available to ensure that adequate replacements exist for the number of transformers that are identified as being at potential risk of damage. Transformer sparing philosophies for transformer banks comprised of single-phase units should consider that multiple phases of a transformer bank may be at risk of damage since all three phases of the transformer would be exposed to similar GIC levels. Additionally, sparing of high-voltage circuit breakers may also be considered due to the uncertainty of their ability to interrupt currents which contain significant levels of GIC. Recovery plans and procedures designed to respond to widespread voltage collapse resulting from E3 EMP should consider the potential effects of E1 EMP on systems that are critical to grid restoration, such as protection and control, SCADA, and communications. The ability of E1 EMP to cause damage to these systems is a major concern since their loss can adversely affect system recovery efforts and timelines. Therefore, E1 EMP hardening of critical electronic systems within transmission control centers and substations along cranking paths may be considered higher priority. As information becomes available on E1 EMP impacts on generating units, distribution systems, and other facets of the electric power grid, assets in addition to those described in this report may also need to be considered in future mitigation plans.

EPRI CONTACT: Randy Horton, Senior Program Manager, rhorton@epri.com

PROGRAM: Substations, P37

ACRONYMS AND ABBREVIATIONS

AGC	automatic generation control
BIL	basic impulse level
BLT	Baum-Liu-Tesche (modeling approach)
CCVT	capacitor coupled voltage transformer
CDF	cumulative distribution function
CM	common mode
CONUS	contiguous United States
CT	current transformer
DHS	U.S. Department of Homeland Security
DOE	U.S. Department of Energy
DPR	digital protective relay
DTRA	Defense Threat Reduction Agency
DUT	device under test
E1 EMP	the early time component of HEMP
E2 EMP	the intermediate time component of HEMP
E3 EMP	the late time component of HEMP
EI	Eastern Interconnection
EMC	electromagnetic compatibility
EMP	electromagnetic pulse
EMS	energy management system
FEM	finite element method
GIC	geomagnetically induced current
GMD	geomagnetic disturbance
GRD	GIC reduction device
GSU	generator step-up transformer

HEMP	high-altitude electromagnetic pulse
HMI	human-machine interface
HOB	height of burst
HVAC	heating, ventilation, and air conditioning
HWFM	half wave full maximum
IBG	inverter-based generation
ICCP	Inter-Control Center Communications Protocol
IEC	International Electrotechnical Commission
IED	intelligent electric device
IEMI	intentional electromagnetic interference
IEN	integrated energy network
LANL	Los Alamos National Laboratory
LCT	longitudinal corrugated copper tape
LLNL	Lawrence Livermore National Laboratory
MOV	metal oxide varistor
MU	merging unit
NBD	neutral blocking device
OEM	original equipment manufacturer
ORNL	Oak Ridge National Laboratory
P&C	protection and control
PDF	probability distribution function
PLC	programmable logic controller
PT	potential transformer
PV	photovoltaic
RF	radio frequency
RFI	radio frequency interference
RMS	root mean square
SCADA	supervisory control and data acquisition
SE	shielding effectiveness
SNL	Sandia National Laboratories
SPD	surge protection device

SSR	subsynchronous resonance
SVC	static var compensator
TRV	transient recovery voltage
TVS	transient voltage suppressing
UPS	uninterruptible power supply
UVLS	under-voltage load shedding
WECC	Western Electricity Coordinating Council (regional entity for the Western Interconnection)

CONTENTS

ABSTRACT	V
EXECUTIVE SUMMARY	VII
ACRONYMS AND ABBREVIATIONS	XIII
1 INTRODUCTION	1-1
1.1 Background	1-1
1.1.1 E1 EMP	1-2
1.1.2 E2 EMP	1-4
1.1.3 E3 EMP	1-5
1.2 Motivation for EPRI's EMP Research Program	1-6
1.3 The EPRI EMP Research Project	1-6
1.3.1 Environment and Modeling	1-7
1.3.2 Testing	1-8
1.3.3 Assessment	1-8
1.3.4 Mitigation, Hardening, and Recovery	1-8
1.3.5 Decision Support	1-9
1.4 Report Organization	1-9
2 HEMP ENVIRONMENT AND MODELING	2-1
2.1 Background	2-1
2.2 Nominal E1 EMP Environment	2-1
2.2.1 Los Alamos National Laboratory (LANL) E1 EMP Environment	2-1
2.2.1.1 Magnitude of Incident E1 Field	2-3
2.2.1.2 Polarization Angle, α	2-7
2.2.1.3 Incidence Angle, ψ	2-8
2.2.1.4 Azimuthal Angle, Φ	2-8
2.2.1.5 Complete Spatio-Temporal E1 EMP Environment	2-8

2.3 Nominal E3 EMP Environment	2-10
2.3.1 Oak Ridge National Laboratory (ORNL) E3 EMP Environment	2-10
2.3.2 Los Alamos National Laboratory (LANL) E3 EMP Environment	2-10
2.4 E1 EMP Modeling.....	2-12
2.4.1 Coupling to Overhead Conductors	2-12
2.4.2 Buried Conductors	2-13
2.5 E2 EMP Modeling.....	2-13
2.5.1 Coupling to Overhead Conductors	2-13
2.6 E3 EMP Modeling.....	2-14
2.6.1 Coupling to Overhead Conductors	2-14
3 E1 EMP TESTING OF SUBSTATION EQUIPMENT.....	3-1
3.1 Background	3-1
3.2 Digital Protective Relays Tested.....	3-1
3.3 Description of Device Performance	3-2
3.4 Free Field Illumination Testing.....	3-3
3.5 Shielding Effectiveness Testing of Substation Control Houses	3-9
3.6 Direct Voltage Surge Injection Testing.....	3-15
3.7 Direct Voltage Surge Injection Testing of Mitigation Options.....	3-25
3.8 Conclusions.....	3-31
4 ASSESSMENT OF HEMP IMPACTS	4-1
4.1 Assessment of E1 EMP Impacts.....	4-1
4.1.1 E1 EMP Assessment Procedure	4-1
4.1.1.1 Initial Step (Performed Once)	4-3
4.1.1.2 Step 1 – Coupling Calculations.....	4-3
4.1.1.3 Step 2 – Creation of Stress PDF at Each Substation Location.....	4-4
4.1.1.4 Step 3 – Determine Voltage Surge Level at DPR Terminals	4-4
4.1.1.5 Step 4 – Determine Damage Threshold of DPR	4-5
4.1.1.6 Step 5 – Assessment.....	4-5
4.1.1.7 Procedure Summary.....	4-5
4.1.2 Example Cases.....	4-6
4.1.2.1 Example 1	4-6
4.1.2.2 Example 2	4-7
4.1.2.3 Example 3	4-8

4.1.3 Summary of E1 EMP Assessment Results.....	4-9
4.2 Assessment of E2 EMP Impacts.....	4-10
4.3 Assessment of E3 EMP Impacts.....	4-14
4.3.1 ORNL Environment.....	4-14
4.3.2 LANL Environment.....	4-14
4.3.2.1 Transformer Thermal Assessment.....	4-14
Step 1: Perform GIC Calculations and Apply Screening Criteria	4-15
Step 2: Time-Domain Thermal Modeling	4-16
Step 3: Application of Temperature Limits	4-17
Step 4: Thermal Assessment.....	4-20
4.3.2.2 Voltage Stability Assessment	4-21
4.4 Assessment of E1 EMP + E3 EMP Impacts.....	4-23
4.4.1 Modeling Uncertainties Associated with Assessment of Combined E1 EMP + E3 EMP Effects	4-25
4.5 Assessment of E1 EMP Impacts on Voltage Stability	4-26
5 APPROACHES FOR MITIGATING THE EFFECTS OF HEMP	5-1
5.1 E1 EMP Mitigation	5-1
5.1.1 Transmission Control Centers.....	5-2
5.1.2 Substations	5-2
5.1.2.1 Mitigation of Radiated Threats.....	5-2
5.1.2.2 Mitigation of Conducted Threats.....	5-3
5.1.2.2.1 Low-Voltage Surge Protection Devices and Filters	5-3
5.1.2.2.2 Control/Signal Cables	5-4
5.1.2.2.3 Fiber Optics (IEC 61850)	5-5
5.1.2.2.4 Cable Trenches and Marshalling Cabinets.....	5-7
5.1.2.2.5 Grounding and Bonding	5-8
5.1.2.3 Example Application.....	5-10
5.1.2.4 Equipment Sparing.....	5-11
5.2 E2 EMP Mitigation	5-11
5.3 E3 EMP Mitigation	5-11
5.3.1 Avoiding Protection System Misoperations	5-12
5.3.2 Blocking or Reducing the Flow of Geomagnetically Induced Currents.....	5-12
5.3.2.1 Neutral Blocking Devices (NBDs)	5-13
5.3.2.2 GIC Reduction Devices (GRDs)	5-14

5.3.2.3 Series Capacitors	5-14
5.3.2.4 Engineering Studies	5-15
5.3.3 Automatic Switching and Load Shedding	5-15
5.3.4 Equipment Sparing	5-15
6 SYSTEM RECOVERY FOLLOWING A HEMP ATTACK.....	6-1
6.1 Power System Restoration Process	6-1
6.2 Potential Impacts of a HEMP-Induced Blackout on Restoration Process	6-2
6.3 Suggestions for Enhancing Preparedness.....	6-2
7 SUMMARY AND CONCLUSIONS.....	7-1
7.1 E1 EMP	7-1
7.2 E2 EMP	7-2
7.3 E3 EMP	7-3
7.4 Combined Effects of E1 EMP and E3 EMP.....	7-3
7.5 System Recovery	7-3
8 RECOMMENDATIONS FOR FUTURE RESEARCH	8-1
8.1 Integrated Energy Network Assets	8-1
8.2 Generation Facilities and End-Use Equipment	8-1
8.3 Software Tools and Methods for Performing HEMP Assessments.....	8-1
8.4 Equipment Testing.....	8-2
8.5 HEMP Environments	8-2
8.6 Field Trials of E1 EMP Hardening of Substations	8-3
9 REFERENCES	9-1
A TRANSFORMER THERMAL MODEL PARAMETERS.....	A-1
Model 1 (Structural Part)	A-1
Model 2 (Structural Part)	A-1
Model 3 (Structural Part)	A-2
Model 4 (Winding)	A-2
B DIRECT INJECTION TESTING OF HIGH-VOLTAGE INSTRUMENT TRANSFORMERS.....	B-1

LIST OF FIGURES

Figure 1-1 Composite elapsed time portrayal of all three components of a HEMP signal, based on IEC 61000-2-9	1-2
Figure 1-2 Compton scattering process	1-3
Figure 1-3 Example of the area affected by E1 EMP resulting from a high-altitude nuclear explosion	1-4
Figure 1-4 Description of the EPRI EMP Project	1-7
Figure 2-1 Normalized smile diagram for benchmark 5 (Yield = 1,000 kT, HOB = 200 km); ground zero location is 40° N, 95° W.....	2-3
Figure 2-2 Normalized E1 EMP waveforms from benchmark 5 for ground locations generally east of ground zero (40° N, 95° W)	2-4
Figure 2-3 Normalized E1 EMP waveforms from benchmark 5 for ground locations generally south of ground zero (40° N, 95° W)	2-5
Figure 2-4 The fraction of energy fluence for ground locations generally east of ground zero (40° N, 95° W) for benchmark 5.....	2-6
Figure 2-5 The fraction of energy fluence for ground locations south of ground zero (40° N, 95° W) for benchmark 5.....	2-6
Figure 2-6 The polarization angle, α , for a 1,000 kT yield weapon detonated at 200 km evaluated at the time when the magnitude of electric field achieves its maximum value at the observer location	2-7
Figure 2-7 The incidence angle for various locations on the ground resulting from a 1,000 kT yield weapon detonated at 200 km above the earth's surface	2-8
Figure 2-8 Example geographic locations for the E1 EMP environment	2-9
Figure 2-9 Map of the instantaneous geoelectric field magnitude of the LANL E3 EMP environment at three different points in time ($t = 20$ sec, $t = 40$ sec, and $t = 100$ sec).....	2-11
Figure 2-10 Illustration of an E1 EMP plane wave incident on an overhead conductor.....	2-12
Figure 2-11 Geometry of buried conductor modeling scenario	2-13
Figure 3-1 Illustration and photographs of EPRI's guided wave simulator based on MIL-STD-461G/RS105.....	3-3
Figure 3-2 Simulated time-lapse portrayal of the plane wave generated during a free field illumination test. (Colors represent the magnitude of the E-field, in sequence of time, T1, T2, and T3.)	3-4
Figure 3-3 Example E1 EMP waveform generated by the EPRI guided wave test facility, and the required MIL-STD waveform determined using analytical equations.....	3-4
Figure 3-4 Illustration of DUT orientation along the horizontal and vertical axes.....	3-5
Figure 3-5 Photograph of a free field illumination test setup with fiber optic video camera	3-6

Figure 3-6 Example of a Type 2 response observed with the fiber optic camera during a free field illumination test	3-6
Figure 3-7 Depiction of a shielding effectiveness test setup	3-9
Figure 3-8 Examples of the various control house constructions where shielding effectiveness tests were performed	3-10
Figure 3-9 Results of shielding effectiveness tests	3-11
Figure 3-10 Measured shielding effectiveness and incident field calculation results for the substation control house constructed of concrete and brick (Type 1).....	3-12
Figure 3-11 Measured shielding effectiveness and incident field calculation results for the substation control house constructed of six-side metal panels with welded seams (Type 4)	3-13
Figure 3-12 Comparison of the measured shielding effectiveness for the six-sided metal structure with proposed 20 dB and 30 dB shielding effectiveness levels.....	3-15
Figure 3-13 Illustration of EPRI's direct injection test based on MIL-STD-188-125-1 Note: DUT is not shown.....	3-17
Figure 3-14 Open circuit voltage pulse generated EPRI direct injection voltage generator and the MIL-STD-188-125-1 waveform	3-18
Figure 3-15 E1 EMP direct injection test setup for application of common mode surges to the voltage inputs of the DPR.....	3-19
Figure 3-16 Depiction of an example direct injection test setup used to test DPRs against line-to-ground surges.....	3-20
Figure 3-17 Test setup to evaluate the performance of mitigation devices	3-26
Figure 3-18 Example measurement data from a mitigation device test (PROT 2)	3-27
Figure 4-1 Approach for performing an E1 EMP assessment of an individual substation	4-1
Figure 4-2 Stress PDF derived from direct injection testing of DPRs.....	4-3
Figure 4-3 Illustration of Steps 1 and 2 of the E1 EMP assessment process.....	4-4
Figure 4-4 Procedure for determining impacts to substations included in the interconnection model	4-5
Figure 4-5 Coupling model for Example 1	4-7
Figure 4-6 Coupling model for Example 2	4-8
Figure 4-7 Coupling model for Example 3	4-8
Figure 4-8 Example configuration used in E2 EMP assessment	4-11
Figure 4-9 E2 EMP waveform defined in IEC 61000-2-9	4-11
Figure 4-10 Results from E2 EMP coupling calculations for vertically polarized wave ($\alpha = 0^\circ$) and line length of 100 km; refer to Figure 4-8 for the definitions of Phi (ϕ) and Psi (ψ)	4-12
Figure 4-11 Results from E2 EMP coupling calculations for horizontally polarized wave ($\alpha = 90^\circ$) and line length of 100 km; refer to Figure 4-8 for the definitions of Phi (ϕ) and Psi (ψ)	4-13
Figure 4-12 Procedure for performing thermal assessment of the U.S. transformer fleet	4-15
Figure 4-13 Example thermal response simulations from a transformer included in the assessment	4-17

Figure 4-14 Example instantaneous hotspot temperature results.....	4-19
Figure 4-15 Procedure for voltage stability assessment evaluating impacts of E3 EMP only.....	4-21
Figure 4-16 Example bus voltages during dynamic simulation of E3 EMP effects	4-22
Figure 4-17 Combined E1 + E3 assessment process diagram	4-24
Figure 5-1 Example radiated and conducted disturbances through a single-barrier substation control house.....	5-1
Figure 5-2 Example of a prototype low-voltage surge protection device designed to protect the analog inputs and control outputs of a DPR	5-4
Figure 5-3 Example of an EMC entry shield	5-5
Figure 5-4 Example architecture of an IEC 61850 based protection and control system	5-6
Figure 5-5 Fiber optic penetration waveguide	5-7
Figure 5-6 Example of a cable trough located within a substation	5-7
Figure 5-7 Example ground ring external to the facility shield.....	5-9
Figure 5-8 Example of a flat bonding strap.....	5-9
Figure 5-9 Examples of various connection methods of grounding conductors that originate externally to the facility shield	5-10
Figure 5-10 Illustration of an E1 EMP hardened substation control house.....	5-11
Figure 5-11 Generic circuit diagram of a neutral blocking device	5-13
Figure 5-12 Physical representation of a neutral blocking device deployed in the field.....	5-14
Figure 6-1 Overview of a step-by-step facility energization procedure.....	6-1
Figure B-1 Calculated frequency response and measured direct voltage surge injection response of a CCVT	B-1
Figure B-2 Calculated frequency response and measured direct voltage surge injection response of a distribution-class PT	B-2

LIST OF TABLES

Table 2-1 Peak incident E1 field corresponding to the five benchmark scenarios.....	2-2
Table 3-1 Description of DPR models that were tested	3-2
Table 3-2 Definition of device responses during and after testing.....	3-2
Table 3-3 Results of field illumination testing of DPRs	3-7
Table 3-4 Estimated levels of attenuated incident E-fields in various structures	3-13
Table 3-5 Results from direct injection testing of DPRs.....	3-21
Table 3-6 Description of mitigation devices that were tested	3-25
Table 3-7 Results of 80 kV voltage pulse applied to various mitigation devices protecting the DUT	3-28
Table 3-8 Results of testing of mitigation devices connected to voltage inputs of DPRs.....	3-29
Table 3-9 Results of testing the ability of mitigation devices to protect the current inputs of relays	3-30
Table 4-1 Summary of E1 EMP impacts.....	4-9
Table 4-2 Temperature limits for condition-based geomagnetically induced current susceptibility categories and percentage of U.S. transformer fleet in each category	4-18
Table 4-3 Number of transformers exceeding temperature limits	4-19
Table 4-4 Transformer thermal assessment results using the LANL E3 EMP environment	4-20
Table 4-5 Comparison of voltage stability assessment results	4-23
Table 4-6 Comparison of voltage stability assessment results: E3 only and E1 + E3	4-24
Table 5-1 Summary of recommended engineering design studies to perform when utilizing GIC mitigation technologies	5-15
Table 6-1 Potential impacts of a HEMP-induced blackout on restoration process	6-2
Table 6-2 Suggestions for preparedness.....	6-3
Table A-1 Asymptotic behavior of Model 1 (structural part)	A-1
Table A-2 Asymptotic behavior of Model 3 (structural part)	A-2

1

INTRODUCTION

1.1 Background

The detonation of a nuclear weapon at high altitude or in space (~ 30 km or more above the earth's surface) can generate an intense electromagnetic pulse (EMP) referred to as a high-altitude EMP or HEMP. HEMP can propagate to the earth and impact various ground-based technological systems such as the electric power grid. Depending on the height of the explosion above the earth's surface and the yield of the weapon, the resulting HEMP can be characterized by three hazard fields, denoted as E1 EMP, E2 EMP, and E3 EMP.

The International Electrotechnical Commission (IEC) [1] defines the three HEMP components based on their distinct characteristics and time scales:

- The early time component (E1 EMP) consists of an intense, short-duration electromagnetic pulse with double exponential waveform characterized by a rise time of 2.5 nanoseconds and amplitude on the order of tens of kV/m (up to 50 kV/m at the most severe location on the ground) [1],[2].
- The intermediate time component (E2 EMP) is considered an extension of E1 EMP and has an electric field pulse amplitude on the order of 0.1 kV/m and duration of one μ sec to approximately ten msec. E2 is comprised of two subcomponents, E2A and E2B.
- The late time component (E3 EMP) is a very low frequency (below 1 Hz) pulse with amplitude on the order of tens of V/km with duration of one second to hundreds of seconds. Like E2 EMP, E3 EMP is comprised of two subcomponents. These are designated as E3A and E3B and are often referred to as the blast wave and the heave wave, respectively.

The composite elapsed time portrayal of all three components of a HEMP signal is illustrated in Figure 1-1. The E3 EMP signal illustrated in Figure 1-1 is bipolar, meaning that the waveform has both positive and negative components. Therefore, the negative portion of the E3 EMP wave is illustrated by a dashed line in the log-log plot.

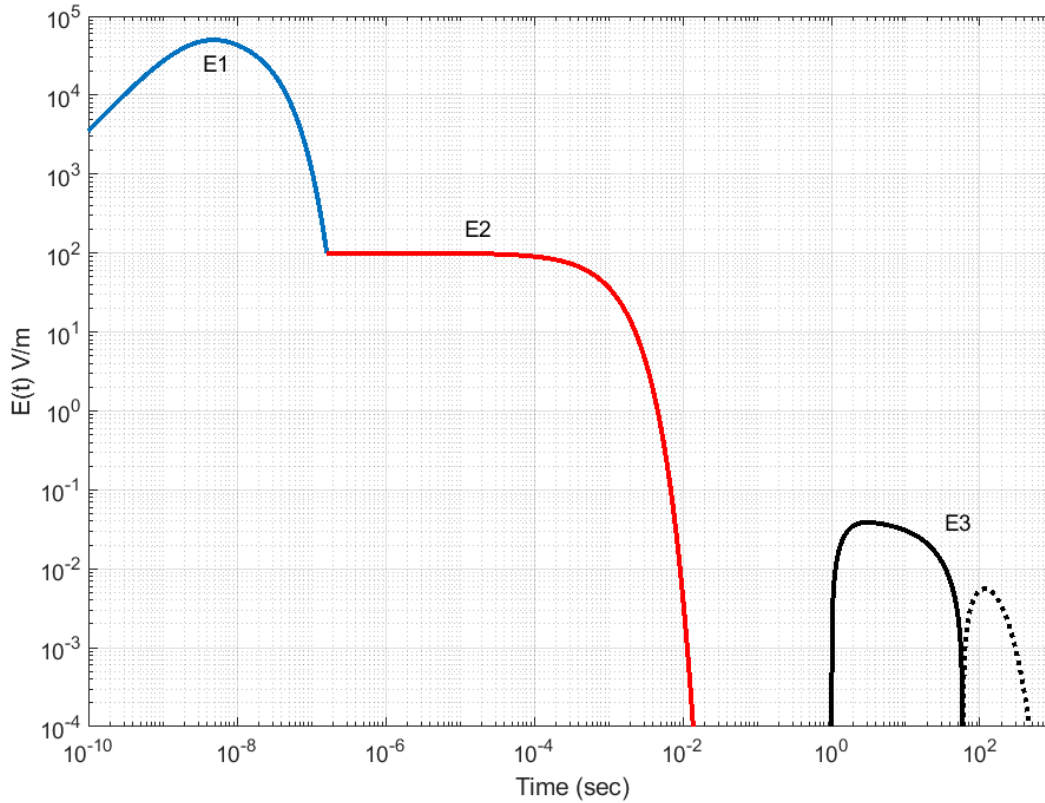


Figure 1-1
Composite elapsed time portrayal of all three components of a HEMP signal, based on IEC 61000-2-9

1.1.1 E1 EMP

The E1 EMP signal is created by the interaction of the prompt gamma rays produced by the nuclear explosion with air molecules that are located approximately 20–40 km above the earth’s surface. This area of the atmosphere, from an EMP generation perspective, is referred to as the source region. The prompt gammas produced by the nuclear explosion expel electrons from air molecules in the source region by a process referred to as Compton scattering. This process is illustrated in Figure 1-2.

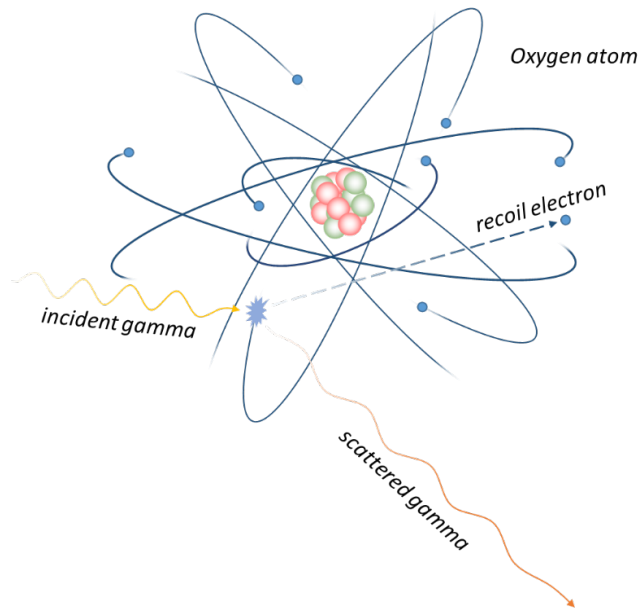


Figure 1-2
Compton scattering process [3]

As illustrated in Figure 1-2, the incident gammas strike electrons, resulting in a recoil response much like that of a struck billiard ball. The incident gammas are also scattered, which becomes important in the generation of E2 EMP. The expelled electrons are then turned by a force resulting from their interaction with the earth's magnetic field. This turning of electrons gives rise to an intense, short-duration electromagnetic pulse referred to as E1 EMP. The geographic region of exposure from E1 EMP is defined by the line of sight distance from the location of the explosion. Thus, weapons that are detonated at high altitudes or in space, for example hundreds of kilometers above the earth's surface, can generate E1 EMP that covers large geographic regions. Although not all locations on the ground experience the same level of E1 EMP field (refer to Figure 1-3), a weapon detonated at 200 km above the center of the contiguous United States (CONUS) can expose an area of approximately 3 million square miles, which includes most of the CONUS and portions of Canada and Mexico. However, not all areas are exposed to the maximum E1 EMP fields, as further illustrated in Figure 1-3 and in Figure 2-1.

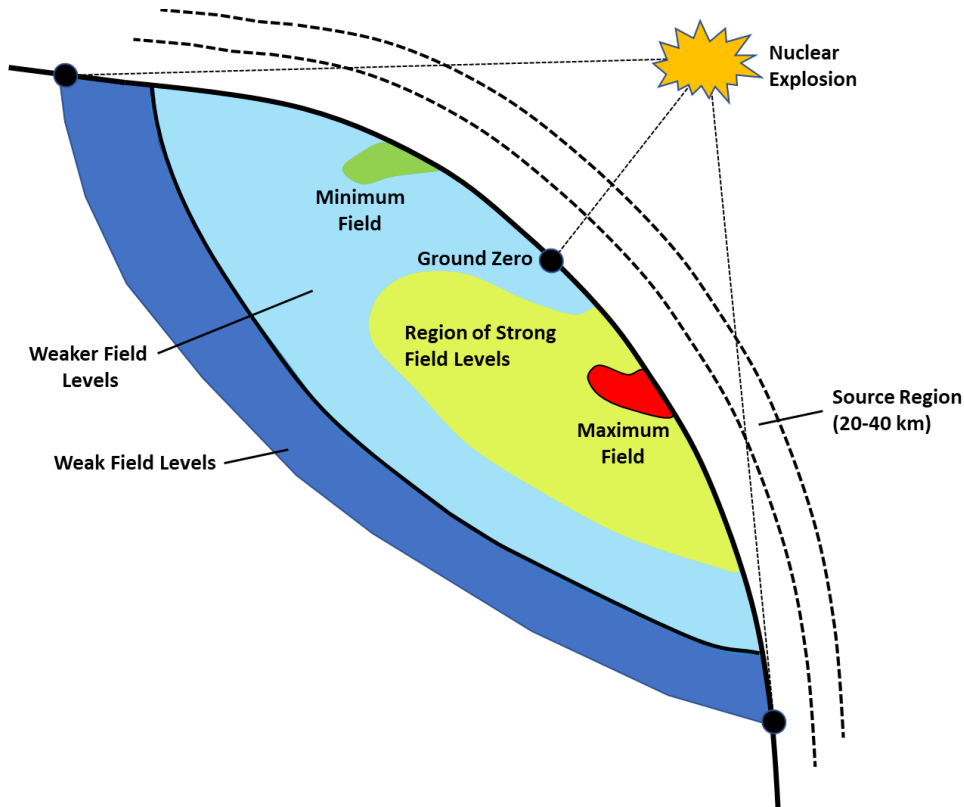


Figure 1-3
Example of the area affected by E1 EMP resulting from a high-altitude nuclear explosion

The incident E1 EMP can be described by an electromagnetic plane wave that travels to the earth's surface at near the speed of light. The shape of the unclassified incident E1 EMP is described by a double exponential waveform [1], [2]. A more detailed description of the phenomenology of E1 EMP is provided in [3].

The incident E1 EMP can couple to overhead lines and cables, exposing connected equipment to significant voltage and current surges (conducted threat). The resulting E1 EMP can also radiate equipment directly (radiated threat). Potential impacts from E1 EMP on the electric transmission system include disruption or damage of electronics such as digital protective relays (DPRs), communication systems, and supervisory control and data acquisition (SCADA) systems.

1.1.2 E2 EMP

The E2 EMP environment is comprised of two components, E2A and E2B. Referring to Figure 1-1, the time scale for E2 is from approximately 1 μ sec to about 10 msec [1]. The first component, E2A, is generated by secondary effects of the gammas that are scattered during the Compton scattering process. The second component, E2B, is generated from gammas that are produced by inelastic collisions between neutrons from the weapon detonation and air molecules.

The characteristics of E2 EMP are often compared with nearby lightning strikes. However, it is important to understand that E2 EMP does not couple to conductive objects in the same way that lightning strikes a transmission tower or conductor. Rather, E2 EMP couples to conductive objects through the air, like E1 EMP. This coupling mechanism is similar to how the field created by a nearby lightning stroke couples to an overhead conductor. Because the amplitude of the incident E2 EMP field is quite low (0.1 kV/m), impacts to the transmission system are not expected to occur.

1.1.3 E3 EMP

The exo-atmospheric detonation of a nuclear weapon can generate a low-frequency (quasi-dc) electric field at the earth's surface. This late-time pulse is referred to as E3 EMP or magnetohydrodynamic electromagnetic pulse (MHD-EMP) [4]. E3 EMP is comprised of two components: E3A, or the blast wave, and E3B, or the heave wave. The resulting geoelectric field is like that created by a severe geomagnetic disturbance (GMD); however, there are two important distinctions. First, E3 EMP can have a much larger amplitude than the geoelectric field created by a severe GMD event (can be an order of magnitude larger), and the duration of E3 EMP is much shorter than a severe GMD event (E3 EMP lasts only 4–5 minutes as compared with a GMD event that can last for several days or more).

The initial blast wave (E3A) is generated within the first 10 seconds after the nuclear explosion, and is a result of the expanding plasma ball created by the nuclear explosion. As the conductive plasma expands, it interacts with or cuts the earth's magnetic field, resulting in a distortion of the field, which in turn induces a geoelectric field at the earth's surface.

The E3B component is generated by the lingering effects of the plasma ball, and the process begins approximately 10 seconds after the initial explosion. The plasma ball generated previously begins to ascend vertically, and the dynamic process of the plasma moving through the earth's magnetic field lines sets up a current system that generates a time-varying electric field at the earth's surface.

An important attribute of E3A is that it does not exist to any significance in the same area that E3B covers. The maximum E3A occurs far north of the ground zero location, whereas E3B is approximately centered around the ground zero location. A more detailed description of the phenomenology of E3 EMP can be found in [3].

The resulting E3 EMP induces low-frequency, quasi-dc currents in transmission lines and transformers. The underlying phenomenon driving the flow of these geomagnetically induced currents (GICs) is like that of a GMD event, and so are the potential impacts. The flow of GIC in transformers causes part-cycle saturation of the transformers' cores, which in turn causes the transformers to:

- Experience increased hotspot heating in windings and structural parts
- Absorb significant levels of fundamental frequency reactive power
- Inject harmonic currents into the grid

Potential impacts to the bulk power system from E3 EMP range from regional voltage instability and collapse (blackout) [5] to possible transformer damage due to excessive hotspot heating [6].

1.2 Motivation for EPRI's EMP Research Program

The issue of potential effects of E1 EMP on electronic equipment has long been recognized by the U.S. military and others. In the 1950s, E1 EMP was investigated as a potential cause of malfunction of electronic equipment during atmospheric nuclear tests [7]. Impacts of E1 EMP on civilian systems soon began to be investigated, and unclassified reference guides such as [2] and [8] began to surface in the mid 1970s. Significant work in this area continued throughout the Cold War. Reference [9] provides a summary of some of the most significant unclassified research that was performed by the U.S. Department of Energy (DOE) during this period. The main findings of this exhaustive research were that E1 EMP can damage unhardened assets over large geographic areas, and E3 EMP can cause regional voltage collapse. However, researchers found that a long-term blackout of many months would be unlikely, because major power system components, such as large power transformers, were not likely to be damaged by the nominal unclassified HEMP environment that was used in the study [9].

Following the Cold War, research efforts by the former Commission to Assess the Threat to the United States from Electromagnetic Pulse (EMP) Attack (former EMP Commission) continued to add to the body of unclassified research available to the industry. Final reports from the former EMP Commission in 2004 [10] and 2008 [11] and subsequent congressional testimony in 2014 [12] provided a different perspective indicating that the potential impacts of HEMP on the electric grid would be dire. Additional work by the former EMP Commission [13] provided further separation from prior findings of DOE and others.

Because of the differences in findings from previous unclassified EMP research, the electric utility industry was left asking two key questions:

1. What are the potential impacts of a HEMP attack on the modern electric transmission system?
2. If impacts are of significant concern, what are possible mitigation options and potential costs and benefits of each?

Because of these questions and the potential impact that a HEMP attack could have on society, EPRI launched a three-year research project in April 2016 to provide the electric utility industry and other stakeholders with a technical basis for making more-informed decisions regarding the potential impacts of HEMP on the electric transmission system and identifying options for mitigating potential impacts. EPRI, in close collaboration with the DOE, developed a Joint Electromagnetic Pulse Resiliency Strategy that was published in July 2016 [14]. A description of the EPRI research project follows.

1.3 The EPRI EMP Research Project

When the project was initiated, publicly available data regarding the HEMP threat, potential impacts of HEMP on the electric transmission system, and field-tested options for mitigating E1 EMP impacts on substation equipment were limited. Thus, the main goal of this research effort was to provide a technical basis for 1) assessing the potential impacts of a HEMP attack on the electric transmission system, and 2) mitigation options that could be used to harden the system against potential impacts, should any be found.

An important aspect of this project was the close collaboration with various government entities that have extensive expertise and knowledge of the HEMP threat. Collaborators included DOE, Lawrence Livermore National Laboratory (LLNL), Sandia National Laboratories (SNL), Los Alamos National Laboratory (LANL), and the Defense Threat Reduction Agency (DTRA).

The initial task of the research project was to determine the state of knowledge of unclassified HEMP research (and other power systems research that could be leveraged) and identify gaps that the current research should focus on. Following this preliminary step, the research project was organized into five areas, which are described below. All three components of HEMP (E1 EMP, E2 EMP, and E3 EMP) were considered in the research.

A visual description of the project, showing the five areas of focus, is provided in Figure 1-4.

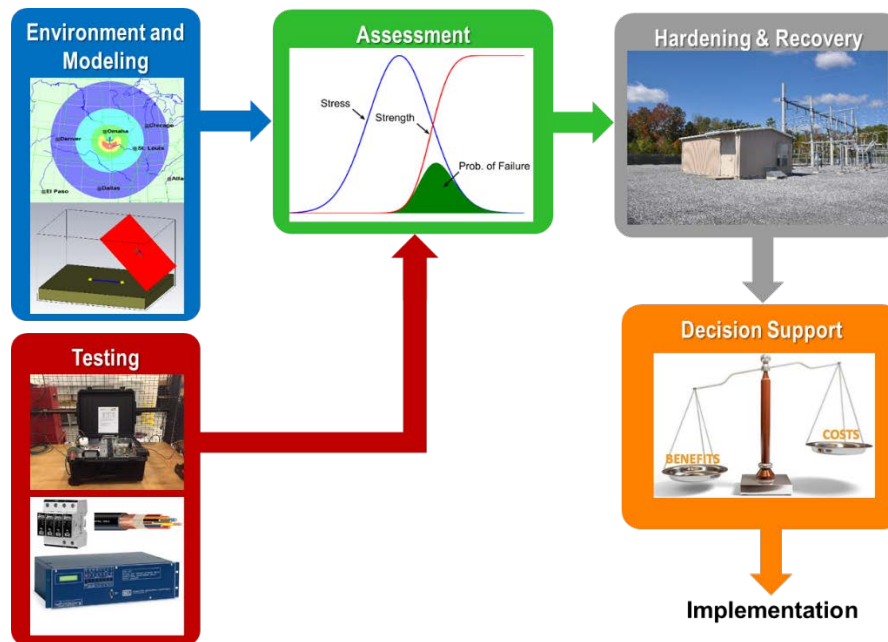


Figure 1-4
Description of the EPRI EMP Project

The details of the project tasks are provided below.

1.3.1 Environment and Modeling

Specific research tasks in the Environment and Modeling area included the following:

- Identifying conservative (bounding) unclassified HEMP environments (electric field amplitude, spatial and time dependent characteristics, etc.) that could be used to assess the potential impacts of HEMP (E1 EMP, E2 EMP, and E3 EMP) on the electric transmission system

- Investigating the physics of how each HEMP component couples to power system infrastructure such as overhead lines, substation bus work, above-ground and below-ground cables, and so on, and developing software tools and methods for performing coupling calculations and assessments
- Collaborating with DOE, DOE weapons laboratories, and other subject matter experts to develop additional unclassified HEMP environments that could be used in assessments

1.3.2 Testing

Laboratory testing of substation equipment such as DPRs was performed to determine the levels of E1 EMP stress that could result in disruption or damage to DPRs if exposed to the HEMP environment(s) defined in the Environment and Modeling task. Free field illumination testing per MIL-STD-461G/RS105 and direct voltage surge injection testing using a voltage surge with waveform defined in MIL-STD-188-125-1 were used to assess vulnerability. Additionally, shielding effectiveness testing of substation control houses was performed to determine the level of shielding that typical control house designs provide. Testing of potential mitigation options such as low-voltage surge protection devices (SPDs) was also performed. E3 EMP damage thresholds of large power transformers were based on prior works related to GMD events [6]. Additional details regarding the development of E1 EMP damage thresholds and the associated tests are provided in Section 3, E1 EMP Testing of Substation Equipment.

1.3.3 Assessment

The goal of this task was to assess, using several unclassified HEMP environments, the potential impacts of a HEMP attack on the transmission system. Assessments included the following:

- E1 EMP impacts on individual substations
- E1 EMP impacts on all substations within an interconnection (wide-area assessment)
- E2 EMP impacts on individual substations
- E3 EMP impacts on an interconnection
- Combined E1 EMP and E3 EMP impacts on an interconnection

Additional details regarding these assessments is provided in Section 4, Assessment of HEMP Impacts.

1.3.4 Mitigation, Hardening, and Recovery

The goal of this task was to assess various mitigation and hardening approaches that could be used by utilities to reduce the potential impacts that were identified in the assessments. Potential unintended consequences of various mitigation and hardening strategies were also evaluated, and system recovery following a HEMP-induced blackout was explored.

Details of these findings are provided in Section 5, Approaches for Mitigating the Effects of HEMP, and Section 6, System Recovery Following a HEMP Attack.

1.3.5 Decision Support

The goal of this task was to develop a framework for supporting risk-informed decisions regarding the implementation of HEMP hardening and mitigation measures.

1.4 Report Organization

The remainder of this final report is organized as follows:

- Section 2 provides a description of the nominal E1 EMP and E3 EMP environments that were developed by LANL and provided for use in this project as well as a brief overview of the E1 EMP and E3 EMP coupling methods that were used in the assessments.
- Section 3 provides a description of the E1 EMP testing that was performed to 1) determine the damage thresholds of DPRs, 2) determine the shielding effectiveness of typical substation control houses, and 3) assess the performance of several potential E1 EMP mitigation options.
- Section 4 provides a description of the E1 EMP assessment that was performed to estimate the potential impacts of two bounding E1 EMP environments on DPRs located in substations across an electrical interconnection. The section also provides a description of the E3 EMP assessment that was performed using the LANL E3 EMP environment as well as the combined E1 EMP + E3 EMP assessment that was performed. Lastly, the section provides a description of the assessment that was performed to determine if E1 EMP alone could result in regional disruption of the bulk power system.
- Section 5 provides a description of the approaches that were identified for hardening transmission assets against the impacts of E1 EMP and E3 EMP.
- Section 6 provides a description of how HEMP can potentially affect system recovery efforts and a listing of opportunities for updating existing recovery plans.
- Section 7 provides a high-level summary of the conclusions that were reached.
- Section 8 provides a summary of research gaps that warrant further study.
- Section 9 is a compiled list of references cited in the report.

2

HEMP ENVIRONMENT AND MODELING

2.1 Background

Unclassified HEMP environments are necessary for assessing the impacts of a HEMP attack on civilian infrastructure. Several unclassified E1 EMP environments exist [15], but in general, these environments have limited usability because they are comprised of a single waveform or in some cases, for example IEC 61000-2-9 [1], provide a generic representation of the peak electric field on the ground as a function of distance from the ground zero location, as reflected in a so-called *smile diagram*. Accordingly, many of the parameters that are important from an effects standpoint, such as polarization, angle of incidence, and so on, must be assumed. Although there are several unclassified E1 EMP environments, albeit with limitations, information on unclassified E3 EMP environments is extremely limited. In fact, when the initial E3 EMP assessments [5], [6] were carried out as a part of this research project, the Oak Ridge National Laboratory (ORNL) E3 EMP environment was the only unclassified environment available that provided the minimum spatio-temporal components necessary to perform interconnection-scale studies. Thus, additional unclassified data on both E1 EMP and E3 EMP were (and still are) needed by the industry.

To further the development of additional unclassified HEMP threat scenarios, EPRI collaborated with DOE, LLNL, and LANL. A description of the E1 EMP environment data provided by LLNL is documented in [16]. The LANL E1 EMP environment is described in [17] and is also provided below, along with a description of the E3 EMP environment that was developed.

2.2 Nominal E1 EMP Environment

2.2.1 Los Alamos National Laboratory (LANL) E1 EMP Environment²

LANL developed unclassified E1 EMP environments for five benchmark high-altitude nuclear burst scenarios [17].

The five benchmark scenarios developed by LANL were as follows:

- Benchmark 1: 25 kT device detonated at 100 km altitude
- Benchmark 2: 25 kT device detonated at 400 km altitude
- Benchmark 3: 125 kT device detonated at 100 km altitude

² The information contained in this section is taken directly from *Coupling of Early-Time High-Altitude Electromagnetic Pulse (E1) into Technological Infrastructure*. EPRI, Palo Alto, CA: 2018. 3002013934, and has been approved for public release and unlimited distribution through LA-UR-18-23547.

- Benchmark 4: 125 kT device detonated at 400 km altitude
- Benchmark 5: 1,000 kT device detonated at 200 km altitude

Calculations to develop these environments were performed using the LANL Compton High-Altitude Pulse (CHAP) code and assumed that the detonation occurred over the central contiguous United States (CONUS) with the ground zero location set to 40°N, 95° W. The benchmark scenarios described, as well as the results from these scenarios, are notional. No actual information about any weapon or weapons platform is contained in these results. Rather, the LANL CHAP code was run using a fictitious gamma source rather than actual weapons outputs and ascribed that source with a given yield of a nuclear device by assuming, as in Glasstone and Dolan [7], that 0.3% of device yield was in the form of 2 MeV gamma rays.

The E1 EMP characteristics for the five benchmark scenarios that were parameterized by device yield and height of burst (HOB) are documented in [17]. The notional weapon yield, height of burst, and peak incident E-field at the worst-case location on the ground associated with the five scenarios provided by Los Alamos National Laboratory under LA-UR-18-23547 are provided in Table 2-1 [17].

Table 2-1
Peak incident E1 field corresponding to the five benchmark scenarios

	Yield (kTon)	Height of Burst (km)	Peak Field (kV/m)
Benchmark #1	25	100	11.4
Benchmark #2	25	400	1.7
Benchmark #3	125	100	19.6
Benchmark #4	125	400	5.6
Benchmark #5	1000	200	24.9

Several general trends were noted from an assessment of the smile diagrams³ and associated normalizations provided in [17]. These include the following:

- The area of influence increases with increasing height of burst. Recall that the E1 EMP field impacts any location on the earth that is within line of sight of the burst location. As the HOB increases, so does the area within view of the burst.
- Increasing the affected area by increasing the HOB comes with a significant reduction in the electric field magnitude on the ground. The two bursts that occur at 400 km altitude experience a considerable drop in maximum electric field magnitude in comparison with their 100 km HOB counterparts.
- There was a weak dependence of the peak electric field with device yield. For example, a 1,000 kT burst achieved a peak electric field only slightly larger than that of the 125 kT burst at 100 km.

³ A smile diagram presents the peak amplitude of the incident E-field at every location on the ground over an impacted area. Because the resulting E-field pattern has a smile shape (refer to Figure 2-1) it is often referred to as a smile diagram.

Because the 1,000 kT benchmark scenario provided the highest peak electric field (~ 25 kV/m at the worst location on the ground) it was selected for use in E1 EMP assessments.⁴ The details of this scenario are described below.

2.2.1.1 Magnitude of Incident E1 Field

To more easily display the spatial electric field amplitude in a simple diagram, the information in the field is frequently condensed to its maximum amplitude at a specific location on the ground. The resultant spatial E1 EMP field is called a *smile diagram* due to its characteristic shape of a smile south of the burst location. A smile diagram normalized by the maximum electric field amplitudes over all locations and times is displayed in Figure 2-1.

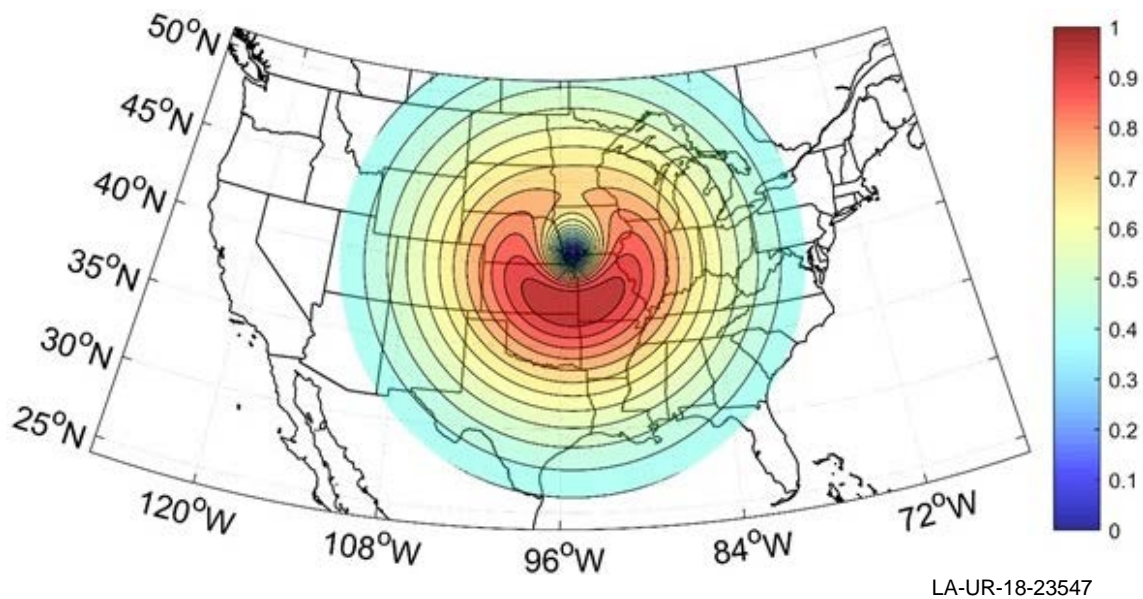


Figure 2-1
Normalized smile diagram for benchmark 5 (Yield = 1,000 kT, HOB = 200 km); ground zero location is 40° N, 95° W

There are few standard smile diagrams that one can compare with the spatial behavior presented in Figure 2-1. One such standard is provided in IEC 61000-2-9 [1]. Although the general shape of the smile diagram and area of coverage displayed in Figure 2-1 is in general agreement with the IEC standard, it is worth noting that there are differences for benchmarks 1, 2, and 4 (not shown) when one considers the decay of the electric field magnitude toward the horizon. For these weaker bursts (weaker due to lower yield or higher burst altitude), the amplitude did not decay to approximately 50% of the peak field at the horizon, as is given in IEC 61000-2-9 [1], but rather tended toward zero. Using the IEC smile diagram for these weaker bursts would exaggerate the potential effects, thus highlighting the need for additional unclassified E1 EMP environments that are physically consistent.

⁴ The peak amplitudes of the fields associated with the 1,000 kT environment were also scaled to 50 kV/m (multiplied by ~ 2) to correspond to the peak electric field described in IEC 61000-2-9.

The smile diagram as defined in Figure 2-1 captures only the maximum amplitude of the incident field at spatial locations within the line of sight of the burst, but at each location. However, at each location on the ground the resulting peak field is derived from a waveform representing the temporal aspects of the field. The E1 EMP waveform can be represented by a double exponential function such as the one described by Equation 2-1.

$$\mathbf{E}(t) = E_0 \cdot k \cdot (e^{-at} - e^{-bt}) \tag{Eq. 2-1}$$

Two popular double exponential functions used in the literature are the IEC waveform [1], which sets $E_0 = 50\text{kV/m}$, $k = 1.3$, $a = 4 \times 10^7\text{s}^{-1}$, and $b = 6 \times 10^8\text{s}^{-1}$, and the Bell Labs waveform [2], which sets $E_0 = 50\text{kV/m}$, $k = 1.05$, $a = 4 \times 10^6\text{s}^{-1}$, and $b = 4.76 \times 10^8\text{s}^{-1}$. These two standard waveforms (normalized by their peak amplitude of 50 kV/m) are shown along with waveforms from benchmark 5 for a selection of locations east and south of ground zero. These waveforms are provided in Figures 2-2 and 2-3. The waveforms associated with benchmark 5 (yield = 1,000 kT, height of burst = 200 km) have also been normalized by the peak electric field of 24.9 kV/m. Also displayed are the Bell Labs [2] and IEC 61000-2-9 [1] standard waveforms, which have been normalized by their peak electric field amplitude of 50 kV/m. The Bell Labs and IEC waveforms were time-shifted to make peaks coincide.

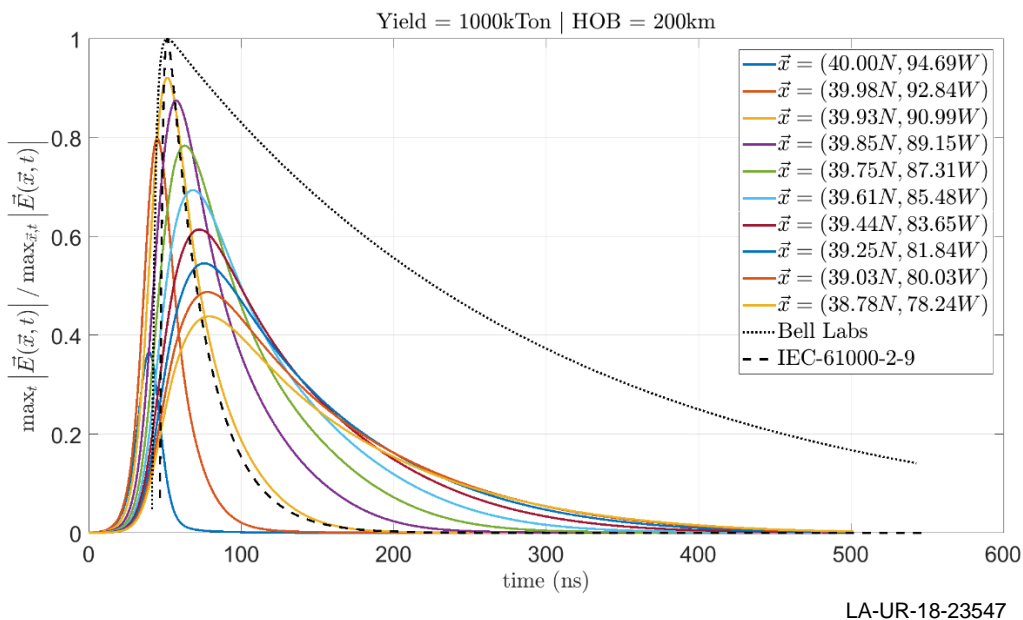


Figure 2-2
Normalized E1 EMP waveforms from benchmark 5 for ground locations generally east of ground zero (40° N, 95° W)

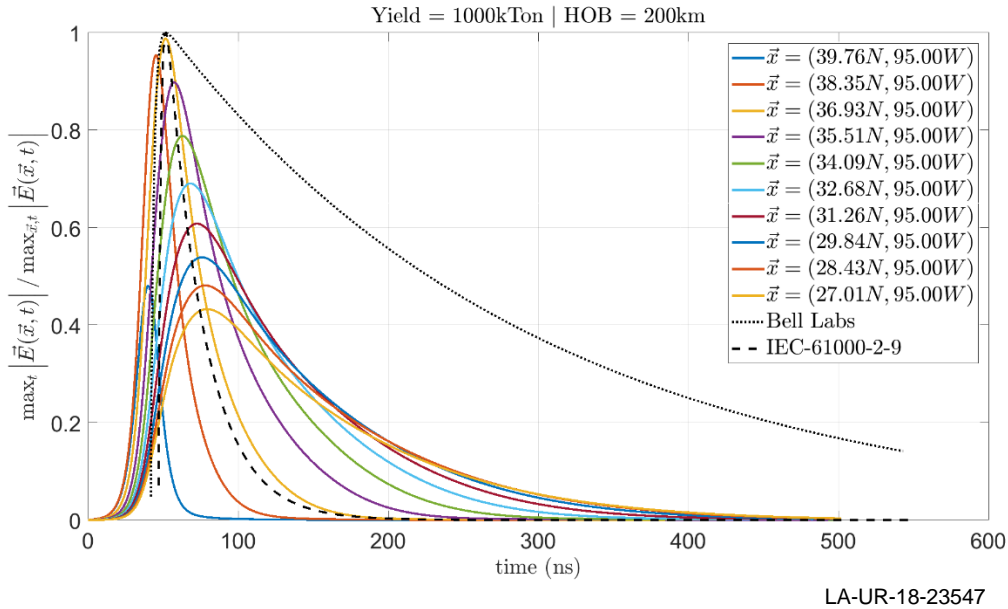


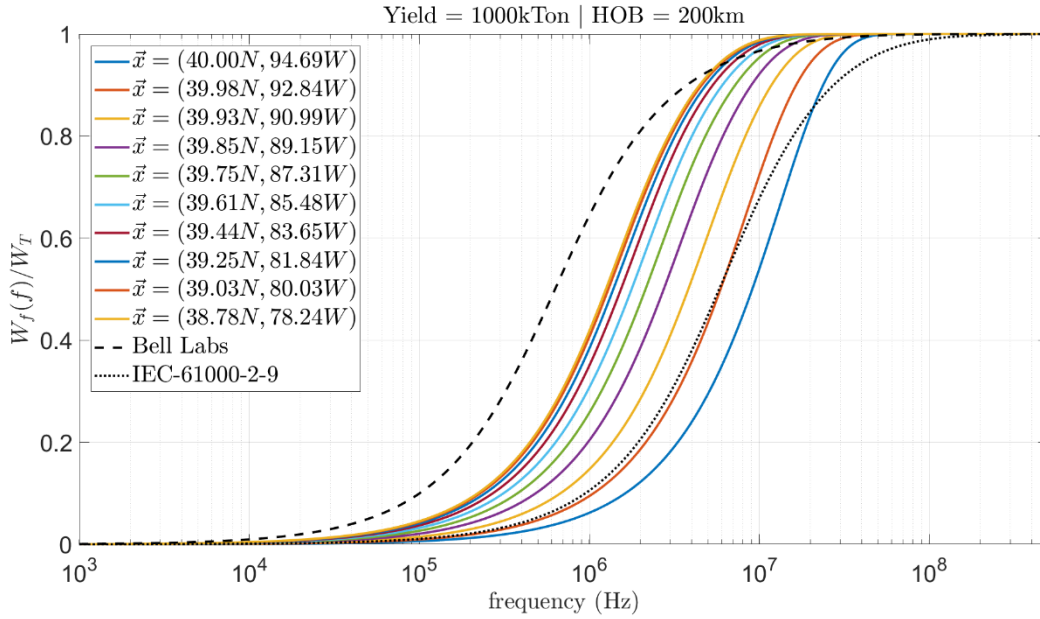
Figure 2-3
Normalized E1 EMP waveforms from benchmark 5 for ground locations generally south of ground zero (40° N, 95° W)

Several general trends can be observed in the time signals illustrated in Figures 2-2 and 2-3. The first general trend is the increase and eventual decay of the peak amplitude as the observer location is moved south or north from ground zero, further illustrating the results shown in the smile diagram shown in Figure 2-1. The second is that the time signals at locations closer to ground zero tend to rise and fall more quickly than their counterparts near the horizon.

The waveform associated with the maximum peak field of benchmark 5 rises and falls more sharply than the IEC waveform. For most of the region around the burst, the peak rise occurs more slowly than both standards, and the decay tails reside somewhere between the IEC 61000-2-9 standard and the slower Bell Labs waveform. This fact is further reflected in the spectral content for each of the signals. The fraction of energy fluence for each of the signals is defined as

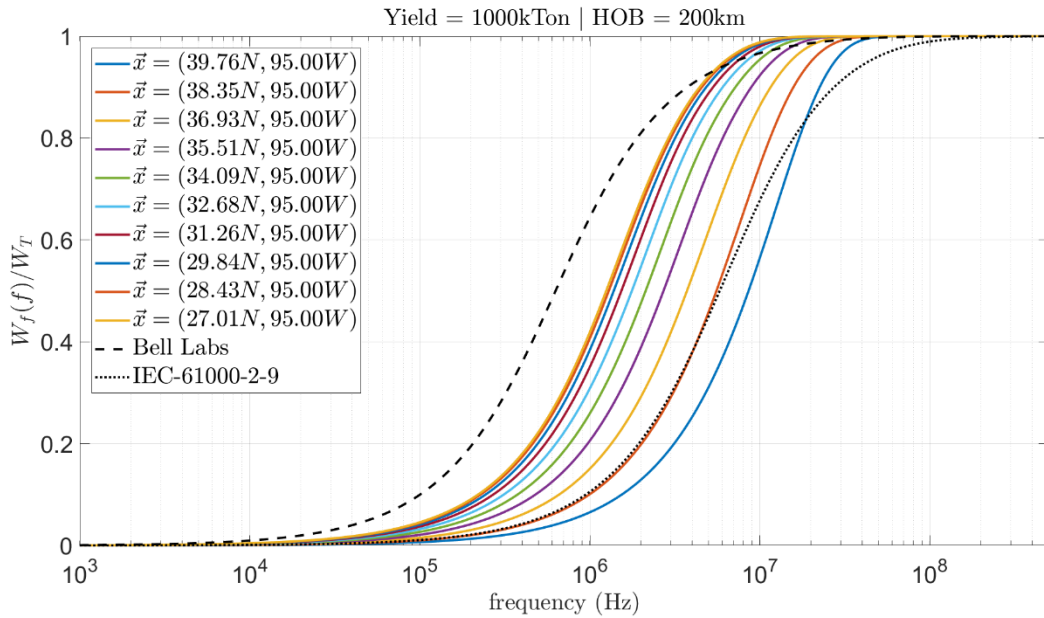
$$\frac{W_f}{W_T} = \frac{\int_{1000}^{f_1} |E(f)|^2 df_1}{\int_{1000}^{\infty} |E(f)|^2 df} \quad \text{Eq. 2-2}$$

where $E(f)$ is the complex Fourier transform of the E1 EMP waveform. The fraction of energy fluence for the IEC 61000-2-9 and Bell Labs waveforms is shown with the fraction of energy fluence for a selection of ground locations east and south of ground zero (Figures 2-4 and 2-5).



LA-UR-18-23547

Figure 2-4
The fraction of energy fluence for ground locations generally east of ground zero (40° N, 95° W) for benchmark 5



LA-UR-18-23547

Figure 2-5
The fraction of energy fluence for ground locations south of ground zero (40° N, 95° W) for benchmark 5

For all the scenarios, as well as both benchmarks, almost all of the energy is contained within frequencies less than 100 MHz.

2.2.1.2 Polarization Angle, α

The polarization of the E1 EMP field is an important parameter in coupling calculations. It is primarily governed by the cross product of \vec{k} , the line of sight vector from the explosion to observer location, with the direction of the geomagnetic field vector where the line of sight vector crosses ~ 30 km altitude (the approximate source region). For details on why this occurs, refer to other available reports, such as LANL's *A Review of EMP Hazard Environments and Impacts* [3].

The polarization angle, as with the field amplitude, is a function of both the observer location and time. The time dependence tends to be weak; thus, for most applications, it can be ignored. In Figure 2-6, the polarization angle α , as defined in Figure 2-10, is displayed for the 1,000 kT scenario evaluated at the time that each location experiences its maximum electric field amplitude.

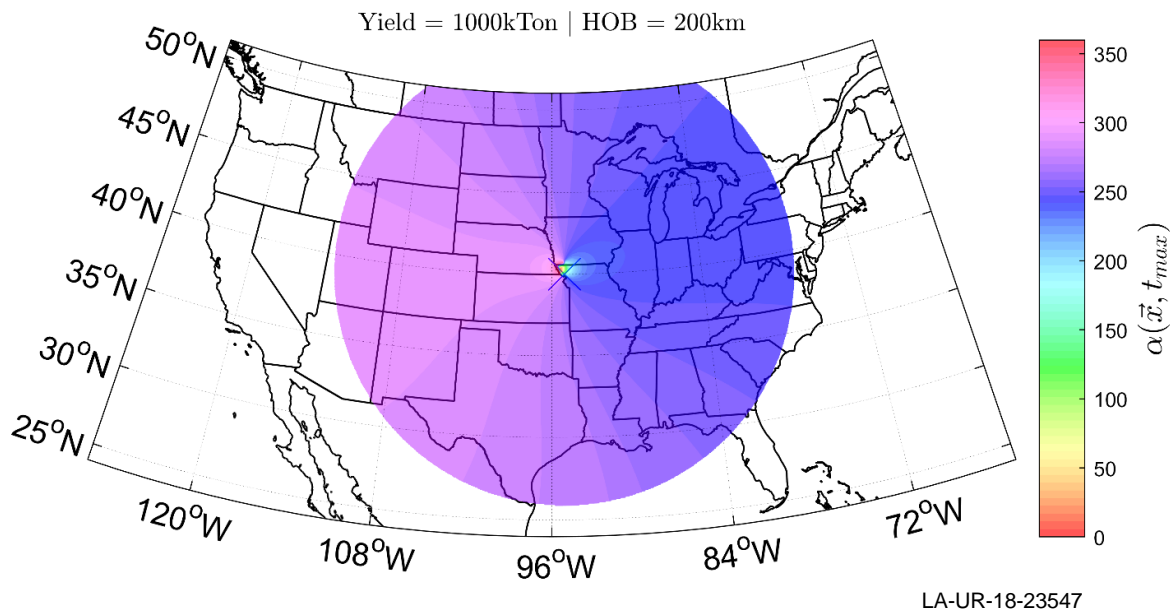


Figure 2-6
The polarization angle, α , for a 1,000 kT yield weapon detonated at 200 km evaluated at the time when the magnitude of electric field achieves its maximum value at the observer location

For the five benchmark scenarios that were evaluated, the region exposed to E1 EMP experiences a polarization angle, α , that generally ranges from 240° to 300° , with the precise value of 270° occurring to the north and south of ground zero. The value near 270° means that most of the energy of the electric field is in the horizontally polarized component rather than the vertically polarized component. This finding also agrees with the conclusions presented in [18] that the incident electric field for a majority of observation locations within the CONUS can be considered horizontally polarized. However, there are smaller regions, near the ground zero location, that are closer to values of 180° or 0° (360°), corresponding to a primarily vertically polarized electric field [17].

2.2.1.3 Incidence Angle, ψ

The angle of incidence, ψ , is fixed by \vec{k} , which is defined by a ray drawn from the burst location to the observer's location on the ground (the *line of sight*) [17], [3]. For example, directly below the burst, the incidence angle would be $\psi = 90^\circ$. In contrast, if the burst occurred on the observer's horizon, the incidence angle would be $\psi = 0^\circ$. The incidence angles for benchmark 5 are shown in Figure 2-7. The incidence angles for identical heights of burst (not shown) are identical; this is a result of the incidence angle depending only on line of sight from the burst point to a location on the ground and is entirely independent of device yield [17].

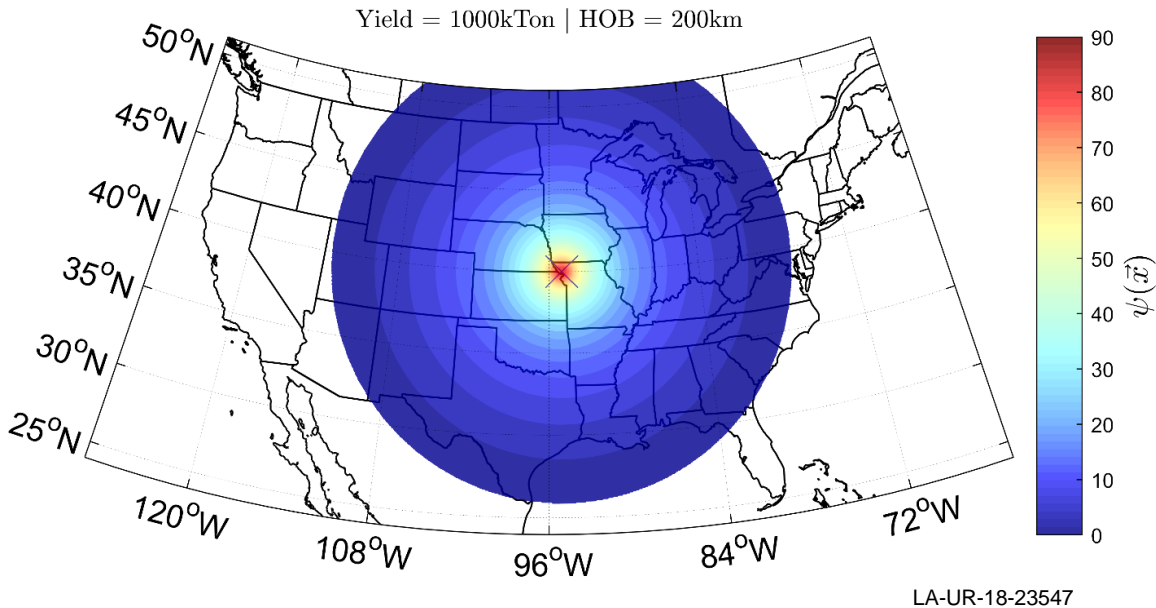


Figure 2-7
The incidence angle for various locations on the ground resulting from a 1,000 kT yield weapon detonated at 200 km above the earth's surface

2.2.1.4 Azimuthal Angle, Φ

The azimuthal angle, ϕ , is the angle that the incident plane wave makes with the conductor (see Figure 2-10). It is also commonly referred to as the line angle. Although the line angle is an important parameter in the E1 EMP coupling problem, it is highly variable because it is related to the orientation of the line (which can be any direction) with respect to the burst location (which is unknown in civilian assessments). Typically, many different line angles are evaluated to estimate a range of potential coupling responses.

2.2.1.5 Complete Spatio-Temporal E1 EMP Environment

Intuitively it would seem that the worst-case impacts would occur where the amplitude of the incident E1 EMP field is a maximum (refer to red portion of Figure 2-1). Using this maximum electric field one could then model the E1 EMP with an enveloping waveform such as the double exponential waveform described in IEC 61000-2-9 or Bell Labs and allow incidence angles and polarization angles to range over $0^\circ \leq \psi \leq 90^\circ$ and $0^\circ \leq \alpha \leq 360^\circ$, respectively. The worst-case results from this analysis could then be used to assess the potential impacts.

This analysis method would result in a worst-case scenario for coupling to conductors. However, because the polarization angle, incidence angle, and waveform for a physically consistent E1 EMP environment are not independent variables, this simplification can lead to an overestimate of the worst-case electrical stress that a component might be exposed to during a HEMP attack [17], [18]. When a complete, self-consistent, spatio-temporal E1 EMP environment is used, maximum coupling generally occurs in areas to the east and west of ground zero and not south of ground zero where the area of maximum electric field amplitude is located. Thus, when performing an analysis of E1 EMP impacts over a large region such as an electrical interconnection, *it is of paramount importance that a physically consistent E1 EMP environment be used.*

In order to perform interconnection-scale E1 EMP coupling simulations (refer to Section 4), a bounding, but physically consistent E1 EMP environment was provided by LANL under LA-CP-18-20631. With the exception of Figures 2-1 through 2-7, the details of this environment (spatio-temporal fields) are not provided in this report, but Figure 2-8 illustrates the density of the geographic locations for which the environment was provided. Note that the ground zero location shown in Figure 2-8 is completely notional and is for illustration purposes only.

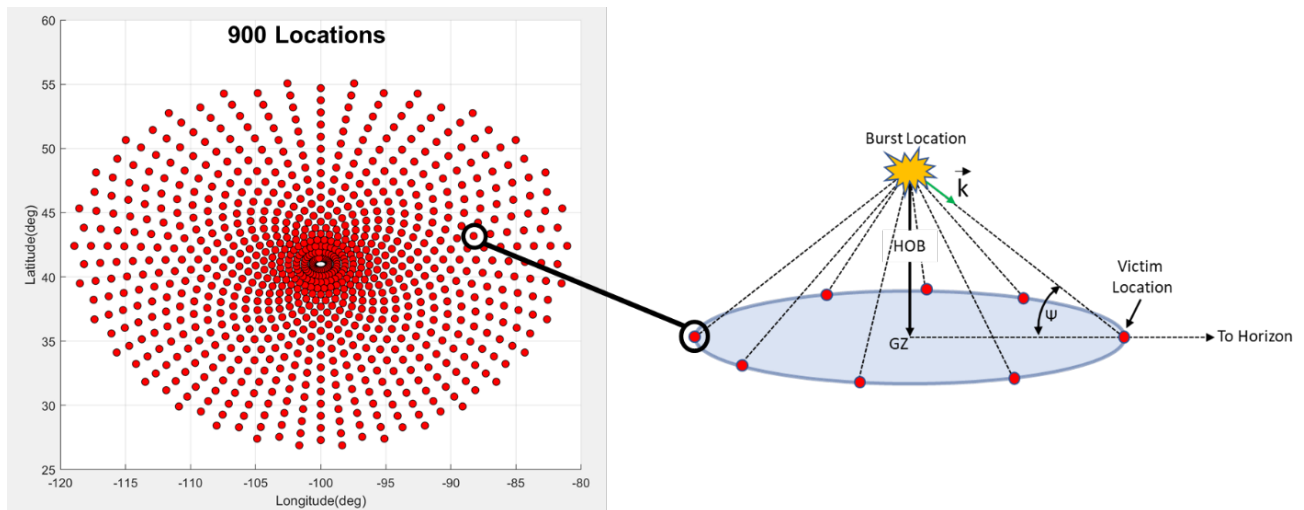


Figure 2-8
Example geographic locations for the E1 EMP environment

There are 900 concentrically spaced geographic locations shown in Figure 2-8 for which data were provided. At each of the 900 locations on the ground, the horizontal and vertical components of the incident E-field and associated waveform were provided. Also, the angle of incidence (refer to the angle ψ in Figure 2-8) was defined for each of the 900 locations on the ground. Thus, for each of the 900 locations on the ground, the following quantities were known: the waveform of the incident E1 EMP, the peak amplitude of the electric field, the angle of incidence (ψ), and the polarization angle (α). The only unknown quantity was the line angle (refer to ϕ in Figure 2-10). As will be shown later, the line angle was varied to evaluate all possible line angles. Details on how this E1 EMP environment was used to perform coupling simulations on a large geographic region such as an electrical interconnection are provided in Section 4.

2.3 Nominal E3 EMP Environment

Brief descriptions of the two E3 EMP environments that were used in the EPRI analysis are provided below. It is important to note that neither E3 EMP environment is related to the previous E1 EMP benchmark scenarios described previously. Both environments are based on different notional weapons and heights of burst.

2.3.1 Oak Ridge National Laboratory (ORNL) E3 EMP Environment

The E3 EMP environment used in the initial E3 EMP assessments performed by EPRI [5],[6] was developed by Oak Ridge National Laboratory (ORNL) and described in [4] and [9]. At the time these initial studies were performed, the ORNL E3 EMP environment was the only unclassified environment available that contained the *minimum* spatio-temporal characteristics⁵ necessary to perform interconnection-scale assessments. The environment, which included both E3A and E3B components, was based on a notional detonation of a 1,400 kT weapon 400 km above the earth's surface. The peak amplitude of the resulting E3A field was approximately 13 V/km, and peak E3B electric field was approximately 24 V/km. Simulations to create the ORNL E3 EMP environment were based on a uniform earth model with conductivity of 0.001 S/m, which is generally considered a conservative worst-case. The full details of the ORNL E3 EMP environment can be found in [4] and [9].

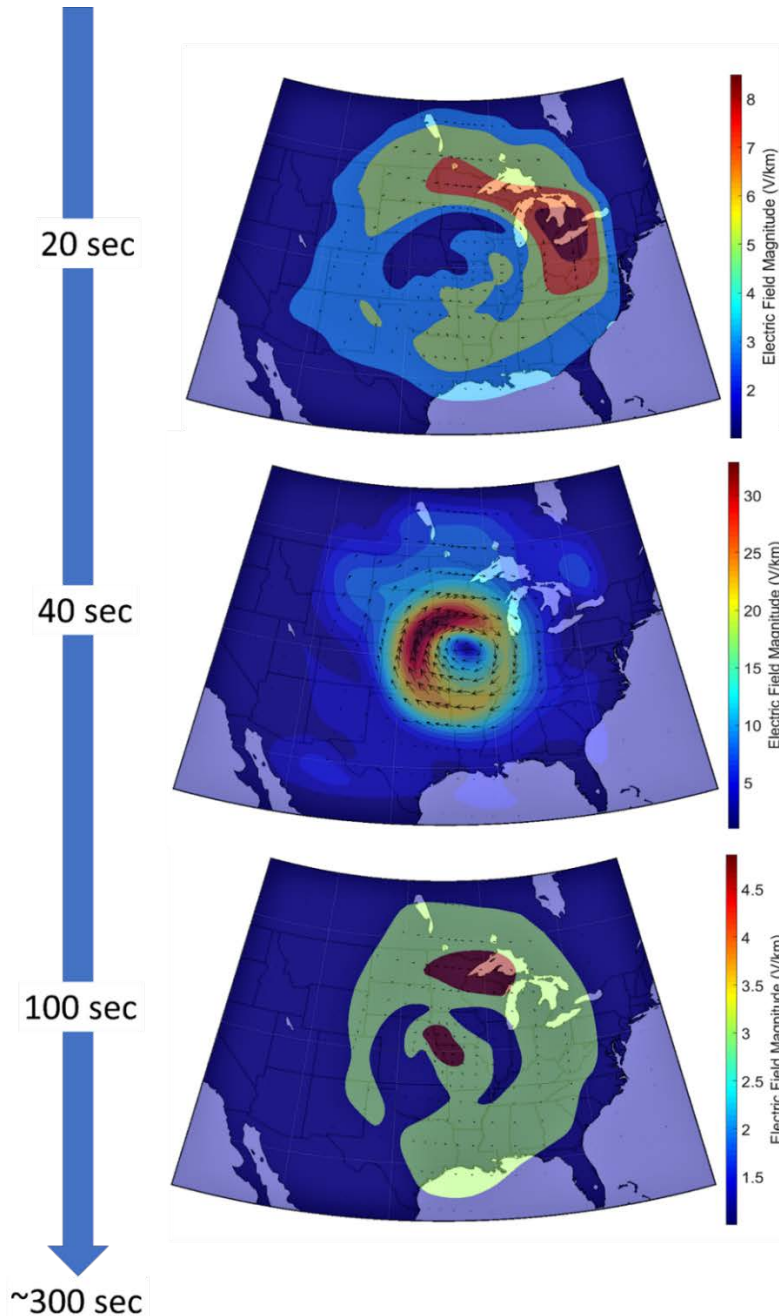
2.3.2 Los Alamos National Laboratory (LANL) E3 EMP Environment

Although the ORNL E3 EMP environment was the only one available at the time of the initial EPRI E3 EMP assessments that included the minimum spatio-temporal components necessary to perform interconnection-scale studies, there were a number of known limitations with the environment. First, the environment included a significant E3A component that covered the entire CONUS while also having a strong E3B component over a portion of the same area. It is well established that the maximum E3A field does not exist to any significance over the same geographic area covered by the E3B pulse [19], [20]. Second, the direction of the geoelectric field vectors for both the E3A and E3B environments remained fixed throughout the duration of the event. This behavior is not consistent with data observed during high-altitude tests over land [20]. Third, only a single waveform was available to represent the temporal effects, which is also known to be inconsistent with test data [20]. These limitations led the EPRI research team to explore options for obtaining additional unclassified data that could be used to improve the fidelity of previous studies. What follows is a description of the unclassified E3 EMP environment that was provided by LANL.

The LANL E3 EMP environment is based on a notional 10,000 kT (10 MT) weapon detonated 200 km above the earth's surface, and no actual information about any weapon or weapons platform was used to develop the environment. The environment does not include an E3A component, since the focus of the impacts, and hence the target locations, are centered over the CONUS. The peak E3B field is approximately 35 V/km and is based on a soil conductivity of

⁵ Spatio-temporal characteristics refer to the time-varying electric field on the ground over a large geographic area. These electric fields are used to compute time-varying geomagnetically induced currents (GICs) that are used in the assessments.

0.001 S/m. The entire spatio-temporal E3B environment is time dependent, meaning that for each location on the ground, a time-dependent geoelectric field (magnitude and direction) was provided to the EPRI research team. A map of the instantaneous geoelectric field magnitude at three different points in time ($t = 20$ sec, $t = 40$ sec, and $t = 100$ sec) for a notional ground zero location within the CONUS is shown in Figure 2-9 to illustrate the spatio-temporal behavior of the environment.



LA-UL-19-22326

Figure 2-9
Map of the instantaneous geoelectric field magnitude of the LANL E3 EMP environment at three different points in time ($t = 20$ sec, $t = 40$ sec, and $t = 100$ sec)

2.4 E1 EMP Modeling

A brief description of the coupling methods that were used to perform the E1 EMP assessment discussed in Section 4 is provided below.

2.4.1 Coupling to Overhead Conductors

Because the source (nuclear detonation at high altitude or in space) of the E1 EMP signal is a significant distance from the earth's surface (10s to 100s of km) ground-based infrastructure (for example, a substation or overhead transmission line) can be assumed to be in the far field. Thus, the incident E1 EMP can be considered a plane wave. An electromagnetic plane wave incident on an overhead conductor is illustrated in Figure 2-10.

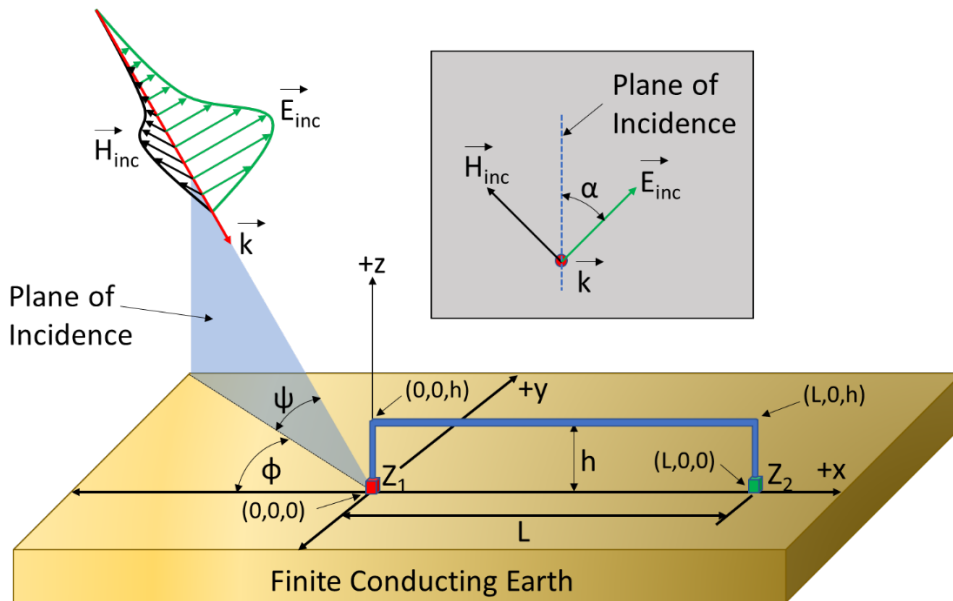


Figure 2-10
Illustration of an E1 EMP plane wave incident on an overhead conductor

In Figure 2-10, E_{inc} is the incident electric field vector, H_{inc} is the incident magnetic field intensity vector, and k , referred to as the Poynting vector, is defined as: $\vec{k} = \vec{E} \times \vec{H}$. Referring to Figure 2-10, the angle ψ is the angle of incidence (or elevation angle), and the angle ϕ is the azimuthal angle or line angle. The upper right portion of Figure 2-10 shows the polarization of the incident field defined by the angle α and is the orientation of the electric field vector (vertical or horizontal) relative to the plane of incidence. A plane wave that is vertically polarized will have a polarization angle of 0° , and a plane wave that is horizontally polarized will have a polarization angle of 90° . Earth conductivity and permittivity are denoted by σ and ϵ , respectively. All of these parameters are important in the coupling process [17].

The primary method used in this research to couple the incident electromagnetic plane wave into an electrical conductor above a finite conducting earth was based on the Baum-Liu-Tesche (BLT) equations [17], [21]. This model accounts for coupling of the incident pulse into the vertical and horizontal segments of the line (refer to Figure 2-10) as well as the response of a

finite conducting earth. Calculations following the BLT equation-based method are carried out in the frequency domain, and Fourier techniques are used to convert the frequency-domain results to the time-domain signals. The reader is referred to References [17] and [21] for further details regarding this coupling model.

2.4.2 Buried Conductors

Coupling models for buried conductors based on the BLT approach were also developed. As with the overhead line coupling method, the response of a finite conducting earth was included. The geometry of a buried conductor scenario is illustrated in Figure 2-11.

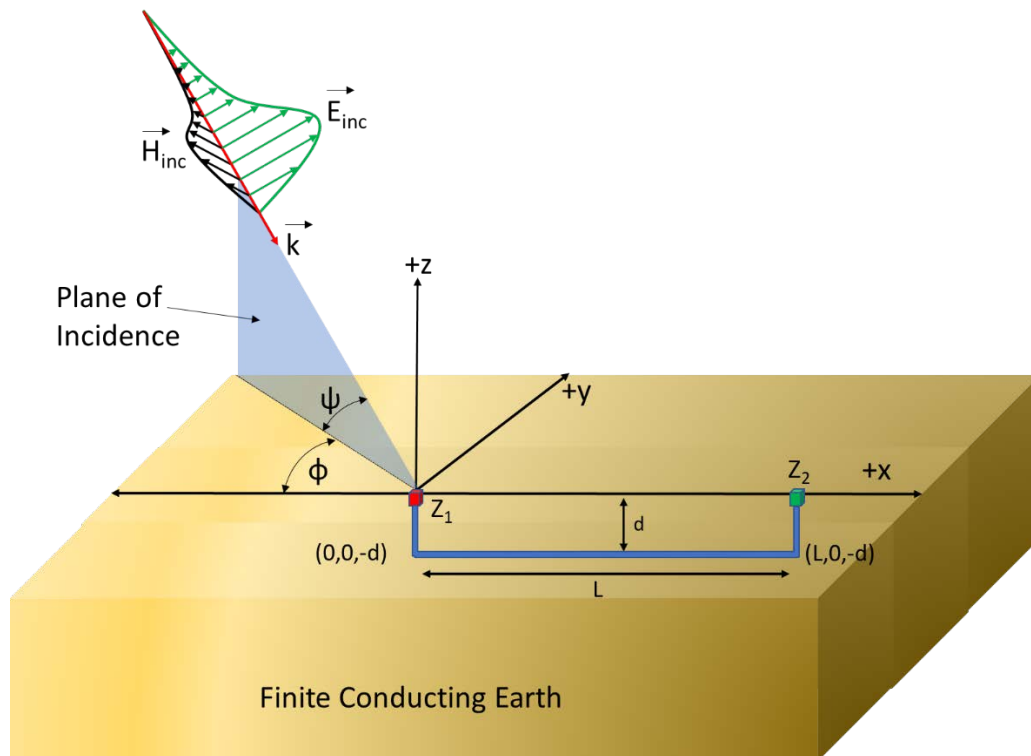


Figure 2-11
Geometry of buried conductor modeling scenario

As with the overhead line coupling models, calculations were carried out in the frequency domain, and Fourier techniques were used to convert back to the time domain. The reader is referred to Reference [21] for further details of the BLT method applied to buried conductors.

2.5 E2 EMP Modeling

2.5.1 Coupling to Overhead Conductors

The coupling model described in Section 2.4.1 was also used to perform the E2 EMP assessment described in Section 4.2.

2.6 E3 EMP Modeling

2.6.1 Coupling to Overhead Conductors

The procedure for coupling the low-frequency E3 EMP signal into overhead transmission lines is the same as that for coupling the quasi-dc geoelectric field associated with a GMD event. The electric field is integrated along the path of the transmission line to determine the induced voltage that drives the GIC. Because of the low-frequency nature of the GIC, a dc model of the power system is used to compute the GIC flows. The procedure used to couple the E3 EMP environment to overhead transmission lines is documented in the EPRI report *Magnetohydrodynamic Electromagnetic Pulse Assessment of the Continental U.S. Electric Grid: Geomagnetically Induced Current and Transformer Thermal Analysis* [6].

3

E1 EMP TESTING OF SUBSTATION EQUIPMENT

3.1 Background

Sections 2 and 4 of this report present the results of modeling that determines the incident electric fields (E-fields) and surge voltages that digital protective relays (DPRs) in a substation could be exposed to as a result of a HEMP attack. This section reports the results of testing that determines the incident radiated E-fields and the surge voltages that the DPRs can withstand so that the vulnerability can be determined. In addition, this section presents the results of testing mitigation methods, including shielding and surge protection.

Testing was performed to investigate how DPRs within a substation control house would perform when subjected to both radiated E-fields and conducted surges. In addition, the levels of shielding provided by typical substation control house designs, which may reduce the E-field magnitudes incident on the DPRs, were evaluated, as well as the performance of surge protection devices. Several tests were performed, such as the following:

- Free field illumination testing based on MIL-STD-461G/RS105 [22] to determine the magnitude of the incident E-field that could cause damage or disruption of a device under test (DUT).
- Shielding effectiveness testing of substation control houses based on the MIL-STD-188-125-1 [23] approach to assess the ability of these structures to shield internal components from incident electromagnetic waves.
- Direct injection testing using a voltage impulse with waveshape defined in MIL-STD-188-125-1 [23] to determine:
 1. the voltage surge magnitude that could cause damage or disruption of a device under test (DUT), and
 2. the performance of potential surge protection devices.

3.2 Digital Protective Relays Tested

As a part of this research, extensive E1 EMP testing of DPRs was performed. A general description of the DPRs that were tested is provided in Table 3-1. For security reasons, names of specific manufacturers and models are not provided. Testing results and levels at which disruption or damage occurred for these devices are provided in later sections. In many cases, multiple units of the same model were tested; however, not all DPR models were exposed to both free field illumination and direction injection testing.

Table 3-1
Description of DPR models that were tested

Digital Protective Relay (DPR) Model Designation	Description
DPR 1	Transmission Line Protection (Differential) and Control
DPR 2	Feeder Protection and Control
DPR 3	Transmission Line Protection and Control
DPR 4	Transmission Line Protection and Control
DPR 5	Transformer Protection (Differential) and Control
DPR 6	Transmission Line Protection (Differential) and Control
DPR 7	Transmission Line Protection
DPR 8	Transmission Line Protection
DPR 9	Over/Under Frequency
DPR 10	Transformer Protection (Differential)
DPR 11	Feeder Protection
DPR 12	Transmission Line Protection (Differential) and Control
DPR 13	Controller System
DPR 14	Transformer Protection (Differential) and Control
DPR 15	Transformer Protection (Differential)
DPR 16	Transformer Protection (Differential)
DPR 17	Feeder Protection and Control

3.3 Description of Device Performance

Test results were characterized by how the DUT responded to the test and the minimum E-field level or voltage surge magnitude at which the response was observed. Device responses were classified into four categories: Pass, Type 1, Type 2, and Type 3, and are defined in Table 3-2.

Table 3-2
Definition of device responses during and after testing

Device Response	Description	Examples
Pass	No disruption or damage of the device was observed during the test	Normal operation observed during and after the test.
Type 1	Device disruption; device able to resume normal operation after test without user intervention	Following the test, the device reboots to a stable operating condition without manual intervention.
Type 2	Device disruption; manual intervention required to resume normal operation	<ul style="list-style-type: none"> Following the test, the device becomes disabled, but manually recycling the power returns the device to a normal operating state. Following the test, settings are changed and manual intervention is required.
Type 3	Device destruction; repair or replacement of device required	The test causes permanent damage to the device.

3.4 Free Field Illumination Testing

Free field illumination testing was performed to determine the ability of a DUT to withstand the effects of an incident electromagnetic plane wave. This type of test is performed by using a guided-wave (or bounded-wave) simulator to generate a transient electromagnetic field that is then applied to a DUT.

The EPRI free field illumination test facility was designed for testing equipment of the size that can be found in a typical substation. MIL-STD 461G/RS-105 prescribes a largest allowable DUT size of one-half the length, one-half the width, and one-third the height of the waveguide structure. Taking into consideration typical DUT sizes, the impedance of the structure, and the overall footprint, the final system has a testing volume (area of uniform E-field that is within specification) of 2m x 2m x 2m. EPRI's test facility, which performs free field illumination testing per MIL-STD-461G/RS-105, is illustrated in Figure 3-1.

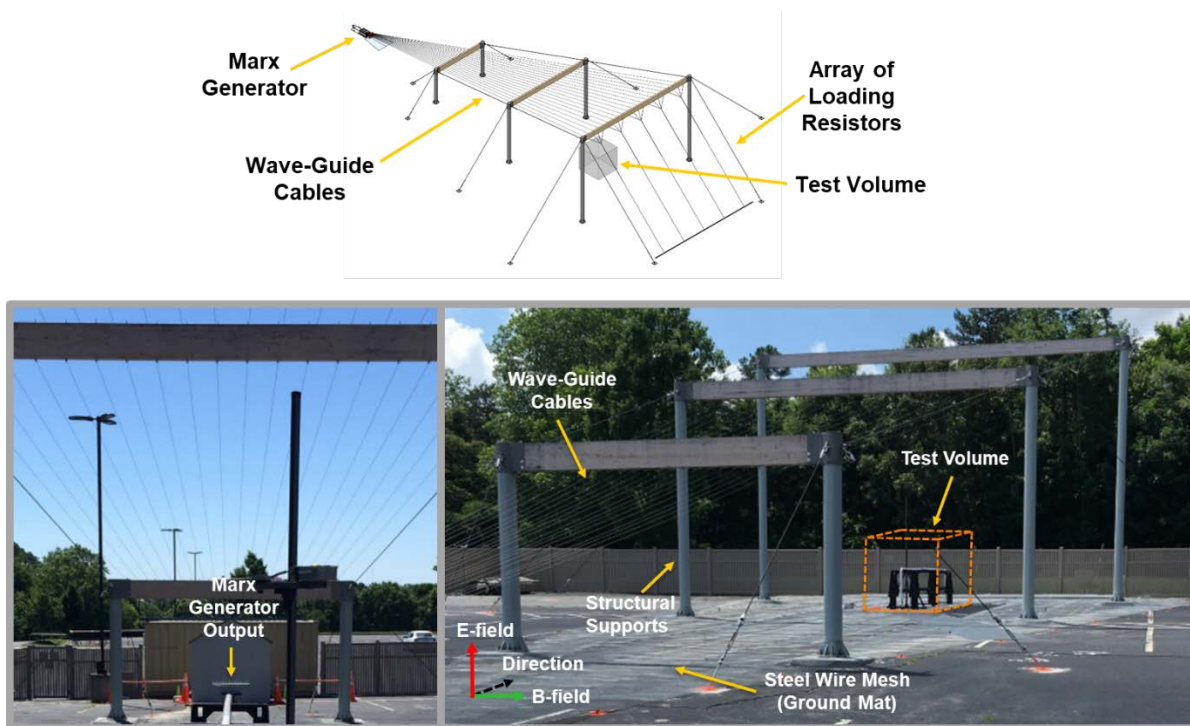


Figure 3-1
Illustration and photographs of EPRI's guided wave simulator based on MIL-STD-461G/RS105

The guided wave simulator shown in Figure 3-1 generates a vertically polarized plane wave that propagates from the source (output of the Marx generator) toward the 2m x 2m x 2m test volume. Figure 3-2 shows a simulated time-lapse portrayal of the propagation of the resulting plane wave.

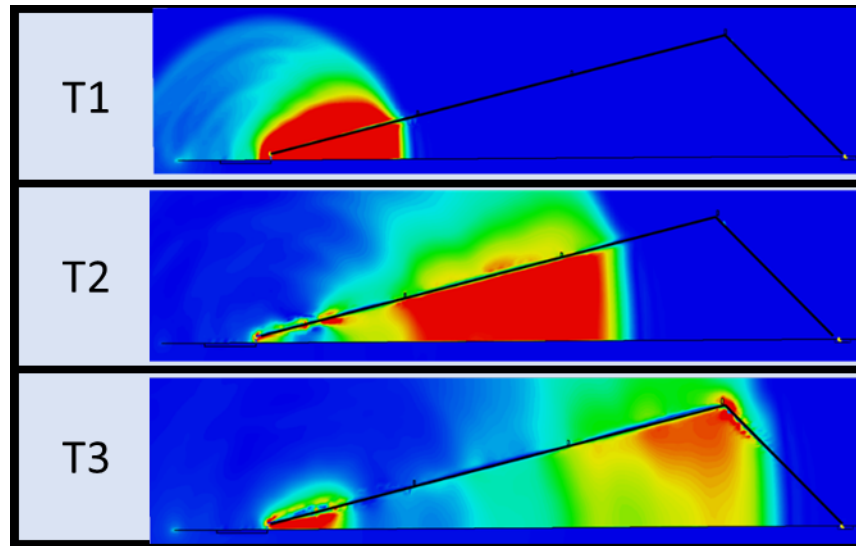


Figure 3-2
Simulated time-lapse portrayal of the plane wave generated during a free field illumination test. (Colors represent the magnitude of the E-field, in sequence of time, T1, T2, and T3.)

The test facility is designed to create a uniform E-field inside the 2m x 2m x 2m test volume illustrated in Figure 3-1. A comparison of the measured E-field pulse inside the test volume and the analytical E1 EMP waveform defined in MIL-STD-461G/RS105 is shown in Figure 3-3.

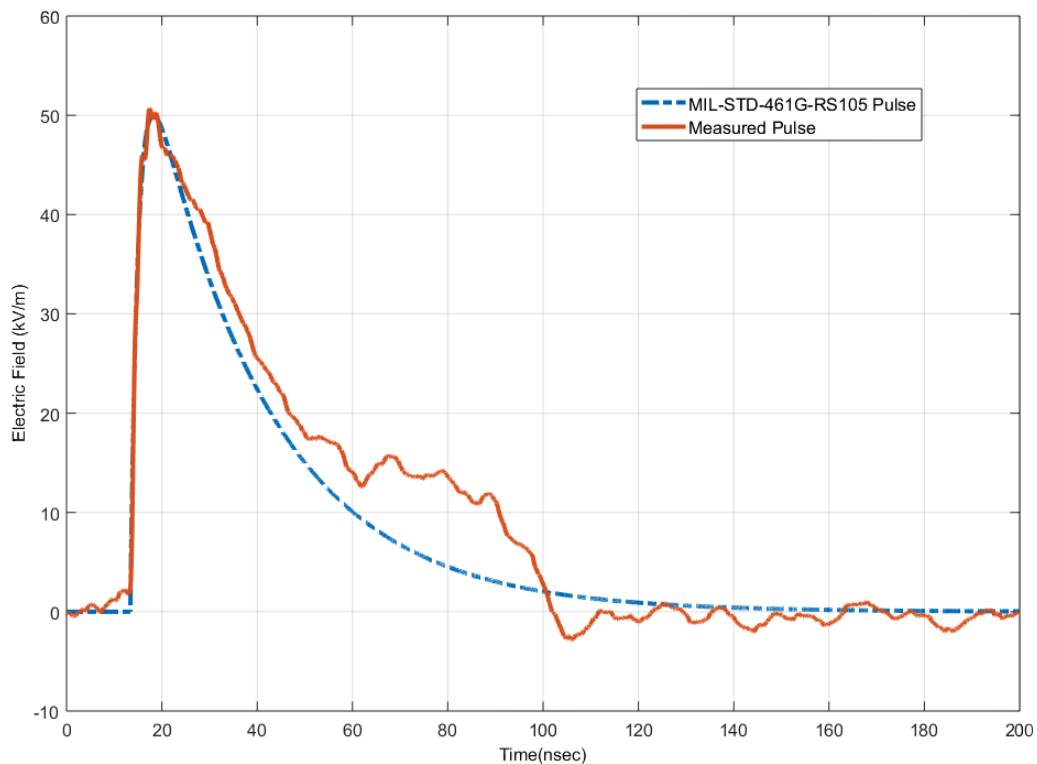


Figure 3-3
Example E1 EMP waveform generated by the EPRI guided wave test facility, and the required MIL-STD waveform determined using analytical equations

Since the generated E-field is vertically polarized (meaning that it is oriented in the vertical direction as illustrated in Figures 3-1 and 3-4) and it is important to determine the response of a DUT to both vertical and horizontally polarized waves, the tests are performed with the DUT oriented along two different axes: 1) along the horizontal (or x) axis, and, 2) along the vertical (or y) axis, as illustrated in Figure 3-4.

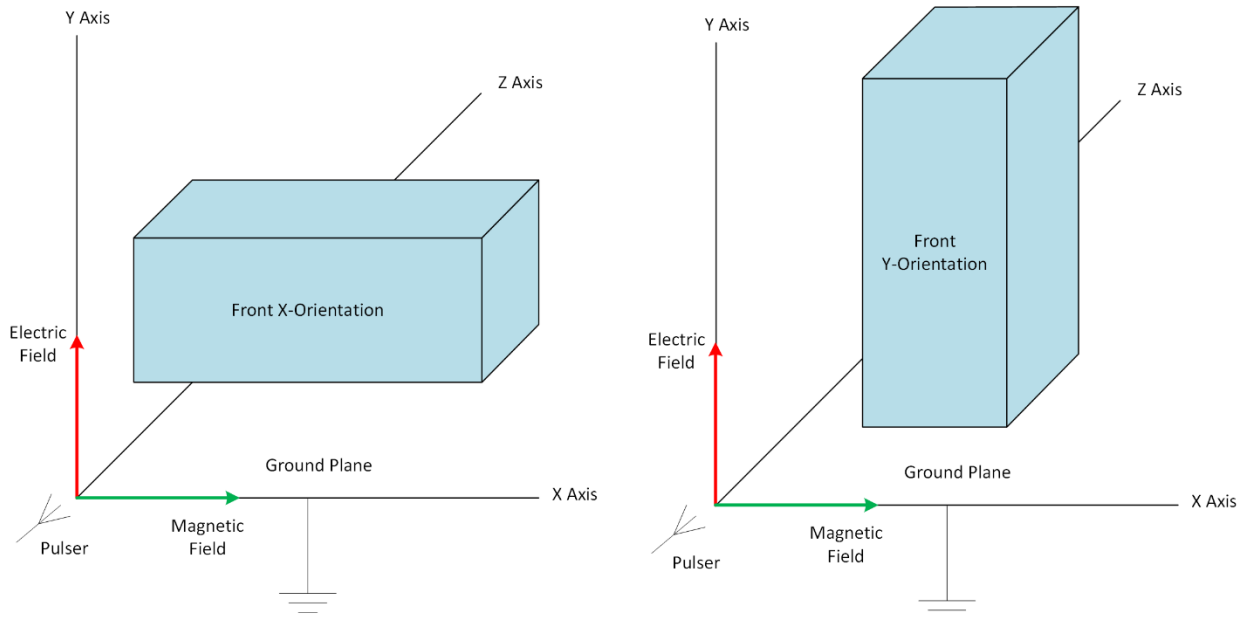


Figure 3-4
Illustration of DUT orientation along the horizontal and vertical axes

Operation of the DUT is observed prior to, during, and immediately after the test using a remote-controlled video camera as shown in Figure 3-5. The camera is EMP hardened and is controlled remotely using fiber optic cables. Figure 3-6 shows a snapshot of a Type 2 response that was observed during a DPR test. During the tests, DPRs were powered on when tested, using an ac generator. The power cables were short (< 10m) and oriented perpendicular to the incident E-field to minimize coupling.

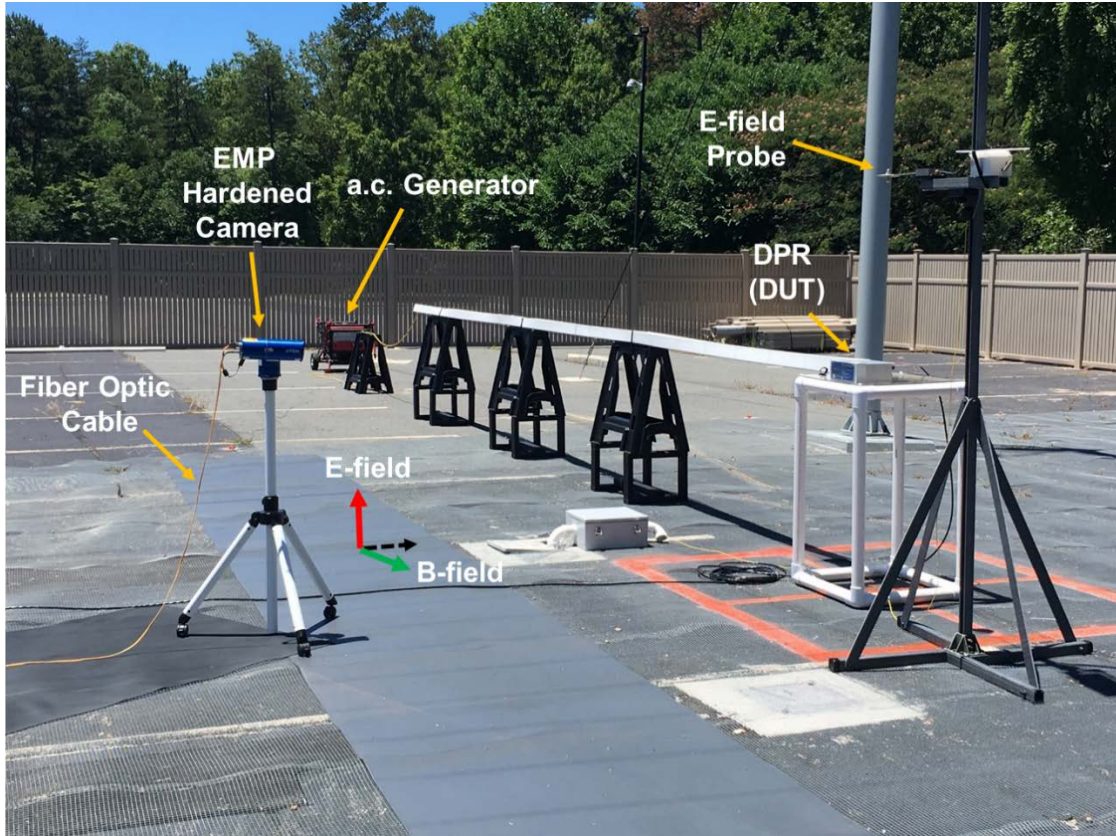


Figure 3-5
Photograph of a free field illumination test setup with fiber optic video camera



Figure 3-6
Example of a Type 2 response observed with the fiber optic camera during a free field illumination test

Free field illumination testing of DPRs was performed using the following test sequence.

1. Verify that the DPR is powered on and in a normal operating mode.
2. Verify the DPR's operating status and health by connecting to the DPR using a laptop computer and appropriate communications cable and perform diagnostics using manufacturer's software.
3. Disconnect the laptop computer and communications cable from the DPR.

4. Apply the MIL-STD-461G/RS105 radiated pulse (50 kV/m).
5. Observe the front panel display of the DPR for errors using the EMP hardened fiber optic camera.
6. Verify the DPR's operating status and health by connecting to the DPR using a laptop computer and appropriate communications cable and perform diagnostics using manufacturer's software.
7. If the DPR experiences a response other than a pass, cycle device power.
8. Repeat for a total of three pulses per DPR per orientation.

When a response other than Pass was observed, the amplitude of the incident field was lowered and testing was performed again to identify the minimum E-field level that resulted in DUT disruption or damage. The results of the free field illumination testing of DPRs that was performed at the EPRI test facility are provided in Table 3-3.

**Table 3-3
Results of field illumination testing of DPRs**

Relay Model		Device Response			
		Pass	Type 1	Type 2	Type 3
		E-Field Level (kV/m)			
DPR 1	Transmission Line Protection (Differential) and Control	50			
DPR 2	Feeder Protection and Control	50			
		50			
DPR 3	Transmission Line Protection and Control			15	
				25	
				30	
				35	
				35	
DPR 4	Transmission Line Protection and Control	50			
DPR 5	Transformer Protection (Differential) and Control	50			
DPR 6	Transmission Line Protection (Differential) and Control	50			
DPR 7	Transmission Line Protection	50			
DPR 9	Over/Under Frequency	50			

**Table 3-3 (continued)
Results of field illumination testing of DPRs**

Relay Model		Device Response			
		Pass	Type 1	Type 2	Type 3
		E-Field Level (kV/m)			
DPR 10	Transformer Protection (Differential)		35		
			40		
			45		
				45	
DPR 11	Feeder Protection	50			
DPR 12	Transmission Line Protection (Differential) and Control			15	
DPR 13	Controller System			35	
				45	
DPR 14	Transformer Protection (Differential) and Control	50			
DPR 15	Transformer Protection (Differential)	50			
		50			
DPR 16	Transformer Protection (Differential)	50			

DPRs that did not exhibit any adverse impacts from the maximum E-field level of 50 kV/m were assigned a Pass with designation of 50 kV/m, for example DPR 16. Other responses are characterized by the E-field level at which they occurred. In some cases, the DPR responded differently depending on the orientation of the device. The values provided in Table 3-3 correspond to the minimum E-field level that resulted in an observed response.

Additional free field illumination testing of DPRs with three-phase voltage and current signals connected to the analog inputs of the DPRs was performed. These tests showed no additional adverse effects; thus, testing results are not provided here.

Test results indicated that many of the DPRs can withstand the MIL-STD-461G/RS105 threat level of 50 kV/m; however, some experienced Type 1 and Type 2 responses (device disruption) at E-field strengths as low as 15 kV/m. There were no Type 3 responses observed during free field illumination testing of DPRs.

Based on the results of the free field illumination testing of DPRs presented in Table 3-3, it can be concluded that some additional shielding of DPRs is needed, but not to the 80 dB level required by MIL-STD-188-125-1. If margin is applied to the test results such that 5 kV/m is used as the limit of E-field strength inside an enclosure, then 20 dB of shielding across the frequency band defined in MIL-STD-188-125-1 (10 MHz – 1 GHz) is adequate. Section 3-5 provides

measured results and analysis of the shielding effectiveness of different control house construction types. Testing demonstrated that some control house designs may be able to provide a level of shielding necessary to reduce E-field levels inside the enclosure sufficiently to avoid Type 1 and 2 responses.

3.5 Shielding Effectiveness Testing of Substation Control Houses

Shielding effectiveness tests are performed to measure an enclosure's ability to provide electromagnetic shielding. Tests were performed on substation control houses of different construction types to determine the level of shielding that they inherently provide. These results were used in conjunction with the results of Section 3.4 on free field illumination testing to determine whether a DPR installed inside a control house could be impacted due to direct radiation by an incident E1 EMP wave.

The general test procedure for determining the shielding effectiveness of a substation control house is illustrated in Figure 3-7.

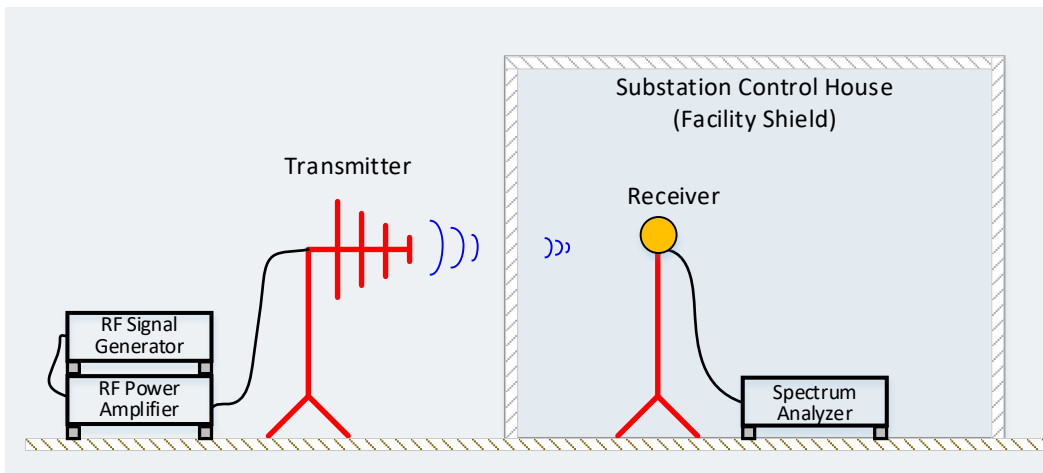


Figure 3-7
Depiction of a shielding effectiveness test setup

As depicted in Figure 3-7, a high-frequency signal is transmitted by an antenna located outside of the substation control house and is received by an antenna located inside the substation control house. The procedure is repeated for many discrete frequencies so that the shielding effectiveness for the desired frequency band is tested. The measurement data are then used to compute the shielding effectiveness (dB) at each discrete frequency that is tested using Equation 3-1,

$$SE = 20 \log_{10} \left(\frac{S_T}{S_R} \right) \quad \text{Eq. 3-1}$$

where SE is the shielding effectiveness or level of attenuation (dB), S_R is the received signal (arbitrary units), and S_T is the transmitted signal (arbitrary units).

Shielding effectiveness testing was performed using a purpose-built system that is designed to perform the shielding effectiveness (SE) test defined in MIL-STD-188-125-1. The system consists of a transmitting unit, a receiving unit, and matched antennas. This system was used to perform SE testing on four substation control houses of differing construction types, which included:

- Type 1: Concrete block walls covered with brick
- Type 2: Concrete walls reinforced with steel rebar
- Type 3: Metal walls with overlapping panels that are fastened together with screws
- Type 4: Metal walls and floor (six-sided) with welded seams

In each of the four scenarios, the control houses were operational, with typical points of entry (doors; power supply cables; control, measurement, and communication cables; HVAC, etc.), and no effort was made to intentionally provide shielding at these locations.

The four construction types are illustrated in Figure 3-8.

Type 1: Concrete Block and Brick



Type 2: Concrete With Steel Rebar



Type 3: Metal with Overlapping Panels



Type 4: Six-Sided Metal with Welded Seams



Figure 3-8
Examples of the various control house constructions where shielding effectiveness tests were performed

When performing the shielding effectiveness tests, measurements were made at various locations within the control house (walls, doors, etc.) The goal of these tests was to quantify the difference in the level of shielding provided by different construction types rather than perform a full evaluation per MIL-STD-188-125-1, which requires that the structure be subdivided into plane areas not greater than 3.05m x 3.05m and testing be performed on each. The measured shielding effectiveness at a single location on a wall for each of the four construction types, and the performance requirements of MIL-STD-188-125-1, are provided in Figure 3-9.

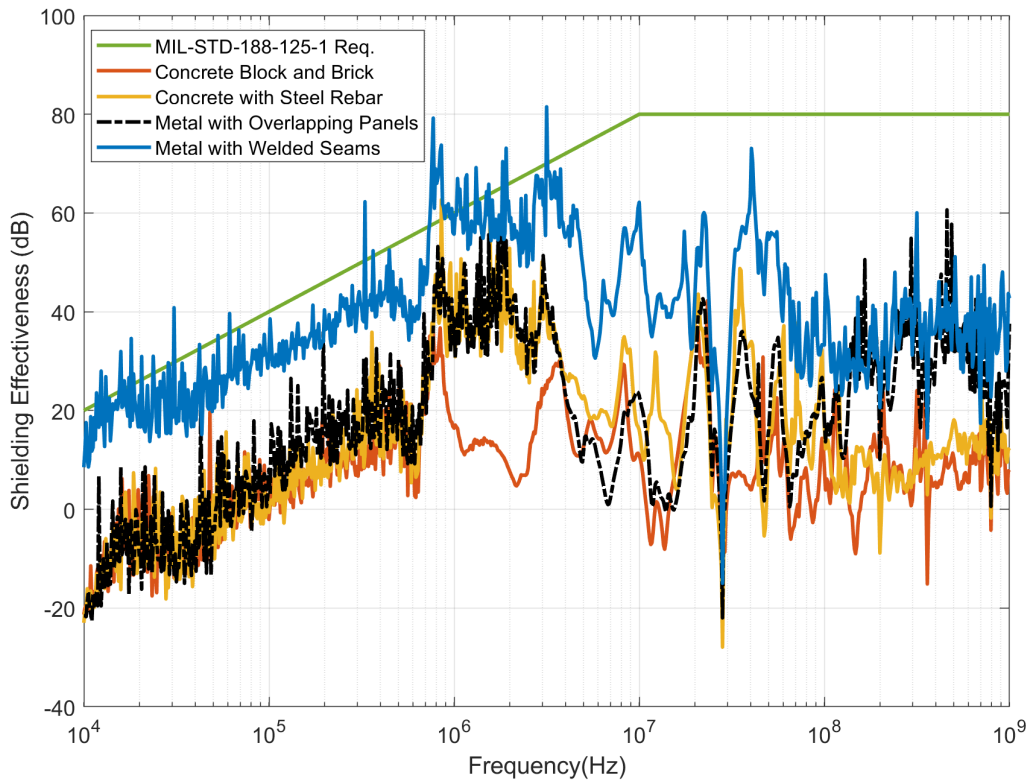


Figure 3-9
Results of shielding effectiveness tests

In order to meet the performance requirements of MIL-STD-188-125-1, the measured shielding effectiveness must be above the green line shown in Figure 3-9. As shown, none of the standard construction types achieved this across the frequency range. The best-performing construction type was the six-sided metal building, whereas the worst-performing construction type was the building constructed with concrete and brick.

As illustrated in the free field illumination testing, most DPRs that were tested were found to be resilient to direct illumination of E-fields, with many of the DPRs being able to withstand the full 50 kV/m E-field. However, some DPRs experienced disruption at levels as low as 15 kV/m, so it is important to understand what the attenuated E-field strengths could be within a given substation control house structure so that the appropriate level of shielding can be determined.

As shown in Figure 3-9, the amount of attenuation (or amplification in the case of a resonance) that a given structure type provides is dependent on frequency. Even when structures provide a modest level of attenuation, for example the six-sided metal structure, there are frequencies

where shielding is poor and other frequencies where the shielding is excellent (where it meets or exceeds MIL-STD-188-125-1). Thus, it is difficult to evaluate the effectiveness of the shielding provided by a given structure based merely on a visual inspection of Figure 3-9 or a similar chart.

A more robust way of evaluating the performance of structures such as substation control houses that are not specifically designed to provide significant levels of shielding is to estimate the E-field that could be transmitted through the structure and illuminate the equipment inside given an assumed threat environment, for example the E1 EMP waveform described in IEC 61000-2-9. This can be done by convolving the shielding effectiveness measurement data, which is essentially a magnitude-only transfer function, with an incident E-field pulse. The data processing and analysis technique described in IEC 61000-5-9 for predicting induced currents in cables was adapted to estimate the E-field that would be transmitted through a substation control house structure using the shielding effectiveness measurement data presented in Figure 3-9. An example of the simulated E-field pulse penetrating the concrete block building is shown in Figure 3-10, and the simulated field penetrating the six-sided metal building is shown in Figure 3-11. The incident E-field pulse used in these calculations was the 50 kV/m IEC 61000-2-9 waveform.

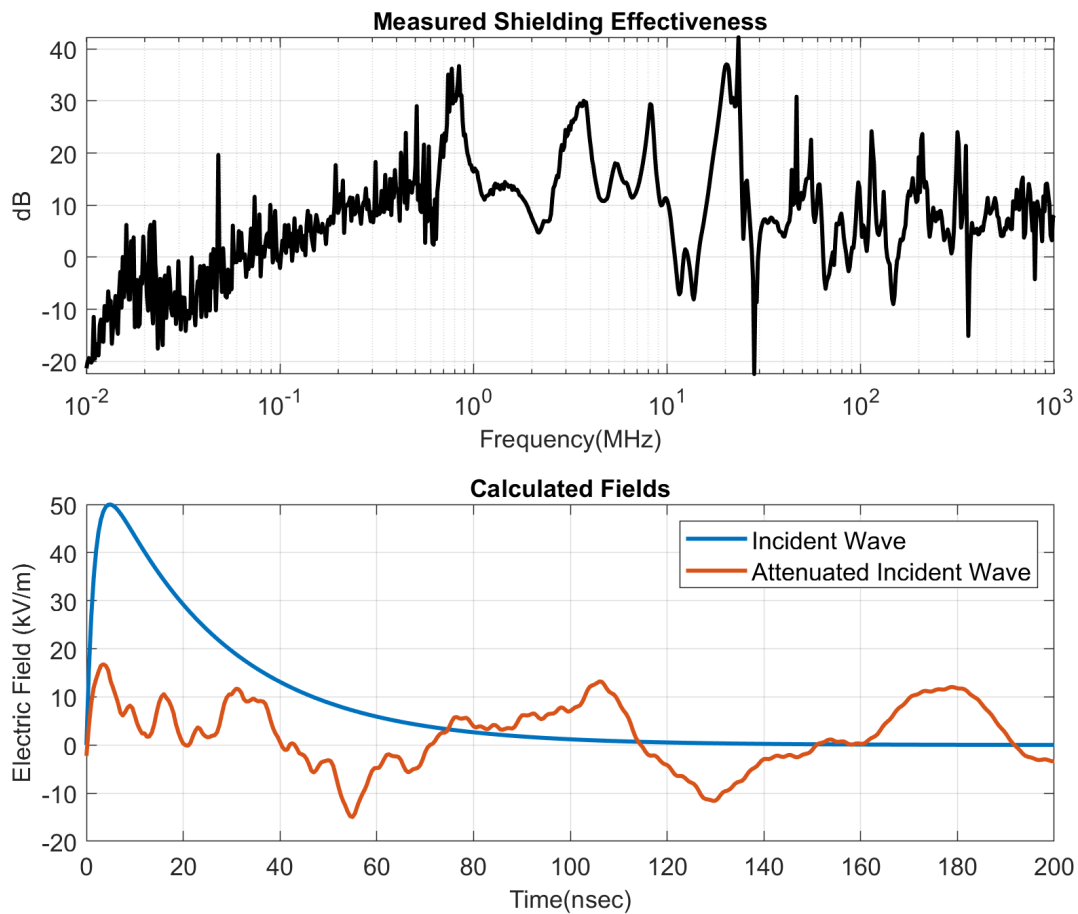


Figure 3-10
Measured shielding effectiveness and incident field calculation results for the substation control house constructed of concrete and brick (Type 1)

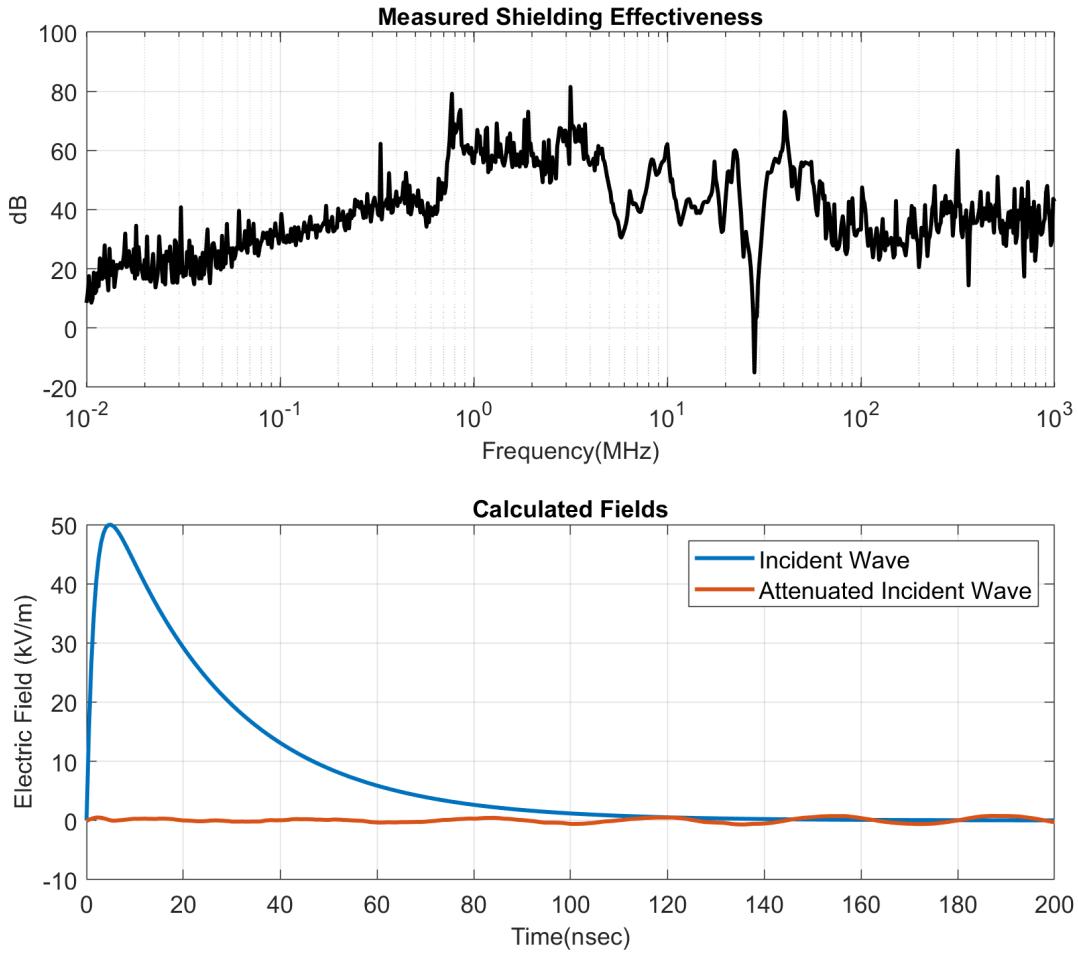


Figure 3-11
Measured shielding effectiveness and incident field calculation results for the substation control house constructed of six-side metal panels with welded seams (Type 4)

A compilation of results for the four control house types that were tested is provided in Table 3-4.

Table 3-4
Estimated levels of attenuated incident E-fields in various structures

Structure Type	Peak Incident E-field (kV/m)	Peak Attenuated Incident E-field (kV/m)	Calculated Attenuation (dB)
Type 1: Concrete Block and Brick	50	17.5	9.1
Type 2: Concrete with Steel Rebar	50	10.3	13.7
Type 3: Metal with Overlapping Panels	50	10.3	13.7
Type 4: Metal with Welded Seams	50	0.5	40

Based on the free field illumination testing of DPRs (refer to Table 3-3) the shielding provided by the concrete and brick structure was not adequate to prevent disruption of some DPRs that were tested, as the peak attenuated incident E-field exceeded the 15 kV/m level where disruption can occur. The peak attenuated incident E-fields associated with other structure types were all found to be below the 15 kV/m level. The six-sided metal control house constructed with metal panels that are welded at the seams was found to provide the best performance at the location measured (wall panel).

The results presented in Table 3-4 show a wide array of responses and appear to suggest that the control house constructed with concrete and steel rebar performs as well as the metal building with overlapping panels fastened with screws. Referring to the shielding effectiveness measurements in Figure 3-9, the two construction types provide similar shielding up to approximately 100 MHz, where they diverge, with the metal building significantly outperforming the concrete control house. However, the amplitude of the IEC E1 EMP waveform at frequencies beyond 100 MHz is very small. Thus, the resulting transmitted E-fields are similar.

Based on these findings and the results of the free field illumination testing of DPRs, it is expected that substation control houses constructed to provide 20 dB of attenuation across the 10 MHz to 1 GHz frequency band defined in MIL-STD-188-125-1 will provide adequate protection of DPRs located within the confines of the structure. For more critical applications, such as substations along cranking paths or those that serve critical loads, substation control houses may require 30 dB of attenuation across the same frequency band. Although not presented here, it is expected that all construction types would provide limited shielding near doors, cable entry, HVAC openings, or other points of entry if specific design features are not included to increase the inherent shielding of such penetrations. Thus, modifications to these points of entry may be necessary if shielding does not meet the required performance level.

A plot of the shielding effectiveness measurement of the Type 4 structure (six-sided metal enclosure with welded seams) with the two proposed shielding effectiveness levels including the 0 dB at 1 kHz coordinate is provided in Figure 3-12.

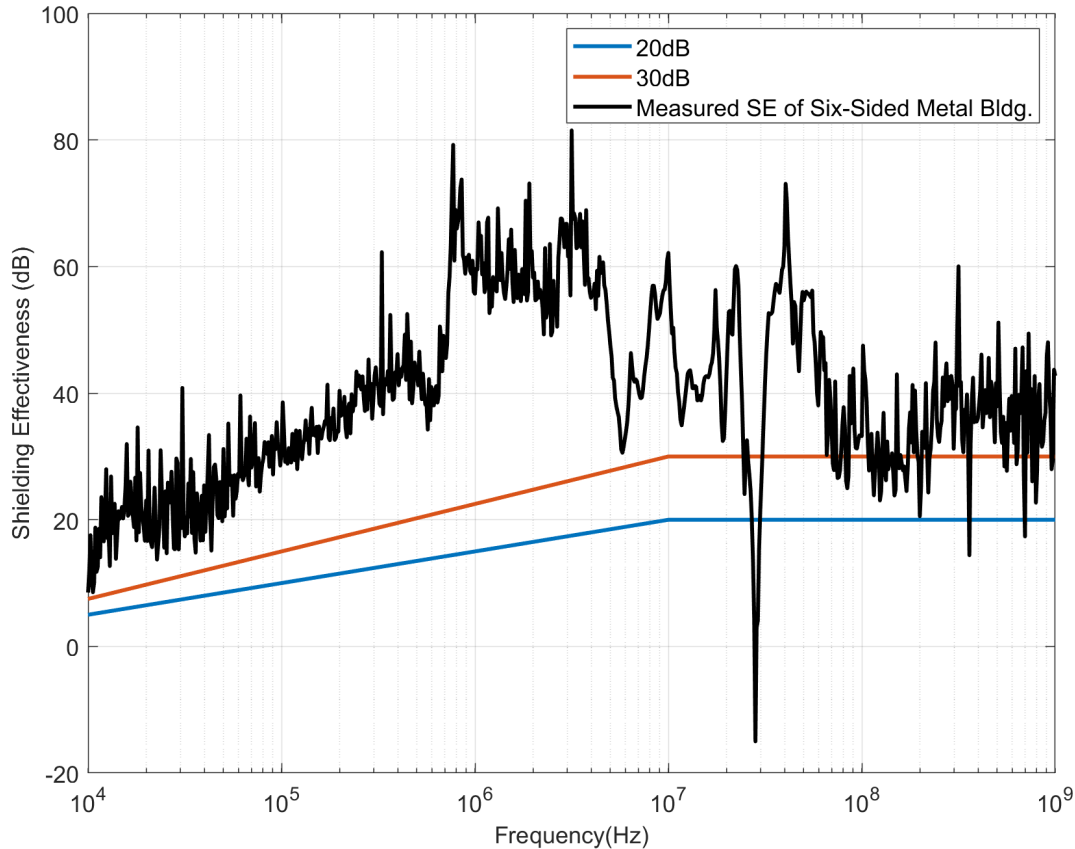


Figure 3-12
Comparison of the measured shielding effectiveness for the six-sided metal structure with proposed 20 dB and 30 dB shielding effectiveness levels

The comparison of the measured data with the proposed shielding effectiveness levels indicates that the six-sided metal enclosure is able to meet the 20 dB requirement at the measurement location (wall panel) with the exception of three frequencies, namely 28 MHz, 360 MHz, and 698 MHz. The enclosure, however, did not meet the 30 dB requirement across the full frequency spectrum. It is expected that design modifications would need to be made in order to meet the higher shielding level. Additionally, other locations within the control house would need to be evaluated to ensure adequate shielding performance is obtained at other locations within the structure, including points of entry such as doors, cable entryways, HVAC, and so on.

3.6 Direct Voltage Surge Injection Testing

Radiating threat-level E1 EMP over an area large enough to include relevant effects, for example testing an entire transmission substation, is not practical. Thus, an alternative is to inject threat-level voltage surges directly into the analog inputs or discrete inputs and outputs (I/O) of a DUT to determine the levels at which damage or disruption of the device occurs. In the assessment process, the levels at which damage or disruption is observed during testing are compared against the levels determined using modeling to determine whether the DPR is at risk.

The shape of the voltage pulse⁶ that was used in the direct injection testing that was performed during this project is defined in MIL-STD-188-125-1 [23]. The impulse waveform is defined in MIL-STD-188-125-1 as a double exponential having a nominal rise time of 10 ns and a half wave full maximum (HWFM) duration of 500 ns. The EPRI direct injection system utilizes a custom-built Marx generator to produce a voltage impulse that meets the waveform specifications of MIL-STD-188-125-1. Photographs taken at EPRI's direct injection test facility are shown in Figure 3-13.

The top panel of Figure 3-13 shows the oscilloscopes and the high-voltage cage that contains the test equipment, and the bottom panel shows an overhead view of the test bench where the Marx generator and other ancillary equipment necessary to carry out the tests are located. The voltage source shown in Figure 3-13 provided three-phase voltage (120/208 Vac) to the analog voltage inputs, and the current source provided approximately 1 A of three-phase current to the analog current inputs of a DUT to simulate nominal field measurements.

A comparison of an example measured open circuit voltage pulse (~20 kV peak) generated by the EPRI Marx generator and the analytical E1 EMP waveform defined in MIL-STD-188-125-1 is shown in Figure 3-14. The EPRI Marx generator used in this testing had a maximum open circuit peak voltage of 80 kV.

⁶ MIL-STD-188-125-1 defines a current pulse rather than a voltage pulse; however, the intent of the MIL-STD test is to test equipment protected by HEMP filters, which provide a low-impedance path to conducted surges. Accordingly, for these applications, a current pulse is appropriate. Typical utility electronic equipment items, such as DPRs, do not have filters or surge protection at the inputs of the device and some inputs present a very large impedance to an incident surge, for example the analog voltage inputs of a DPR. Therefore, a voltage pulse is more appropriate for testing susceptibility of DPRs to conducted transients.



Figure 3-13
Illustration of EPRI's direct injection test based on MIL-STD-188-125-1
Note: DUT is not shown

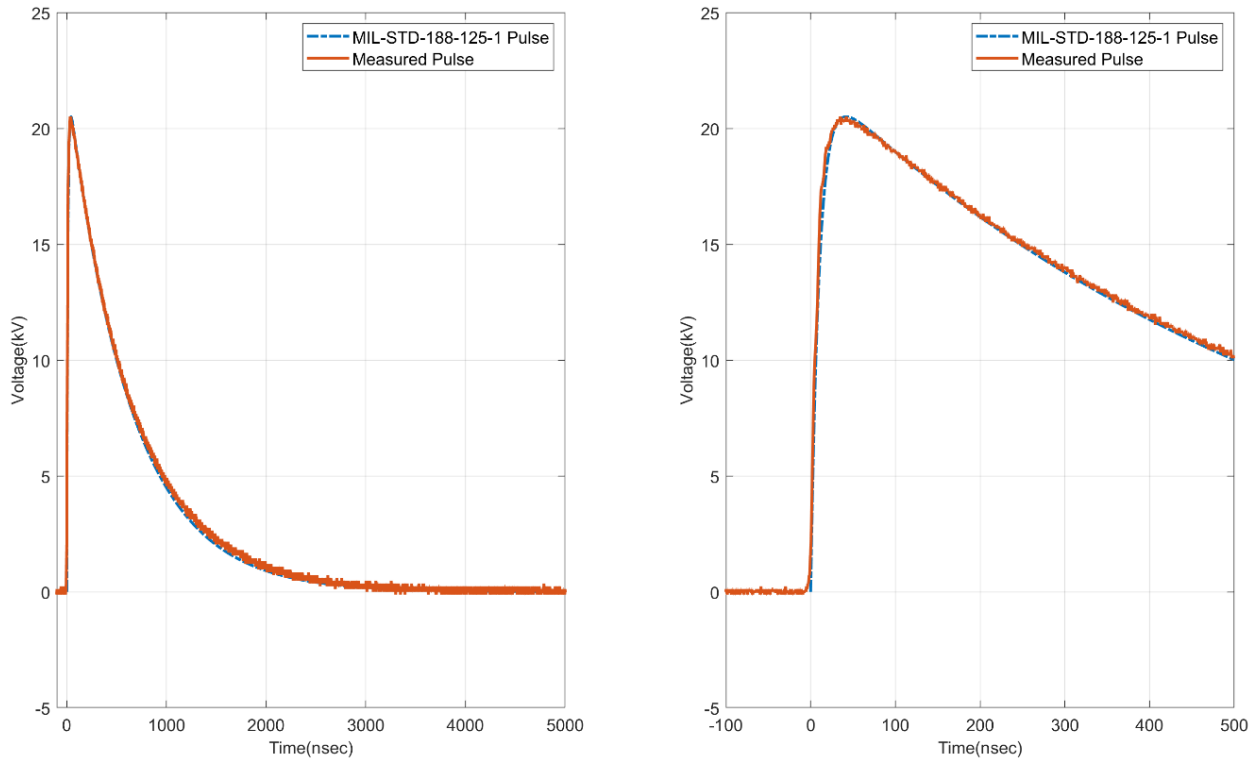


Figure 3-14
Open circuit voltage pulse generated EPRI direct injection voltage generator and the MIL-STD-188-125-1 waveform

The pulse that is generated was coupled to the DUT through large metal oxide varistors (MOVs) to prevent the fundamental frequency ac voltages and currents from being applied directly to the output of the Marx generator. An example test setup used to couple a common mode voltage surge into the voltage inputs of a DPR (the DUT) is shown in Figure 3-15.

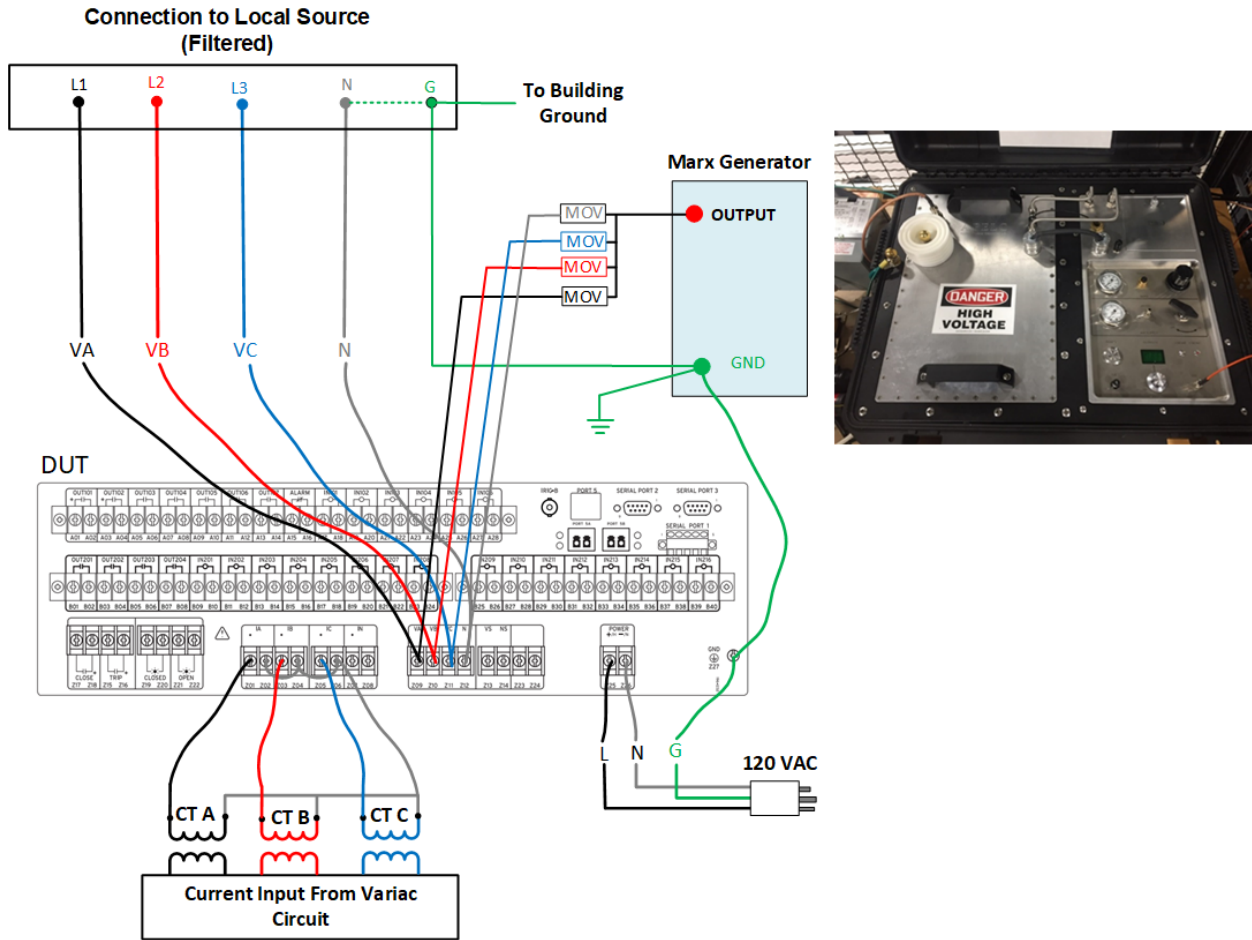


Figure 3-15
E1 EMP direct injection test setup for application of common mode surges to the voltage inputs of the DPR. (Common mode surges are applied between the L1, L2, L3, and N voltage inputs of the DPR and ground. CT A, CT B, and CT C are the inputs to the current inputs of the DPR. L, N, and G are the ac power supply voltages and grounding connections; the dashed green line indicates that the source neutral is connected to the building ground.)

Both common-mode and line-to-ground tests were performed. An example of a direct injection test setup that was used to test DPRs against line-to-ground surges is shown in Figure 3-16.

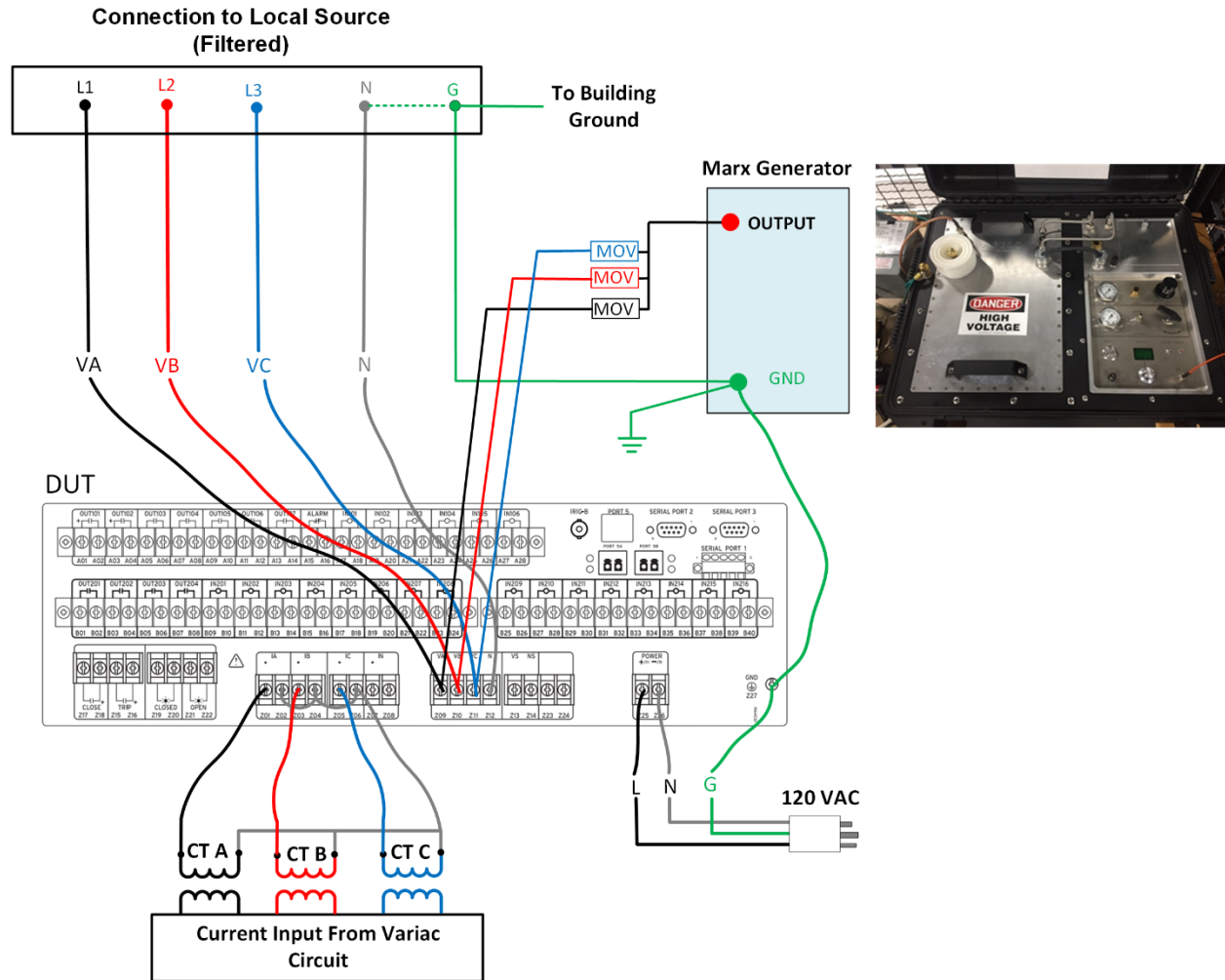


Figure 3-16
 Depiction of an example direct injection test setup used to test DPRs against line-to-ground surges. (Line-to-ground surges are applied between the L1, L2, and L3 voltage inputs of the DPR and ground. CT A, CT B, and CT C are the inputs to the current inputs of the DPR. L, N, and G are the ac power supply voltages and grounding connections; the dashed green line indicates that the source neutral is connected to the building ground.)

As shown in Figures 3-15 and 3-16, the devices were powered from 120 Vac as opposed to dc from a battery. The neutral of the local source was grounded to the building ground, which was also connected to the ground of the Marx generator and the DUT.

Although Figures 3-15 and 3-16 show testing of voltage inputs only, the current inputs, output contacts, power supply input, and digital inputs were also tested. All tests were performed with the units powered on and with nominal three-phase voltage and current applied to the analog voltage and current inputs (three-phase voltage (120/208 Vac), 1 Amp of three-phase current).

The Marx generator that was used for direct injection testing of DPRs has a maximum open circuit voltage of 80 kV. Thus, DPRs that did not exhibit Type 1, Type 2, or Type 3 responses for voltages up to 80 kV were assigned a Pass at this maximum voltage level. The ability of the DPRs tested to withstand surge voltages above 80 kV was not explored.

Results from direct injection testing of DPRs are provided in Table 3-5. Table 3-5 includes results from several different kinds of tests:

1. *Individual tests that were performed on individual DPRs all the way to failure (Type 3 response).* An example of this scenario is unit 4 (first listing of DPR 2) which shows an asterisk (*) by the relay designation (DPR 2*). In this test, the voltage inputs of the relay were tested with line-to-ground surge voltages of various levels. At 35 kV, a Type 3 response was observed, but Type 1 or Type 2 responses were not observed prior to the Type 3 response.
2. *Individual tests that were performed on individual DPRs that stopped at a Type 1 or Type 2 response.* An example of this scenario is unit 48 (DPR 15). In this test, the voltage inputs of the relay were tested with common-mode surge voltages of various levels. At 15 kV, a Type 1 response was observed, and the testing was stopped to preserve the unit for other purposes.
3. *Multiple tests of a single DPR where one or more of the tests were taken to failure (Type 3 response).* An example of this scenario is unit 1 (DPR 1). In this scenario, the voltage inputs of the relay were initially tested (Test #1) with line-to-ground surge voltages of various levels. At 70 kV, a Type 3 response was observed, but Type 1 or Type 2 responses were not observed prior to the Type 3 response. Next, based on an evaluation of the unit, it appeared that only the voltage inputs were damaged so the current inputs of the same DPR were then tested (Tests #2 and #3). Test #2 was a common-mode voltage surge test of the current inputs, and no abnormal response was observed up to 80 kV; thus, the test was given a Pass. The last test (test #3) was a line-to-ground voltage surge test of the current inputs, and a Type 3 response was observed at 80 kV. Neither Type 1 or Type 2 responses were observed prior to the Type 3 response at 80 kV.

Table 3-5
Results from direct injection testing of DPRs

Relay	Unit	Test #	Mode	Pass	Type 1	Type 2	Type 3
				Voltage Surge Level (kV)			
DPR 1	1	1	VL-G		NF	NF	70
		2	CCM	80	NF	NF	NF
		3	CL-G		NF	NF	80
DPR 1	2	1	VL-G		NF	NF	60
		2	CL-G	80	NF	NF	NF
		3	CCM	80	NF	NF	NF
DPR 1	3	1	CCM		NF	NF	25
		2	VCM		NF	NF	50
		3	VL-G		NF	NF	25
DPR 2*	4	1	VL-G		NF	NF	35
DPR 2*	5	1	Serial Port		NF	NF	25

Table 3-5 (continued)
Results from direct injection testing of DPRs

Relay	Unit	Test #	Mode	Pass	Type 1	Type 2	Type 3
				Voltage Surge Level (kV)			
DPR 2*	6	1	Serial Port		NF	NF	15
DPR 2*	7	1	CCM		NF	NF	35
DPR 2*	8	1	CCM		NF	NF	35
DPR 2*	9	1	VL-G		NF	35	40
DPR 2*	10	1	CP VL-G		NF	NF	32
DPR 2*	11	1	VL-G		NF	NF	35
DPR 2*	12	1	VCM		NF	NF	15
DPR 2*	13	1	CL-G		NF	NF	70
DPR 2*	14	1	OUTPUT		NF	NF	45
DPR 2*	15	1	CCM		NF	35	55
DPR 2*	16	1	VL-G		NF	NF	30
DPR 2*	17	1	CP		NF	60	70
DPR 2*	18	1	VCM		NF	NF	15
DPR 2*	19	1	INPUT		NF	20	NF
DPR 2*	20	1	CL-G		NF	NF	80
DPR 2*	21	1	CL-G		NF	NF	30
DPR 2*	22	1	CL-G		NF	NF	55
DPR 2*	23	1	CCM		NF	NF	45
DPR 2*	24	1	CP VCM		NF	NF	10
DPR 2*	25	1	OUTPUT		NF	NF	15
DPR 2	26	1	OUTPUT		NF	60	NF
		2	OUTPUT		NF	60	NF
		3	OUTPUT	80	NF	NF	NF
		4	OUTPUT		NF	NF	60
		5	OUTPUT		NF	NF	10
		6	OUTPUT		NF	NF	10
DPR 2	27	1	VCM		NF	14	NF
		2	CCM		NF	15	NF
		3	CL-G	80	NF	NF	NF
DPR 2	28	1	VCM		NF	NF	15
		2	CCM	80	NF	NF	NF
		3	CL-G	80	NF	NF	NF

Table 3-5 (continued)
Results from direct injection testing of DPRs

Relay	Unit	Test #	Mode	Pass	Type 1	Type 2	Type 3
				Voltage Surge Level (kV)			
DPR 2	29	1	CCM		15	----	----
		2	OUTPUT		NF	NF	10kV
		3	OUTPUT		NF	NF	5kV
DPR 3	30	1	VCM		NF	20	----
		2	CCM		NF	5	60
		3	CP		NF	NF	70
DPR 3	31	1	VL-G		NF	30	----
		2	VCM		NF	23	----
		3	CCM		NF	5	----
		4	CL-G		NF	10	----
		5	CP		NF	NF	23
DPR 3	32	1	CP VL-G		NF	NF	50
		2	CP VCM	80	NF	NF	NF
		3	VL-G		NF	NF	25
		4	CP VCM	80	NF	NF	NF
		5	CP		NF	NF	80
DPR 3	33	1	VCM		25	30	----
		2	VL-G		NF	NF	15
		3	CCM		NF	30	60
		4	CL-G		NF	50	----
		5	CP		NF	NF	15
DPR 3	34	1	CL-G		NF	20	----
DPR 3	35	1	VL-G		NF	NF	30
DPR 3	36	1	VL-G		NF	NF	30
DPR 4	37	1	VL-G		NF	NF	80
DPR 6	38	1	OUTPUT	80	NF	NF	NF
		2	VL-G		50	60	70
DPR 7	39	1	VL-G		30	NF	40
DPR 7	40	1	VL-G		NF	50	NF
		2	VCM		NF	60	NF
		3	INPUT		NF	NF	70
DPR 8	41	1	VL-G	80	NF	NF	NF
		2	VCM	80	NF	NF	NF
DPR 8	42	1	VL-G		NF	80	NF
		2	VCM		NF	70	NF

Table 3-5 (continued)
Results from direct injection testing of DPRs

Relay	Unit	Test #	Mode	Pass	Type 1	Type 2	Type 3
				Voltage Surge Level (kV)			
DPR 9	43	1	VCM		NF	NF	30
DPR 10	44	1	VL-G		NF	NF	20
DPR 10	45	1	VL-G		NF	NF	15
DPR 12	46	1	INPUT		NF	NF	30
		2	INPUT	80	NF	NF	NF
		3	INPUT		NF	NF	10
		4	INPUT		NF	NF	10
DPR 15	47	1	VCM		NF	NF	20
		2	VL-G		NF	NF	60
		3	CL-G	80	NF	NF	NF
		4	CCM	80	NF	NF	NF
DPR 15	48	1	VCM		15	----	----
DPR 17	49	1	VL-G		NF	NF	60
		2	CCM		NF	NF	15
		3	VL-G		NF	NF	60
		4	CL-G		NF	NF	15
Table Notes							
VCM		Voltage Input (Common Mode)					
VL-G		Voltage Input (Line to Ground)					
CCM		Current Input (Common Mode)					
CL-G		Current Input (Line to Ground)					
CP		Control Power 120 Vac/Vdc					
NF		No Failure - Did not respond with a failure					
INPUT		Voltage surge applied to digital input					
OUTPUT		Voltage surge applied to output contact					
*		Only one type of test conducted on the DPR					
----		Not tested					

Thresholds at which disruption or damage occurred varied widely based on relay manufacturer and model and the specific device input/output that was tested. Based on the results of DPR direct injection tests, if the peak voltage surge magnitudes can be limited to less than 5 kV, all of the inputs for all of the DPRs tested can be protected. If the voltage surge magnitude is limited to less than 10kV, all but one input of one DPR could be protected.

3.7 Direct Voltage Surge Injection Testing of Mitigation Options

As the research began to show that E1 EMP could cause damage or disruption of DPRs, mitigation devices were evaluated to determine their ability to protect DPRs from conducted threats. The mitigation devices that were tested included low-voltage SPDs, a radio frequency interference (RFI) power line filter, individual surge protection components such as transient voltage suppressing (TVS) diodes and shunt connected filters, an EMP power line filter, and an auxiliary current transformer (CT). A listing of the devices that were tested is provided in Table 3-6. As with other devices, specific manufacturer and model information is not provided in this report.

Table 3-6
Description of mitigation devices that were tested

Protection Device	Type	Description
PROT 1	Surge Protection Device	120/208V three-phase, MOV based, with neutral protection
PROT 2	Surge Protection Device	120V single-phase, TVS diode and gas tube, requires multiple devices to protect three phases and neutral
PROT 3	Surge Protection Device	480V three-phase, MOV based, no neutral protection
PROT 4	Surge Protection Device	120/208V three-phase, MOV based, no neutral protection
PROT 5	Surge Protection Device	120V single-phase, MOV based, requires multiple devices to protect three phases and neutral
PROT 6	Surge Protection Device	120V single-phase, TVS diode and gas tube, requires multiple devices to protect three phases and neutral
PROT 7	Surge Protection Device	120/208V three-phase, hybrid (TVS diode and MOV), includes neutral protection. Single device designed to have enough inputs to protect a Feeder Protection and Control DPR
PROT 8	HEMP Power Line Filter	480V single-phase, 10A
PROT 9	RFI Power Line Filter	240V single-phase, 40A
PROT 10	Surge Protection Device	120/208V three-phase, hybrid (TVS diode and MOV), no neutral protection
PROT 11	TVS Diode (Component)	240V TVS diode
PROT 12	RC Filter (series RC connected in parallel with load)	250V, R = 100 Ω , C = 0.5 μ F
PROT 13	TVS Diode (Component)	30V TVS diode (only appropriate for current inputs)
PROT 14	Auxiliary Current Transformer	5A to 5A auxiliary current transformer (only appropriate for current inputs)

When mitigation devices were initially tested their ability to respond to protect a DPR from fast front surges was not known. Thus, to minimize the number of DPRs that could potentially be damaged, preliminary tests were performed with the mitigation device protecting an auxiliary stepdown transformer taken from a DPR.⁷ The test setup and measurement locations are shown in Figure 3-17. The auxiliary stepdown transformer was loaded with a resistance of 3.75 kΩ to simulate the input impedance of the voltage input of a DPR. The mitigation device (refer to Surge Protective Device in Figure 3-17) was connected in parallel with the DUT (auxiliary stepdown transformer and load combination). The SPD and DUT were then subjected to various levels of surge voltages up to the maximum level that the Marx generator could produce (80 kV open circuit pulse), and the resulting voltage and current at various locations within the circuit were measured.

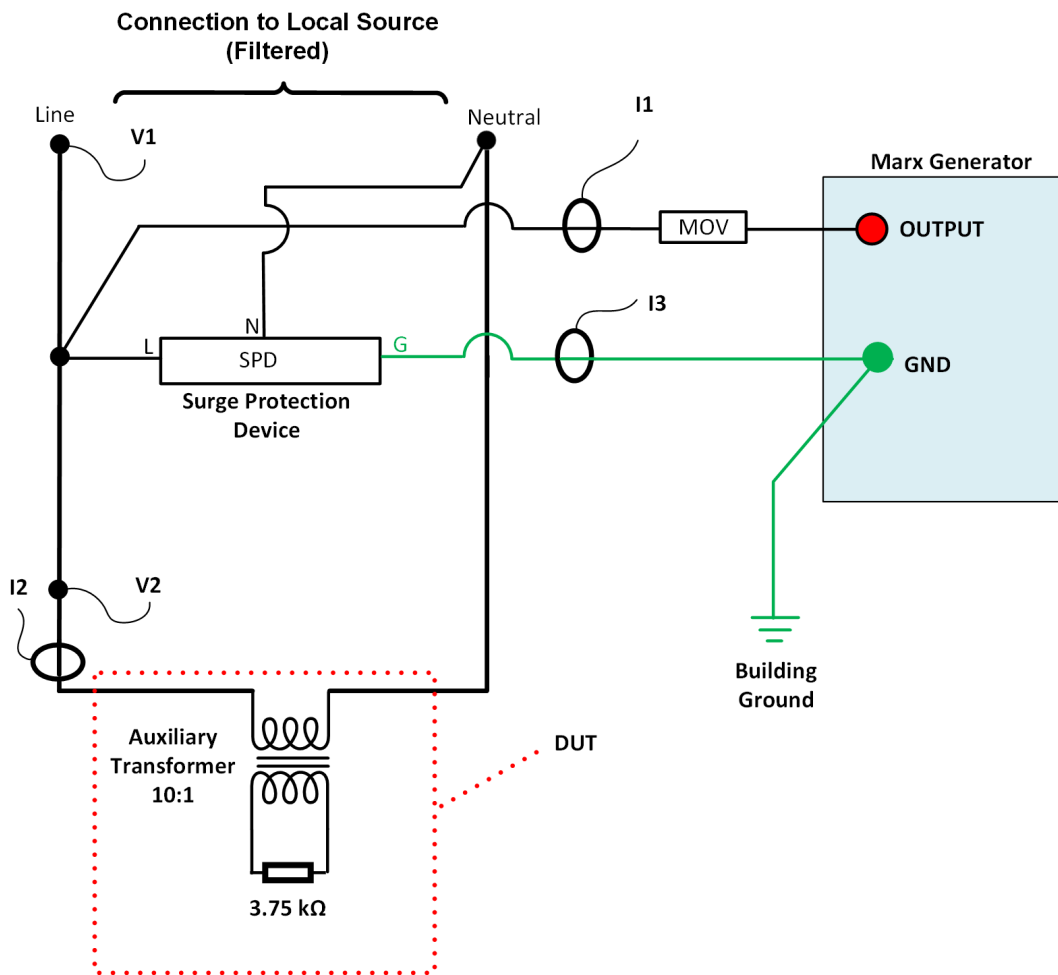


Figure 3-17
Test setup to evaluate the performance of mitigation devices

⁷ The purpose of the auxiliary step-down transformer is to reduce the nominal voltage applied to a DPR's voltage inputs to a level that can be utilized by the internal analog to digital converter inside the relay.

The voltage measurements shown in Figure 3-17 (V1 and V2) were made with respect to ground. Figure 3-18 is an example of the measured voltage and current waveforms resulting from an 80 kV (open circuit voltage) test of one of the mitigation devices (PROT 2).

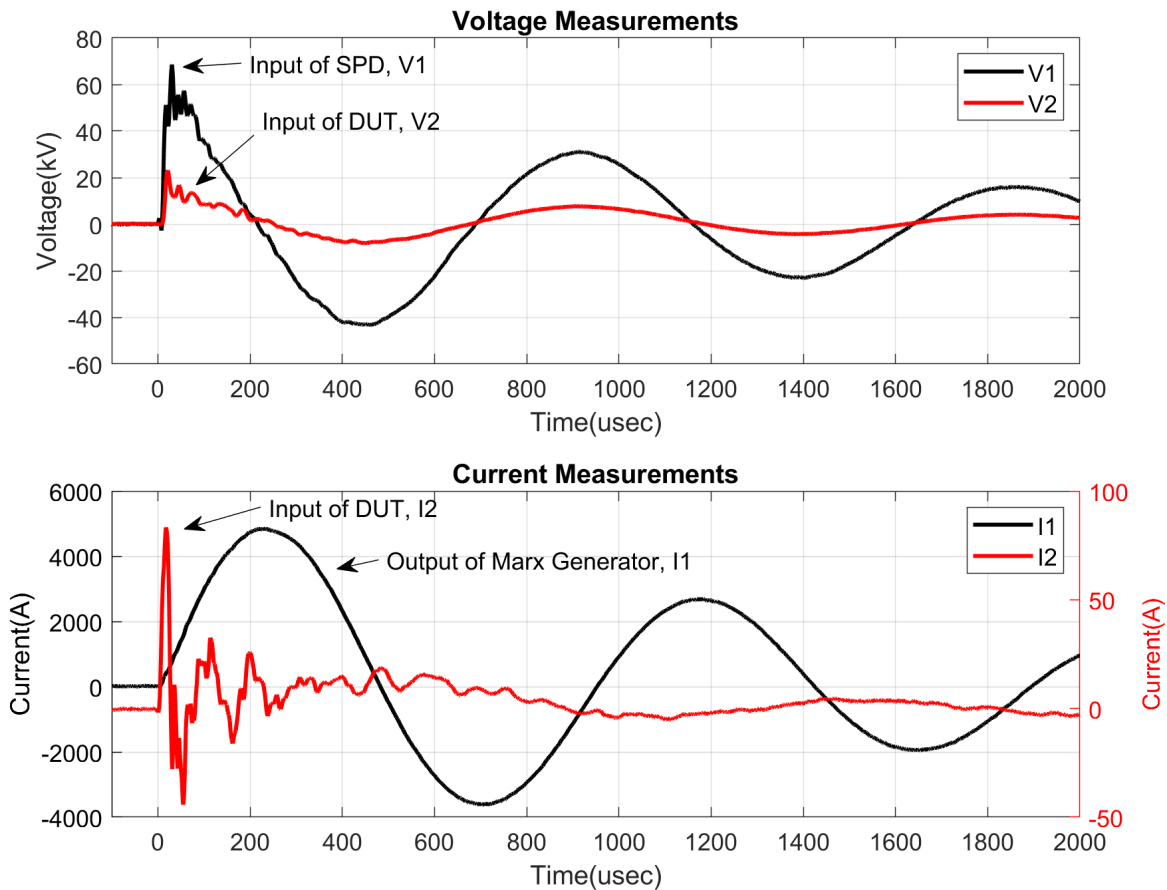


Figure 3-18
Example measurement data from a mitigation device test (PROT 2)

The top panel of Figure 3-18 shows the measured voltage across the input of the SPD (voltage to ground from the input of the SPD, V1) and the voltage at the input of the DUT (voltage to ground from the input of the auxiliary transformer, V2). The bottom panel of Figure 3-18 shows the measured current from the output of the Marx generator, I1 and the measured current into the DUT, I2 (refer to Figure 3-17). Because of the significant difference in amplitude between the two current measurements, I1 and I2, the bottom panel has dual y axes, with the right axis being associated with the current flow into the DUT. The measurements illustrated in Figure 3-18 show a significant reduction in both voltage and current (V2 and I2) into the DUT as a result of the SPD being in the circuit.

By evaluating the voltage and current at the input terminals of the auxiliary transformer (input of the DUT) it was determined whether a mitigation device was an acceptable candidate for further testing connected to a DPR. A summary of the initial test results using an open circuit voltage pulse of 80 kV to identify potential candidates for further testing is provided in Table 3-7. (Note that PROT 13 and PROT 14 were not tested in this manner since they are only appropriate for current inputs.)

Table 3-7
Results of 80 kV voltage pulse applied to various mitigation devices protecting the DUT
(auxiliary step-down transformer with attached load)

Protection Device	Device Description	80 kV Protection Device Test		
		Marx Generator Output Current, I1 (kA)	Peak Voltage across DUT, V2 (kV)	Peak Current into DUT, I2 (A)
PROT 1	MOV based	4.29	28.0	1,200
PROT 2	hybrid (TVS diode and gas tube)	4.88	23.3	85
PROT 3	MOV based	4.35	33.6	193
PROT 4	MOV based	4.10	31.6	232
PROT 5	MOV based	4.48	42.5	367
PROT 6	TVS diode based	4.75	24.1	367
PROT 7	hybrid (TVS diode and MOV)	7.38	9.5	26
PROT 8	480V single-phase, 10A EMP Filter	4.72	31.2	216
PROT 9	240V single-phase, 40A RFI Power Line Filter	4.22	3.2	40
PROT 10	hybrid (TVS diode and MOV)	4.28	37.8	396
PROT 11	TVS diode (component)	5.04	15.3	124
PROT 12	RC Filter, R = 100 Ω, C = 0.5 μF	4.10	16.0	1,520

Based on the results of line-to-ground direct injection testing of DPR voltage inputs presented in Table 3-6, disruption and/or damage of unprotected DPRs can occur at voltage surge levels as low as 15 kV. Thus, it would be preferred that the mitigation device limit the voltage applied to input of the auxiliary step-down transformer to less than 15 kV. However, as shown in the testing results provided in Table 3-7, only two devices met this criterion (PROT 7 and PROT 9), with a third (PROT 11) slightly exceeding the 15 kV threshold. To increase the number of devices to include in further testing, a second criterion (peak current < 500A) was used to select additional devices, namely PROT 2, PROT 3, PROT 4, PROT 5, PROT 7, PROT 9, and PROT 11. In some cases, where similar technologies met the second criterion, the device that performed best was selected for additional testing with a DPR connected. For example, PROT 2 was selected over PROT 10.

Table 3-8 shows the results of the additional tests that were performed with the mitigation device connected to the voltage inputs of three different DPRs (DPR 2, DPR 3, and DPR 4).

Table 3-8
Results of testing of mitigation devices connected to voltage inputs of DPRs (N/A means that no test was performed)

Protective Device	Device Description	Relay	Minimum Surge Voltage Level Where Type 3 Response Was Observed (refer to Table 3-5)	Test Mode	Pass	Type 1	Type 2	Type 3
					Voltage Surge Level (kV)			
PROT 2	hybrid (TVS diode and gas tube)	DPR 2	15	VCM		NF	NF	60
PROT 3	MOV based	DPR 4	80	VL-G	80	NF	NF	NF
PROT 5	MOV based	DPR 2	15	VCM		NF	NF	50
PROT 7	hybrid (TVS diode and MOV)	DPR 2	15	VCM	80	NF	NF	NF
PROT 9	240V single-phase, 40A RFI Power Line Filter	DPR 2	15	VCM	80	NF	NF	NF
PROT 11	TVS diode (component)	DPR 2	15	VCM	80	NF	NF	NF
PROT 11	TVS diode (component)	DPR 2	15	VCM	80	NF	NF	NF
PROT 11	TVS diode (component)	DPR 3	15	VL-G		NF	70	NF
Table Notes								
CCM	Current Common Mode							
CL-G	Current Line to Ground							
NF	Did not respond with a failure							

Additional testing of DPRs with mitigation options to include analog current inputs was also performed. Table 3-9 presents the results of these tests.

Table 3-9
Results of testing the ability of mitigation devices to protect the current inputs of relays

Protective Device	Device Description	Relay	Minimum Surge Voltage Level Where Type 3 Response Was Observed (refer to Table 3-5)	Test Mode	Pass	Type 1	Type 2	Type 3
					Voltage Surge Level (kV)			
PROT 3	MOV based	DPR 3	NA	CL-G		NF	30	NF
PROT 3	MOV based	DPR 3	60	CCM		NF	30	NF
PROT 13	TVS Diode (Component)	DPR 2	35	CCM	80	NF	NF	NF
PROT 14	Auxiliary Current Transformer	DPR 2	35	CCM		15	50	NF
PROT 14	Auxiliary Current Transformer	DPR 2	30	CL-G		NF	20	NF
Table Notes								
CCM	Current Common Mode							
CL-G	Current Line to Ground							
NF	Did not respond with a failure							
N/A	Data not available							

Based on the testing results presented in Tables 3-8 and 3-9, the following conclusions can be made regarding the mitigation devices that were tested:

- Devices that used only MOVs were not able to provide an acceptable level of protection.
- Hybrid technologies, those which use a combination of TVS diodes and MOVs or gas tubes, exhibited improved performance, with the TVS diode and MOV combination performing best.
- TVS diodes (component only) connected directly to the input terminals of a device performed well, but currently this is not a practical application in substation environments since SPDs should include mounting hardware and a means, such as a fuse, to isolate the device from the circuit should a failure of an internal surge protection component (e.g., the TVS diode) occur.
- The auxiliary current transformer that was tested was unable to protect analog current inputs of the DPR models that were tested.

3.8 Conclusions

The following conclusions may be drawn from the testing that was performed:

- Based on the free field illumination testing results, some additional shielding of DPRs is needed, but the 80 dB level specified in MIL-STD-188-125-1 is not required.
- The shielding effectiveness testing showed that a metal control house with welded seam construction may be sufficient to reduce the E-field incident on the DPR sufficiently to avoid disruption or damage.
- Direct voltage injection testing showed that many of the inputs of DPRs are susceptible to voltage surge levels that are lower than those predicted by modeling. In many cases permanent damage was observed.
- Surge protection devices were identified and tested; some were found to provide adequate protection of DPR inputs when subjected to direct injection voltage surges.
- Before applying surge protection devices to DPRs to mitigate potential E1 EMP effects further work is needed to:
 1. Improve SPD designs to perform better against fast-front surges.
 2. Develop appropriate methods for applying SPDs in the field to maintain their protective capability.
 3. Improve understanding of life expectancy and potential failure modes that could affect reliability of protection and control systems.
 4. Develop inspection and maintenance practices.

4

ASSESSMENT OF HEMP IMPACTS

Research was performed to improve understanding of the potential impacts that E1 EMP, E2 EMP, and E3 EMP individually, and E1 EMP and E3 EMP in combination, could have on the electric transmission system. The results of these extensive investigative efforts are described in this section.

4.1 Assessment of E1 EMP Impacts

An interconnection-scale E1 EMP assessment was performed to provide a first-order approximation of the potential impacts of E1 EMP on DPRs located within an electrical interconnection. The assessment was limited to DPRs performing transmission line protection functions, and sought to answer the following basic question: If a HEMP attack occurred that generated an E1 EMP environment like that of the nominal LANL environment or the scaled environment, could it cause damage to DPRs on an interconnection scale? The details of the assessment that was performed to answer this question are provided below.

4.1.1 E1 EMP Assessment Procedure

A general approach that can be used to perform an E1 EMP assessment of an individual substation is illustrated in Figure 4-1.

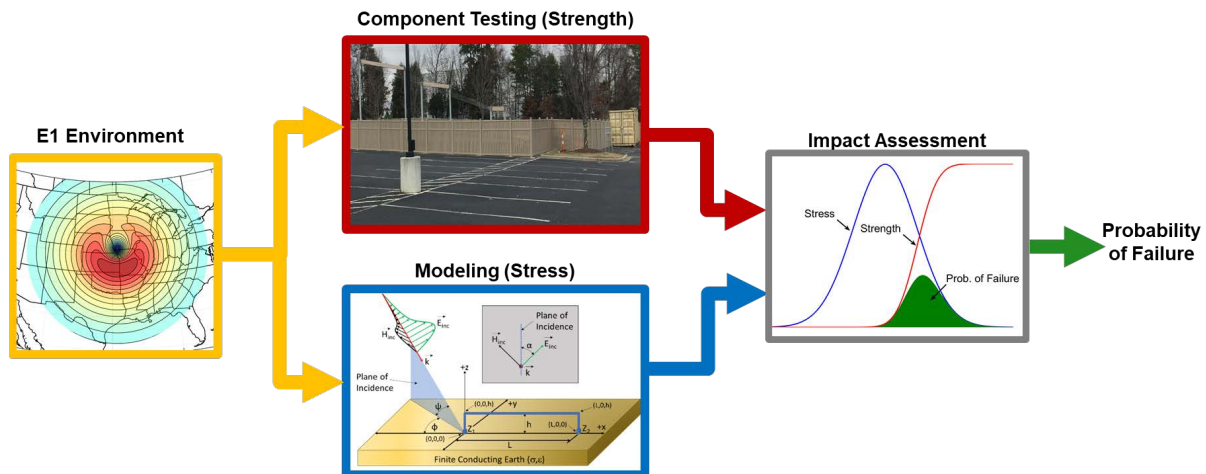


Figure 4-1
Approach for performing an E1 EMP assessment of an individual substation

Referring to Figure 4-1, the E1 EMP environment represents the bounding E1 EMP environment (spatio-temporal electric field) that substations might be exposed to during a HEMP attack (refer to Section 2). Modeling is done to estimate the E1 EMP induced voltage surge (stress) that a critical asset, for example a DPR in a substation, could be exposed to during a HEMP attack

(refer to Section 2). Laboratory testing of critical assets is performed to determine the levels of E1 EMP induced voltage surges that could cause disruption or damage of the device (refer to Section 3). Once modeling and testing data are available, an impact assessment can be carried out by comparing the expected stress with the device strength (refer to the rightmost portion of Figure 4-1).

The procedure described in Figure 4-1 is like that of an insulation coordination study that is performed to inform the design of substations or transmission lines. A probability distribution function (PDF) is created to represent the electrical stress that a critical asset might be exposed to. Next, a cumulative distribution function (CDF) is created that represents the strength of the asset to E1 EMP induced surges. A third PDF is created by convolving the strength CDF with the stress PDF. The probability of failure is then estimated by computing the area underneath the third PDF (refer to green PDF in Figure 4-1). In general, neither the stress PDF nor the strength CDF are purely Gaussian, but are shown for illustration purposes only.

There are several limitations of this approach that must be addressed when adapting it to an interconnection-scale E1 EMP assessment. First, when evaluating an individual substation, the angle that the incident E1 EMP wave makes with the conductor (refer to the angle ϕ in Figure 2-10) is known, if the ground zero location is known, so the stress can be determined with much more precision. In the case of an interconnection-scale assessment, the line angles are generally unknown and are assumed to vary randomly. This results in a range of stresses (overvoltages) that must be considered. Second, when evaluating an individual substation, the specific types and models of critical assets are known; thus, specific damage thresholds can be developed through testing and used in the assessment. In an interconnection-scale assessment, the construction details of the substation including the types and models of equipment are unknown, and thus, a distribution of damage thresholds must be used. To account for these limitations and uncertainties, the assessment approach described in Figure 4-1 was modified for the interconnection-scale study.

There were two main differences between the procedure used in the interconnection-scale study and the one illustrated in Figure 4-1. First, because the data could not be properly described by a more traditional parametric distribution such as the Gaussian distributions illustrated in Figure 4-1, the stress and strength data were both fitted with kernel PDFs [24]. Second, a deterministic approach based on a comparison of random values obtained from the two kernel PDFs was utilized, as opposed to computing the probability of failure directly as illustrated in Figure 4-1. The binary outcome of the deterministic approach was necessary for including the results in the combined E1 EMP + E3 EMP assessment and for estimating the number of line terminals with DPRs that might be at risk of potential damage. The procedural steps that were followed in the interconnection-scale assessment are described below.

4.1.1.1 Initial Step (Performed Once)

A PDF of DPR responses was created based on results of direct line-to-ground voltage surge injection tests of DPR voltage inputs. Line-to-ground voltage surge injection test results, as opposed to results from common mode testing, were used because the coupling results from the BLT equation based methods are line-to-ground values. Because Type 1 and Type 2 responses (device disruption) were rarely observed during direct injection testing of DPR voltage inputs, voltage levels that resulted in Type 3 responses (refer to Table 3-5), meaning the DPR was completely damaged, were used to create the PDF. The resulting PDF is illustrated in Figure 4-2.

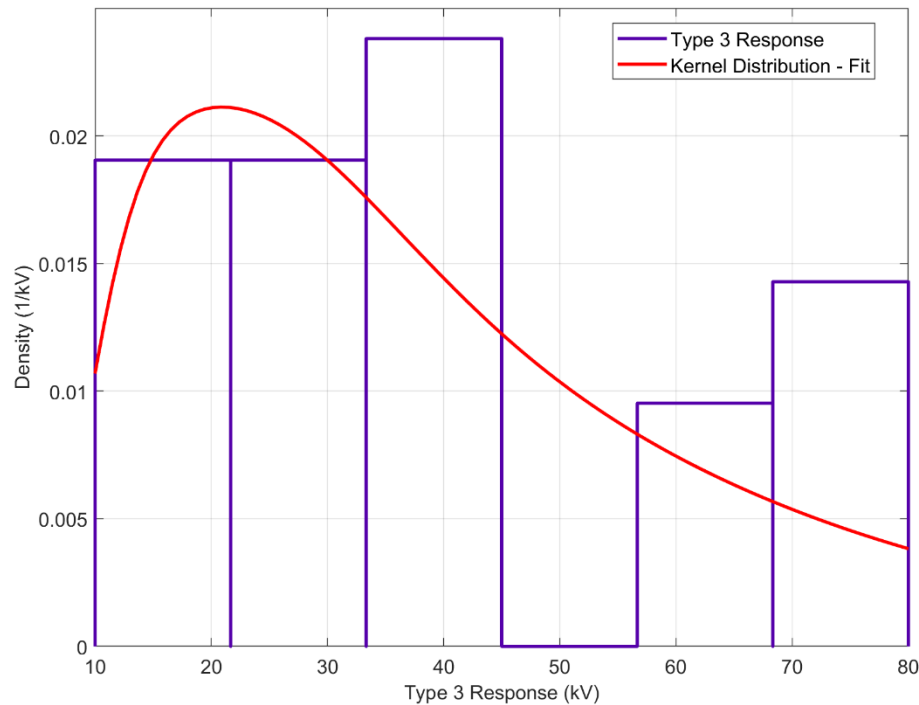


Figure 4-2
Stress PDF derived from direct injection testing of DPRs

It is worth noting that the tail of the distribution shown in Figure 4-2 extends beyond 80 kV. One relay was not disrupted or damaged at the maximum test voltage of 80 kV so the extension of the PDF tail beyond 80 kV is a reasonable approximation.

4.1.1.2 Step 1 – Coupling Calculations

Coupling calculations were performed using the BLT method [17], [21] at each geographic location for which the E1 EMP environment was provided (900 locations in total, concentrically located around the target location – refer to Section 2.2.1.5). Because the actual topology of the lines and cables at each substation location was unknown, the line angles were assumed to be uniformly distributed between -180° and $+180^\circ$ in 5° increments. Thus, 73 simulations were performed at each of the 900 locations on the ground. The peak amplitude of each of the simulations was determined, and a table of peak voltage surge amplitudes (73 total) was created for each location.

4.1.1.3 Step 2 – Creation of Stress PDF at Each Substation Location

The resulting overvoltages at the actual substation locations were determined by interpolating between a) the 900 ground-based locations where the E1 EMP environment data were provided and simulations were performed (refer to Step 1), and b) the actual geographic locations of all of the substations included in the interconnection model. These data were then used to create a table of voltage surge amplitudes that the stress PDFs for each substation were based on. Because the data could not be properly described by a more traditional parametric distribution, a kernel distribution was used instead.

The process described in Steps 1 and 2 is illustrated in Figure 4-3. For clarity, only two locations are shown as the basis of the interpolation, but the interpolation algorithm used incorporated data from multiple locations.

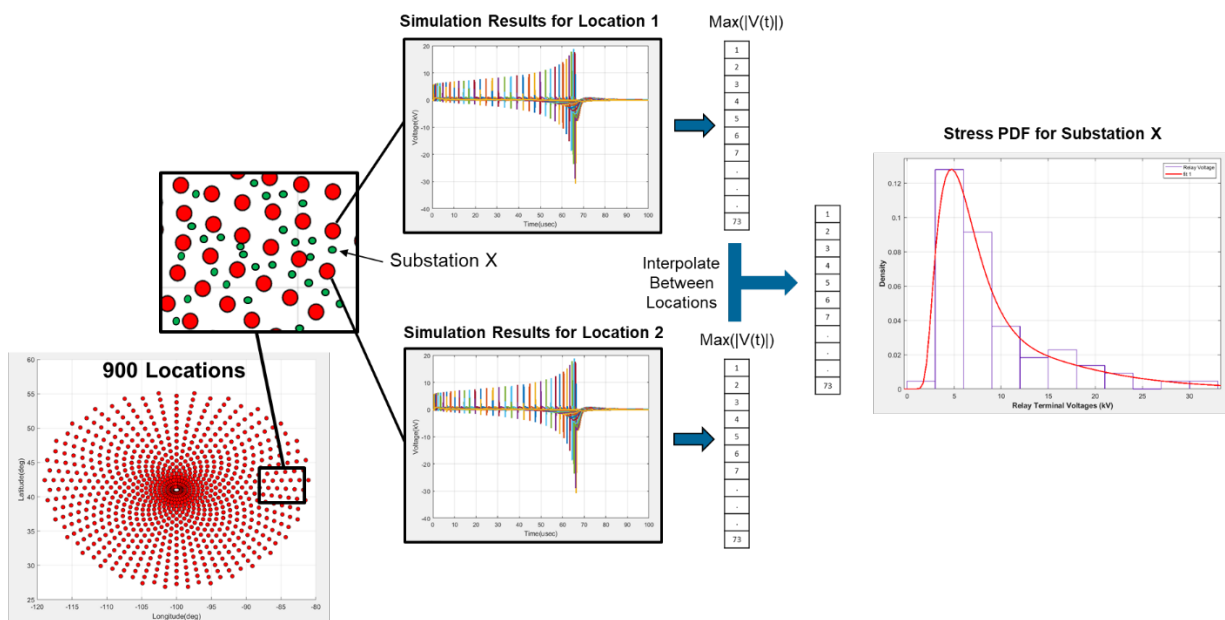


Figure 4-3
Illustration of Steps 1 and 2 of the E1 EMP assessment process

4.1.1.4 Step 3 – Determine Voltage Surge Level at DPR Terminals

Using the stress PDFs created in Step 2, the voltage surge that a DPR could be exposed to was randomly selected from the PDF. For the examples evaluating overhead lines (refer to Section 4.1.2.1, Example 1) the procedure was performed separately for each line terminal located within a given substation. For the examples evaluating cables (refer to Section 4.1.2.2, Example 2, and Section 4.1.2.3, Example 3) the voltage surge level was determined once for each substation since all cables were assumed to be in the same cable trough, and then that value was used for each line terminal in the station.

4.1.1.5 Step 4 – Determine Damage Threshold of DPR

The surge voltage level at which damage would occur to a DPR at a given substation was randomly selected at each substation location separately using the strength PDF created in the initial step. The procedure for this step is based on the assumption that all substations contain DPRs, and that all of the DPRs at a given substation are of the same manufacturer and model. Not all substations within the CONUS contain DPRs, so this assumption will tend to overpredict the level of damage.

4.1.1.6 Step 5 – Assessment

At each substation location, the voltage surge at the voltage input of the DPR was compared with the damage threshold of the DPR. If the terminal voltage of the DPR (stress) was greater than or equal to the DPR damage threshold (strength) it was assumed that a Type 3 failure occurred. For the examples evaluating overhead lines (refer to Section 4.1.2.1, Example 1) the procedure was performed separately for each line terminal located within a given substation. For the examples evaluating cables (refer to Section 4.1.2.2, Example 2, and Section 4.1.2.3, Example 3) the procedure was performed once, and then the result (damaged DPR or OK) was assumed for all other line terminals in the substation.

4.1.1.7 Procedure Summary

Steps 3 through 5 are illustrated in Figure 4-4. This process was carried out for each substation included in the interconnection-scale model. When coupling to overhead lines was evaluated, the process was followed separately for each line located in the substation. In other words, random values for both the stress and strength and the comparison of each were done for each line terminal in each substation separately. In the case of coupling to cables, it was assumed that all cables were in the same cable trough, so the initial random selection of the stress and strength was assumed to be the same for all lines in the substation.

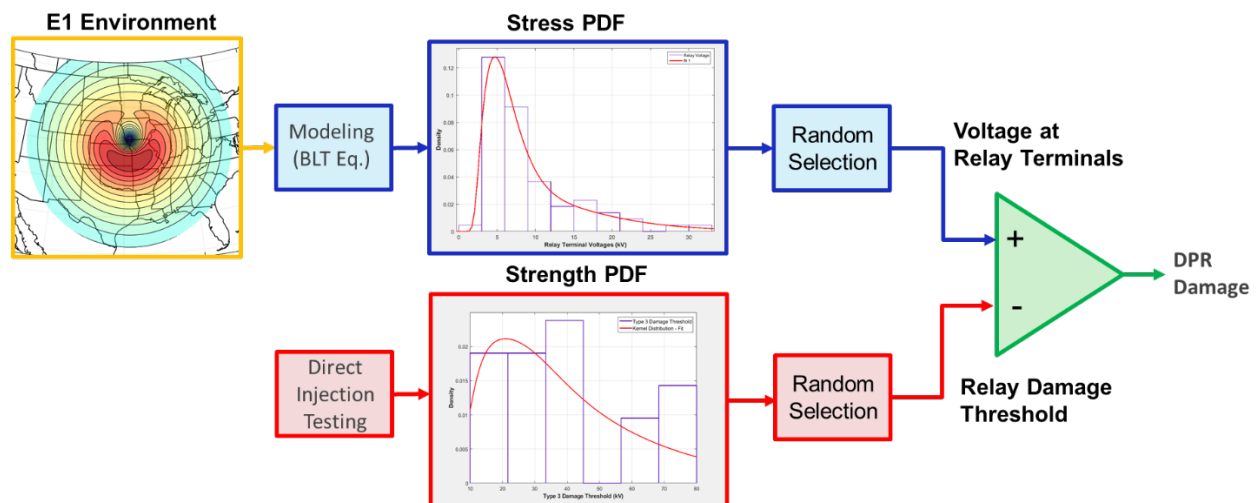


Figure 4-4
Procedure for determining impacts to substations included in the interconnection model

Random selections of both voltage surge levels (stress) and DPR damage thresholds (strength) were required for this assessment because the data necessary to perform a more specific evaluation, for example overhead line and cable topologies and DPR specifics for each substation, were not available. This results in a first-order approximation of potential impacts. Additional modeling fidelity could be achieved by using actual circuit topologies, but such an extensive evaluation was beyond scope.

4.1.2 Example Cases

To evaluate the potential impacts of E1 EMP on line protection DPRs in the interconnection-scale model, a single target location in the Eastern Interconnection (EI) and a single target location in the Western Interconnection (WECC) were evaluated. Both the EI and WECC target locations were notional and no sensitive information was used in determining these locations.

For each target location, three example scenarios were evaluated. In each of the three examples, it was assumed that all substations in the interconnection were of the same construction. In each example that follows it was assumed that the substation control house provided at least 30 dB of attenuation across the full spectrum of frequencies, so potential effects of radiated E1 EMP on DPRs were ignored (it is important to note that this was an assumption to simplify the assessment so that conducted effects could be isolated, and it is not expected that all substation control houses currently provide 30 dB of attenuation across the full spectrum of frequencies). Earth conductivity was assumed to be uniform across the interconnection. Conductivity values of 0.002 S/m and 0.004 S/m were assumed for the EI and WECC cases, respectively. Earth conductivities of 0.01 S/m and 0.001 S/m were also evaluated to provide bounding conditions.

The assessments were based on two bounding E1 EMP environments. The first environment was the nominal LANL E1 EMP environment with peak incident field of approximately 25 kV/m (refer to Section 2). The second E1 EMP environment was a scaled version of the nominal LANL environment where the nominal E1 EMP environment was scaled by a factor of 2 such that the maximum peak incident field at the worst-case location on the ground corresponded to the 50 kV/m level specified in IEC 61000-2-9 [1]. All other parameters, such as waveform, angle of incidence, polarization, and so on, were consistent in both environments.

4.1.2.1 Example 1

The first example was designed to determine the potential for E1 EMP induced surges on overhead lines to damage DPRs if shielded signal/control cables or devices using IEC 61850 (fiber optics) were utilized. In this example, an overhead transmission line with height of 22.9 m (~75 ft) and length of 5 km was terminated into a CCVT with either shielded signal cable or IEC 61850 equipment connected to the secondary. Coupling to low-voltage signal cables was ignored. The source end of the overhead line was terminated into its surge impedance to eliminate unwanted reflections, and the load end of the overhead line was terminated into the parallel combination of the surge impedance of the overhead line (or substation bus) and the input impedance of the CCVT. This example is illustrated in Figure 4-5.

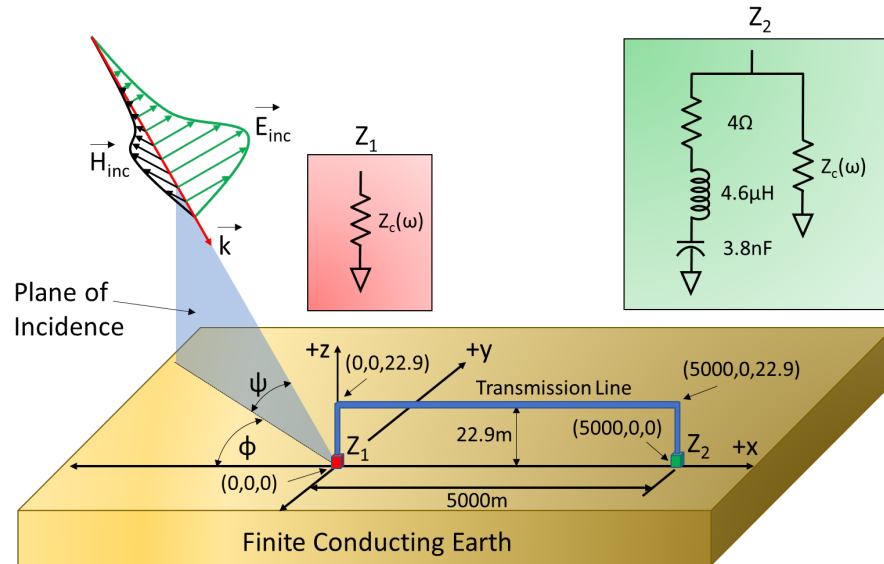


Figure 4-5
Coupling model for Example 1

The resulting voltage at the input of the DPR was determined as follows. First, the voltage at the input of the CCVT (voltage across Z_2 in Figure 4-5) was determined and convolved with the frequency response of the CCVT to obtain the value at the output of the CCVT. The CCVT response was described by a constant gain of 0.15 and zero phase (refer to Appendix B); thus, the time-domain signal at the CCVT input was merely multiplied by 0.15 and the resulting signal was assumed to propagate to the DPR terminals. Testing of a CCVT and signal cable indicated that this is a conservative approach [24].

4.1.2.2 Example 2

The second example was designed to determine the potential for E1 EMP induced surges on unshielded signal cables alone to damage DPRs. To evaluate this potential damage mechanism, the incident E1 EMP pulse was coupled to a 100 m long unshielded signal cable lying on top of the ground (height = 4 mm). The source end of the signal cable was connected to the secondary (low-voltage) terminals of a CCVT, and the load end of the signal cable was assumed to be terminated into the voltage input of a DPR. No coupling effects from the overhead line or high-voltage substation bus were included. This example is illustrated in Figure 4-6.

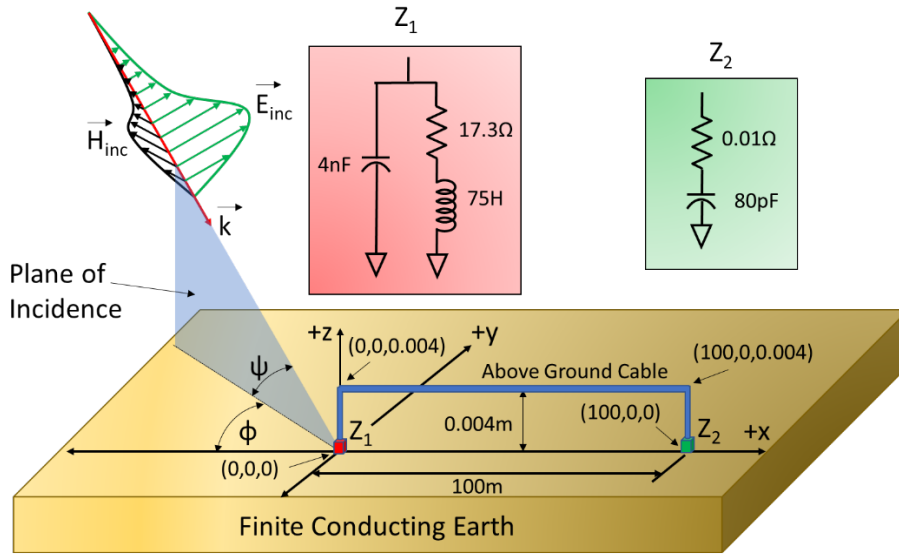


Figure 4-6
Coupling model for Example 2

4.1.2.3 Example 3

The last example was designed to assess the mitigating effect of burying signal cables below grade. Example 3 was the same as Example 2 except the unshielded signal cable was assumed buried 0.5 m below grade. This example is illustrated in Figure 4-7.

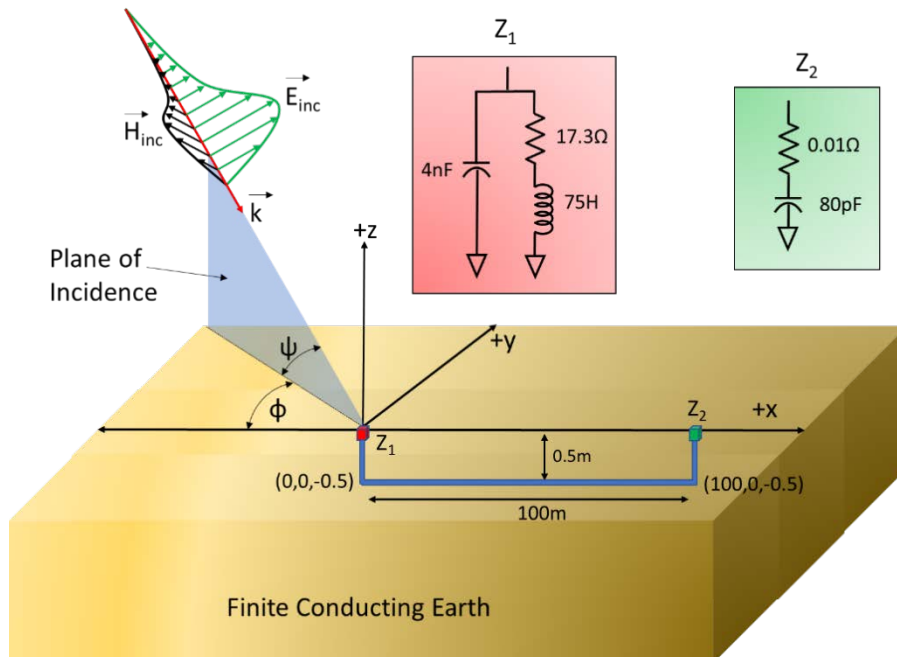


Figure 4-7
Coupling model for Example 3

4.1.3 Summary of E1 EMP Assessment Results

Following the procedure described previously, a first order approximation of the number and geographic locations of the line terminals with DPRs that could potentially be damaged by E1 EMP were assessed. The percentage of line terminals with damaged DPRs for each of the three example cases and bounding earth conductivity values are summarized in Table 4-1.

**Table 4-1
Summary of E1 EMP impacts**

Target Location in Eastern Interconnection							
	Earth Conductivity (S/m)	Example 1 OH Line		Example 2 Unshielded Cable on Ground		Example 3 Buried Cable	
		25 kV/m	50 kV/m	25 kV/m	50 kV/m	25 kV/m	50 kV/m
Percentage of Line Terminals in Eastern Interconnection with Damaged DPRs	0.002	1.3%	4.6%	5.3%	15.5%	0.2%	3.0%
	0.001	1.3%	4.7%	8.8%	19.4%	0.7%	5.3%
	0.01	1.3%	4.6%	1.0%	6.5%	0.0%	0.1%
Target Location in Western Interconnection							
	Earth Conductivity (S/m)	Example 1 OH Line		Example 2 Unshielded Cable on Ground		Example 3 Buried Cable	
		25 kV/m	50 kV/m	25 kV/m	50 kV/m	25 kV/m	50 kV/m
Percentage of Line Terminals in Western Interconnection with Damaged DPRs	0.004	1.4%	5.9%	3.3%	13.6%	0.0%	0.9%
	0.001	1.4%	5.8%	9.4%	20.9%	0.6%	5.7%
	0.01	1.3%	5.5%	2.3%	9.2%	0.0%	0.0%

The results shown in Table 4-1 provide several key insights:

- Effects from bounding E1 EMP environments with characteristics like those presented in this report can potentially disrupt or damage DPRs over a considerable portion of an electrical interconnection. The scaled environment (peak field of 50 kV/m) resulted in a non-linear increase in the number of DPRs that might experience damage from the nominal environment (25 kV/m).
- Example 1 demonstrated that DPRs could be at risk of potential disruption or damage if shielded cables are used exclusively as a mitigation measure.

- Comparing the results from Example 2 with the results from Example 3 illustrates the shielding effect that a conductive earth provides. Impacts to DPRs connected to buried cables were found to be considerably less than impacts to a signal cable lying on the ground (ignoring overhead line coupling). When the earth conductivity was assumed to be 0.01 S/m, impacts in the buried cable scenarios were negligible. Earth conductivity effects were negligible for the overhead line cases (Example 1).
- The spatial voltage profiles (not shown) for the Eastern Interconnection case and the Western Interconnection case were similar, but more DPRs were damaged in the Eastern Interconnection case due to the larger number and density of substations and line terminals. Differences in simulation results using base conductivity levels of 0.002 S/m for the Eastern Interconnection and 0.004 S/m for the Western Interconnection were also evident, but not pronounced. In general, the 0.004 S/m conductivity value yields less severe results as compared with 0.002 S/m.
- In the case of interconnection-scale assessments, specific parameters and data that are important from both a modeling and an assessment perspective are typically unknown and must be assumed or varied. As such, there is considerable uncertainty involved in the analysis; thus, results from interconnection-scale assessments should always be viewed with these limitations in mind. Bounding scenarios using bounding earth conductivity values were also evaluated to provide additional context. Additional modeling fidelity with less uncertainty could be obtained by using actual design data and circuit topologies.

4.2 Assessment of E2 EMP Impacts

An assessment of the potential impacts that E2 EMP could have on substations was performed. The assessment evaluated the potential overvoltages that might occur at a substation entrance if the line were exposed to the maximum threat level of 100 V/m defined in IEC 61000-2-9 [1]. The results were then compared with standard basic impulse levels (BILs) of equipment and an assumed E2 EMP withstand level for DPRs.

Because a spatio-temporal E2 EMP environment was not available, the effects could not be combined with E1 EMP, nor could interconnection-scale effects be evaluated. Thus, only simple scenarios based on the example illustrated in Figure 4-8 were evaluated. In one scenario, the incident wave was assumed to be vertically polarized and the conductor was assumed to be 100 km long and 22.9 m (75 feet) above the ground. In the second scenario, the incident wave was assumed to be vertically polarized and the length of the conductor was assumed to be 5 km, which is more appropriate for distribution systems. In the third scenario, the incident wave was assumed to be horizontally polarized and the conductor was assumed to be 100 km long. All other parameters were consistent among the three scenarios. In order to produce worst-case results, the earth conductivity was selected to be 0.001 S/m. The substation entrance was modeled as a capacitance of 0.5 nF to ground. The sending end of the line was modeled as the line's surge impedance to eliminate unwanted reflections.

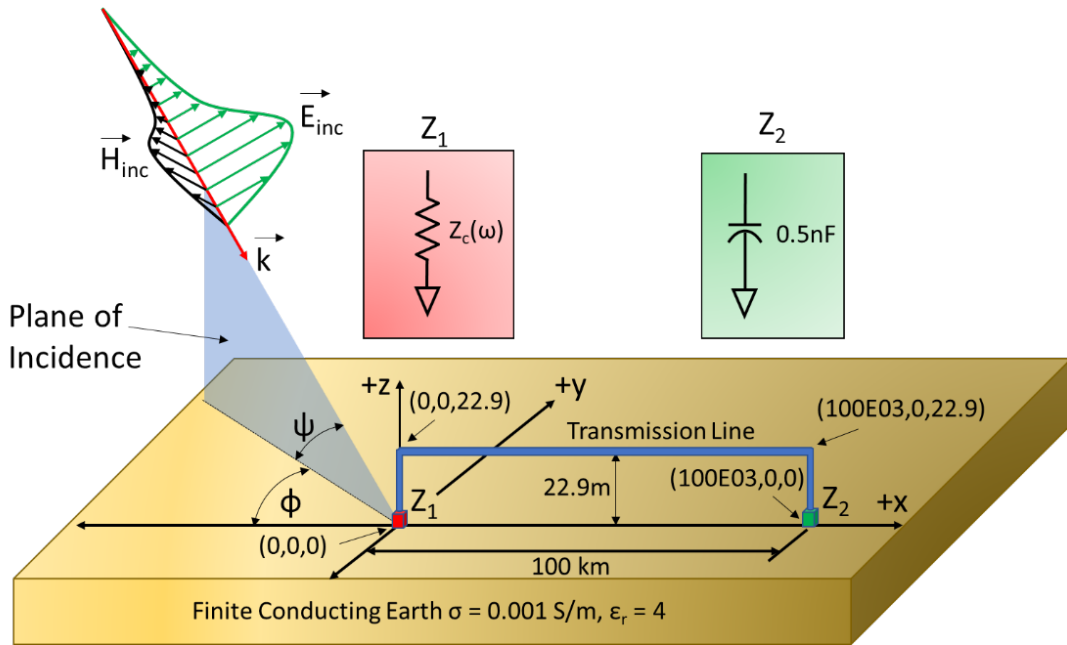


Figure 4-8
Example configuration used in E2 EMP assessment

The incident wave, E_{inc} , illustrated in Figure 4-8 was represented by the E2 EMP pulse defined in IEC 61000-2-9. The maximum field level of 100 V/m was assumed. The resulting E2 EMP waveform is illustrated in Figure 4-9.

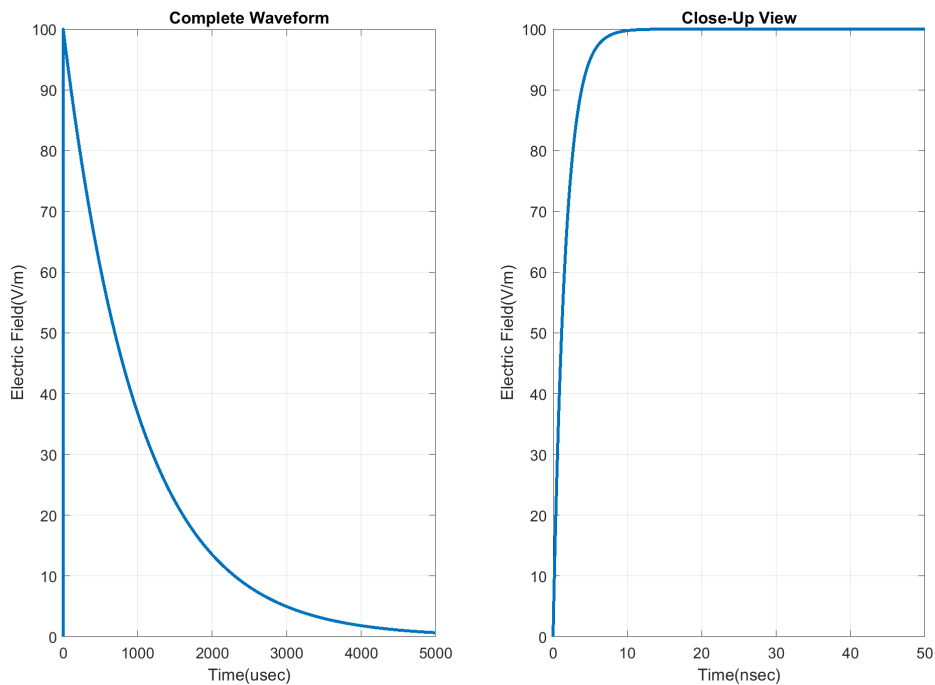


Figure 4-9
E2 EMP waveform defined in IEC 61000-2-9

The analysis was performed by coupling the incident wave shown in Figure 4-9 to the system shown in Figure 4-8 using the BLT equation based approach [17]. To find the worst-case overvoltage that could potentially occur, simulations were performed by varying the line angle, the polarization angle, and the angle of incidence. The line angles were varied between 0° and 180° in 10° increments, and the angle of incidence was varied between 1° and 90° in 1° increments. In total, 1,710 simulations were performed for each scenario. For each simulation, the resulting waveform was analyzed to obtain the maximum peak voltage. A plot of the peak voltages associated with the vertically polarized case with line length of 100 km is illustrated in Figure 4-10.

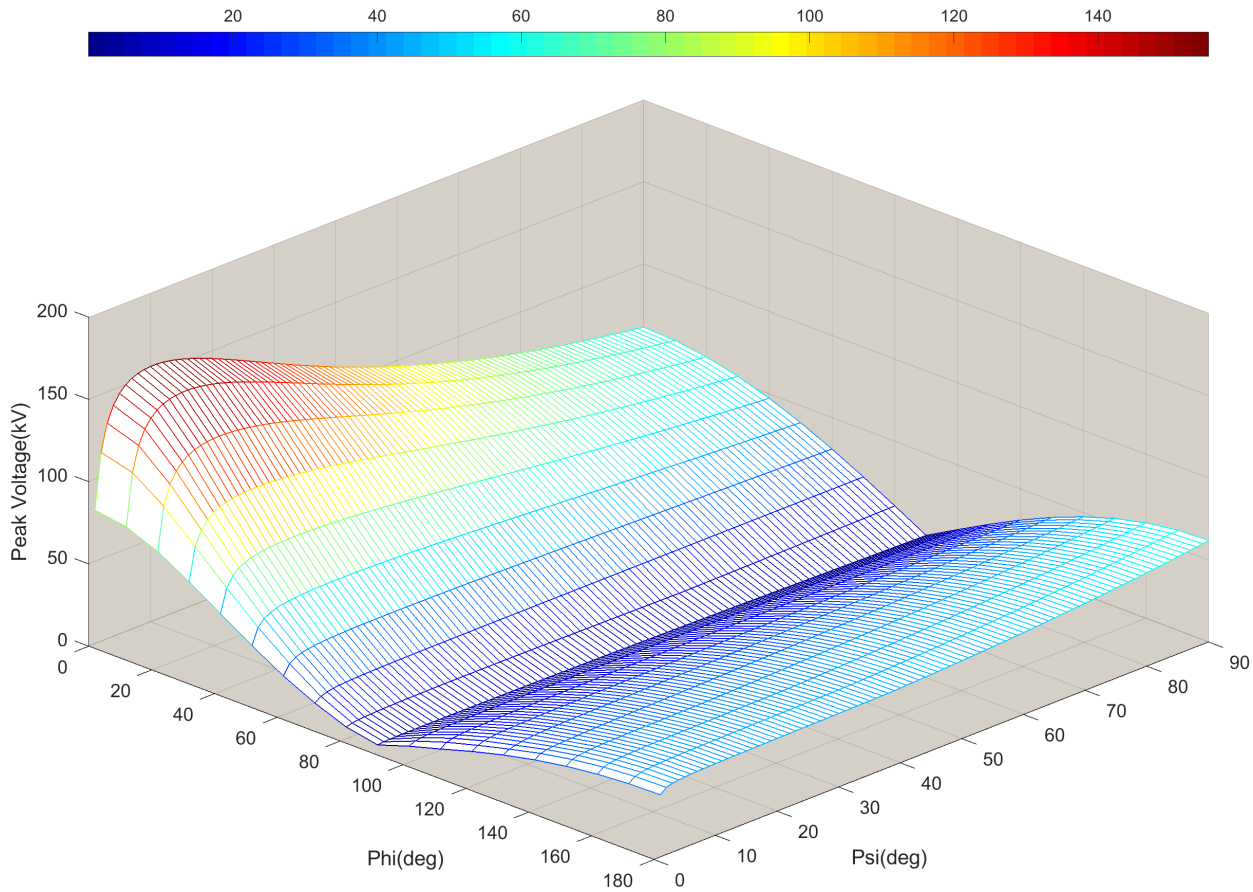


Figure 4-10
Results from E2 EMP coupling calculations for vertically polarized wave ($\alpha = 0^\circ$) and line length of 100 km; refer to Figure 4-8 for the definitions of Phi (ϕ) and Psi (ψ)

As with coupling of E1 EMP fields, the line angle and incidence angle are important parameters. For this example, the worst-case voltage of approximately 155 kV occurred with an incidence angle of approximately 10 degrees. The maximum peak voltage associated with the 5 km case with vertically polarized incident wave was found to be approximately 45 kV.

The results of the 100 km line illuminated by a horizontal polarized incident E2 EMP wave are provided in Figure 4-11.

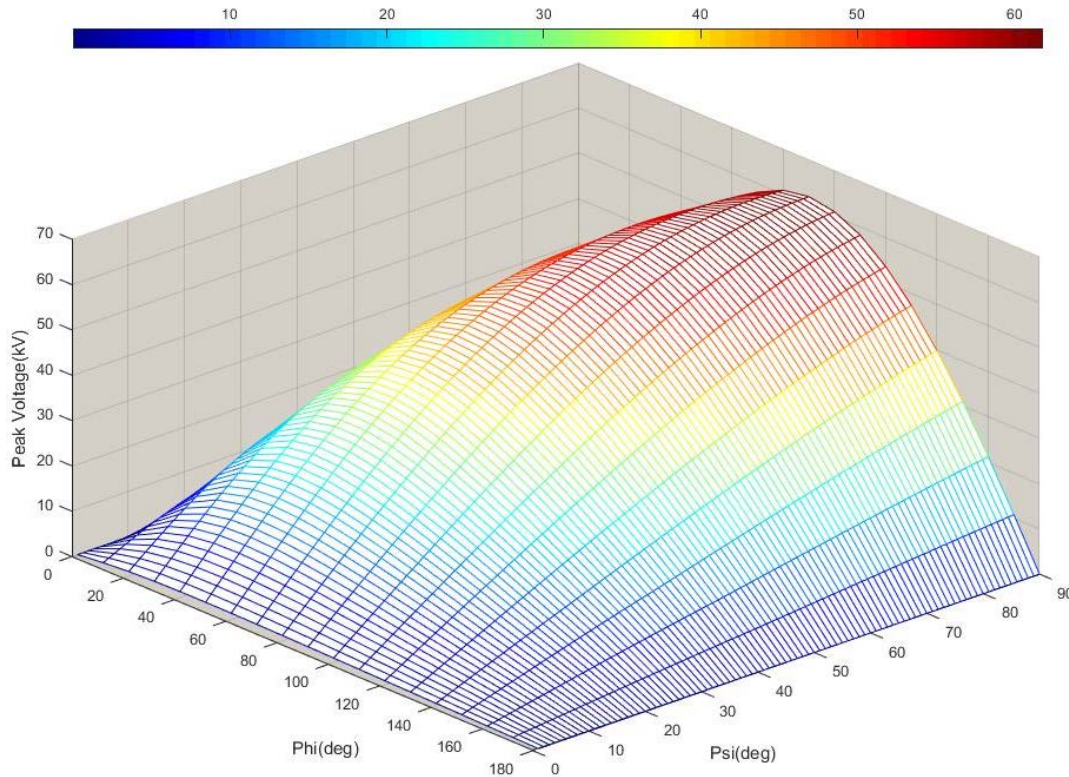


Figure 4-11
Results from E2 EMP coupling calculations for horizontally polarized wave ($\alpha = 90^\circ$) and line length of 100 km; refer to Figure 4-8 for the definitions of Phi (ϕ) and Psi (ψ)

The peak voltage associated with the horizontally polarized case was found to be approximately 62 kV and occurred when the line angle and angle of incidence were both 90 degrees.

A conservative approach is to compare the maximum peak voltage obtained from the simulations with the lowest expected BIL in a substation. The standard BIL provided in IEEE Std. 1313.1-1996 for 46 kV systems is 250 kV. Comparing the maximum peak overvoltage, ~155 kV, with the 250 kV BIL suggests that E2 EMP is not expected to impact systems rated 46 kV and above. The shorter line length, 5 km, is more appropriate for distribution lines. The minimum standard BIL provided in IEEE Std. 1313.1-1996 for 15 kV systems is 95 kV. Comparing the peak overvoltage for this scenario, ~45 kV, with the minimum BIL of 95 kV suggests that E2 EMP does not pose a threat to medium-voltage systems either.

Overtages generated by E2 EMP that are incident on the substation entrance were found to be well below those that can be generated by lightning events, where they can approach and/or exceed the BIL of equipment. It is expected that some amount of E2 EMP generated surge will propagate from the high-voltage terminals of an instrument transformer, for example a PT or CCVT, to the low-voltage terminals and then propagate along the signal cable to the DPR. DPRs are exposed to these threats on a continual basis, and thus it is expected that a majority, if not all, DPRs that are tested per the surge levels defined in IEC 61000-4-5 would be resilient to worst-case levels of E2 EMP induced stress.

4.3 Assessment of E3 EMP Impacts

4.3.1 ORNL Environment

Initial studies by EPRI [5], [6] assessed the potential for E3 EMP alone to cause widespread voltage collapse and/or damage to large power transformers. Eleven different notional target locations across the CONUS were evaluated. The results of these initial studies, based on the ORNL E3 EMP environment, concluded that E3 EMP alone could result in regional voltage collapse. Although it is difficult to precisely determine the geographic area that could be impacted by voltage collapse, it was estimated that the impacts could be on the order of several states or larger, but smaller than either the Eastern or Western Interconnections. None of the scenarios that were evaluated resulted in a nationwide grid collapse. The initial transformer thermal assessment found that only a small number (3 to 14, depending on the target location evaluated) of these transformers were found to be at potential risk of thermal damage. In addition, the at-risk transformers were found to be geographically dispersed. The results of these initial EPRI studies are in agreement with earlier work by ORNL, which indicated that voltage collapse was possible, but the failure of hundreds of large power transformers from E3 EMP is unlikely [9].

4.3.2 LANL Environment

As described in Section 2, the ORNL environment has several known limitations, so the availability of the LANL E3 EMP environment provided an opportunity to evaluate the potential impacts of E3 EMP using a much higher fidelity environment. Thus, the same voltage stability and transformer thermal assessments that were performed previously were carried out again using the LANL E3 EMP environment (refer to Section 2.3.2) to gain a better understanding of the potential impacts that the late-time HEMP field could have on bulk power systems.

The transformer thermal assessment was performed using the same 11 notional target locations that were evaluated in the previous initial study. However, due to time constraints, only a single target location in the Eastern Interconnection and a single target location in the Western Interconnection were evaluated in the voltage stability assessment. However, the two target locations that were selected were chosen to provide a meaningful test, as they were identified in the previous study [5] as target locations that were not likely to cause voltage stability impacts. Therefore, experiencing voltage collapse in the updated study would be an indicator that the LANL E3 EMP environment was more severe than the previous ORNL E3 EMP environment.

4.3.2.1 Transformer Thermal Assessment

Using the higher-fidelity LANL E3 EMP environment, a transformer thermal assessment was performed to determine the potential for the resulting GIC flows generated by E3 EMP to cause immediate thermal damage to a significant number of large power transformers such that recovery efforts could be severely impacted by the resulting damage. The assessment was carried out for each of the 11 notional target locations separately (assuming a single nuclear weapon detonation). The assessment procedure that was followed is illustrated in Figure 4-12 and described below.

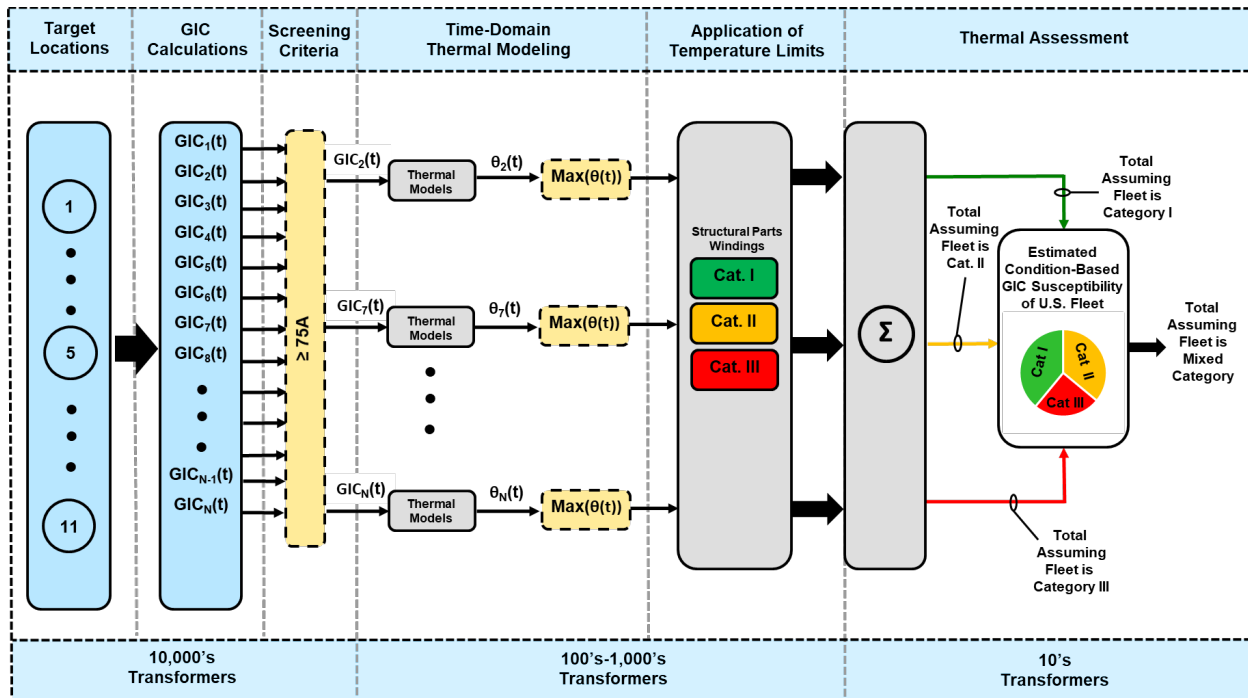


Figure 4-12
Procedure for performing thermal assessment of the U.S. transformer fleet

Step 1: Perform GIC Calculations and Apply Screening Criteria

The time-domain GIC flows in all 69 kV and above transformers included in the interconnection-scale models were computed. Although previous studies have demonstrated that regional voltage collapse from E3 EMP is possible, it was assumed that the system remained stable throughout the duration of the event with system operating voltages at their nominal values. GIC flows were simulated for the entire duration of the E3 EMP event, which is approximately 5 minutes. These assumptions provide a worst-case scenario for assessing the potential impacts of transformer hotspot heating during these events.

To fully simulate the effects of transformer hotspot heating after the effects of E3 EMP have dissipated, the resulting GIC(t) waveforms were extended to 1200 seconds with amplitude of 0.0 amps/phase. Extending the GIC(t) waveform in this manner allowed for the observation of transformer cooling and the amount of time a given hotspot temperature limit was violated in cases in which the instantaneous hotspot temperature exceeded specified temperature limits.

For most target locations, there were tens of thousands of transformers included in the GIC calculations. Because of the geographic coverage of the LANL E3 EMP environment, some target locations required that GIC calculations be performed in multiple interconnections. In these cases, GIC calculations were performed separately for each interconnection.

Once the time-series GIC flows were computed, they were screened to determine which transformers required additional thermal analysis. The screening criterion adopted by NERC and used in TPL-007-2 [25] was used. Each transformer that experienced a peak instantaneous *effective* GIC level of 75 amps/phase or more was selected for additional analysis.

Transformers with effective GIC levels less than 75 amps/phase were assumed to have hotspot heating well below the conservative temperature limits that were used. Additional analysis has shown that the 75 amps/phase criterion is very conservative for E3 EMP impacts because of the short duration of the late-time pulse.

Step 2: Time-Domain Thermal Modeling

The effective GIC flows in the transformers that had peak amplitudes exceeding 75 amps/phase were used as inputs to the time-domain thermal model that was used to compute the total hotspot temperatures of transformer structural parts and windings. There were four sets of model parameters that were used in the assessment. Model parameters included data describing the thermal response of structural parts in three different transformers, described in [26] and [6], and data describing the thermal response of a transformer winding, described in [6].

The time-domain thermal response of each transformer was modeled as a non-linear difference equation of the following form:

$$y(k+1) = \left(\frac{K(k)}{1 + \frac{2\tau}{\Delta t}} \right) (x(k+1) + x(k)) - \left(\frac{1 - \frac{2\tau}{\Delta t}}{1 + \frac{2\tau}{\Delta t}} \right) y(k) \quad \text{Eq. 4-1}$$

Where

y is the hotspot temperature rise (°C)

k is the increment of the difference equation ($k = 1, 2, 3, \dots$ number of samples)

τ is the thermal time constant (seconds)

x is the effective GIC (amps/phase)

K is the non-linear asymptotic thermal response (°C/amp)

Δt is the time step (seconds)

The asymptotic thermal response of large power transformers experiencing part-cycle saturation has been shown to be a nonlinear function of GIC. This effect can be accommodated in the model by computing K at each time step using a look-up table, denoted by $K(k)$ in Equation 4-1.

To determine the total hotspot temperature, THS , the hotspot rise found using Equation 4-1 is added to the top oil temperature, θ_{TO} :

$$THS(k+1) = \theta_{TO} + y(k+1) \quad \text{Eq. 4-2}$$

Because the time constant of the transformer oil is on the order of hours, the top oil temperature can be assumed constant during the short period associated with E3 EMP events. For the simulations here, the top oil temperature was assumed to be 80°C for all transformers [6].

To determine worst-case effects, time-domain temperature calculations using all four thermal models were performed for each transformer that was screened into the process—that is, all transformers with effective GIC flows greater than 75 A/phase. The maximum *instantaneous* temperatures from each of the four models were then obtained from these thermal responses. Example thermal responses from a transformer included in the assessment are shown in Figure 4-13.

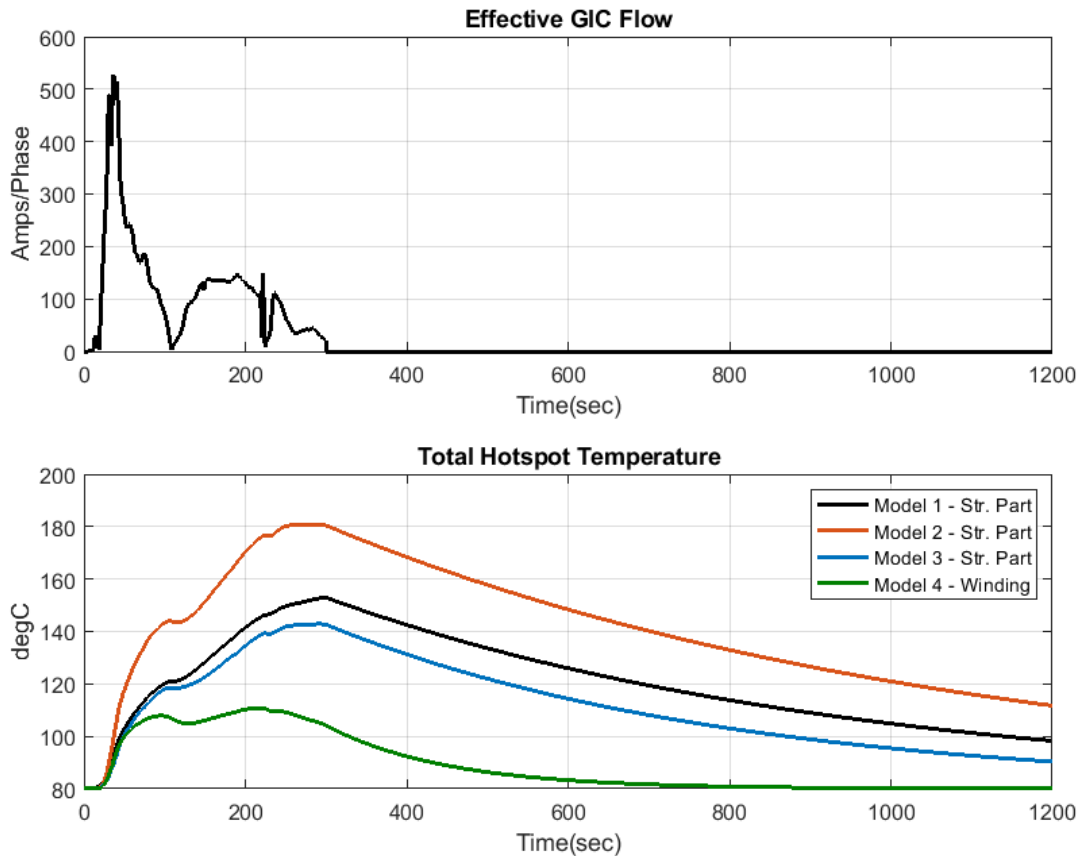


Figure 4-13
Example thermal response simulations from a transformer included in the assessment

The top panel in Figure 4-13 shows the corresponding effective GIC flow in the transformer. The bottom panel in Figure 4-13 illustrates the thermal response from the four different thermal models. Models 1–3 represent structural parts, and Model 4 represents the thermal response of a transformer winding. Parameters for the four thermal models are provided in Appendix A.

Step 3: Application of Temperature Limits

The maximum *instantaneous* hotspot temperatures from the simulations were evaluated against conservative temperature limits derived from IEEE Std. C57.163 and assumed condition-based GIC susceptibility categories of the U.S. transformer fleet. Temperature limits associated with each of the three GIC susceptibility categories and the corresponding percentage of U.S. transformers assumed in those categories are summarized in Table 4-2.

Table 4-2
Temperature limits for condition-based geomagnetically induced current susceptibility categories and percentage of U.S. transformer fleet in each category

Condition-Based Geomagnetically Induced Current Susceptibility Category	Percentage of Fleet	Hotspot Temperature Limit	
		Structural Parts (°C)	Windings (°C)
I	36%	200	180
II	25%	180	160
III	39%	160	140

The condition-based GIC susceptibility categories described in Table 4-3 were based on an analysis of 1,451 transformers with high-voltage windings rated 230 kV and above that were included in EPRI’s transformer database. The analysis evaluated the EPRI PTX Abnormal Condition Codes [27] for these transformers, which account for trends in ethylene and ethane, and the age of each of the transformers, which was used as a proxy for moisture content. Trends in ethylene and ethane can detect transformers with potential conditions that may be exacerbated by short-term hotspot heating caused by part-cycle saturation. Moisture-in-paper is a critical parameter in the formation of bubbles during short-duration overloads. Unfortunately, it is difficult to differentiate moisture-in-paper (which cannot be measured directly) from moisture-in-oil (which can be measured); however, transformer age can be used as a rough proxy for moisture-in-paper since older transformers are more likely to experience conditions such as ingress from aged gaskets.

Using the temperature limits shown in Table 4-2, the number of transformers that experienced hotspot temperatures with maximum instantaneous values exceeding the specified limits was identified. This initial portion of the assessment was performed by evaluating the hotspot temperature of each transformer separately using all four thermal models, and assuming that all transformers included in the interconnection-scale model were of the same GIC susceptibility category. Figure 4-14 shows the results of these calculations for one of the target locations that was evaluated. The maximum instantaneous hotspot temperatures obtained from each of the thermal models for structural parts for each of transformers experiencing an effective GIC flow of 75 amps/phase or more are illustrated in the figure.

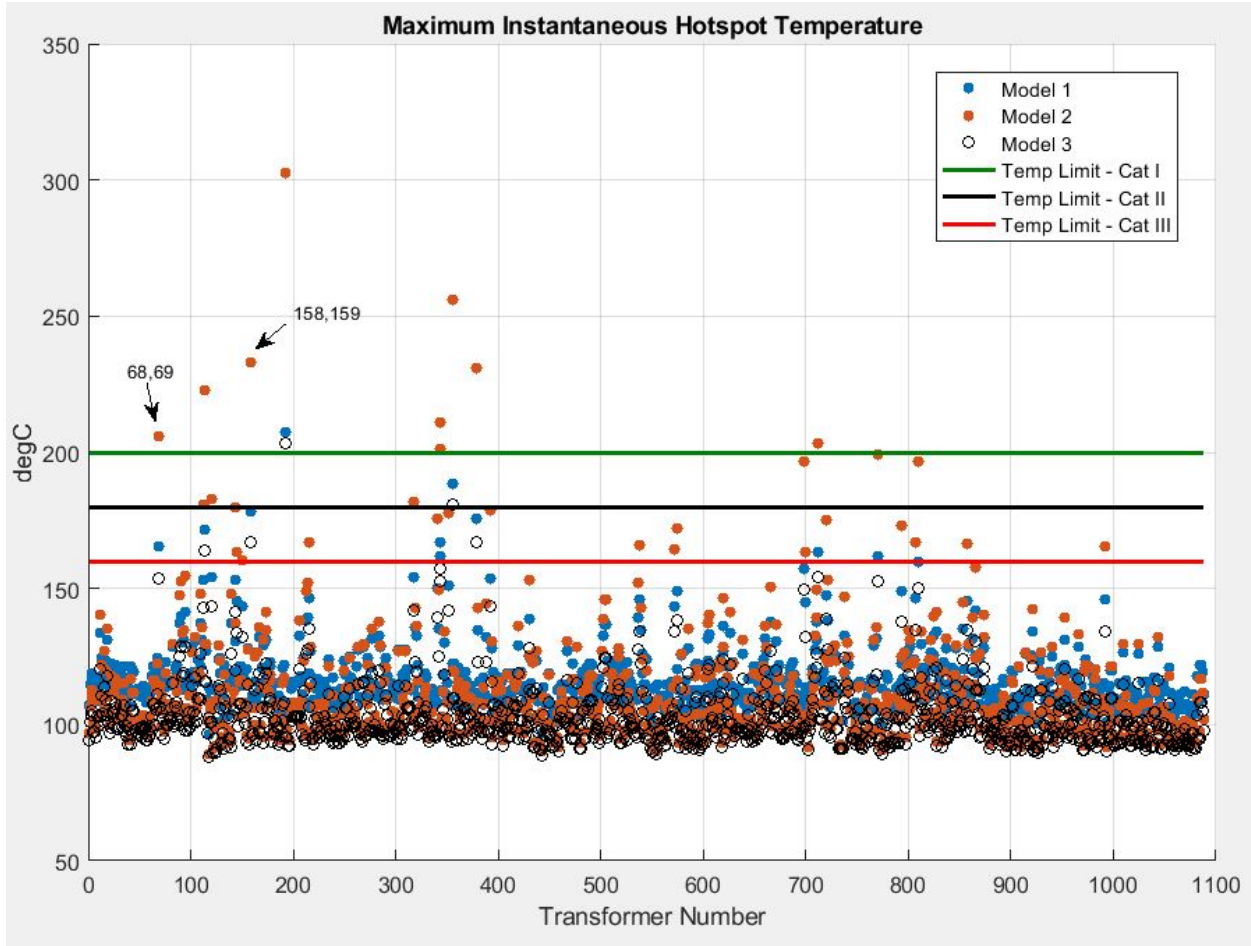


Figure 4-14
Example instantaneous hotspot temperature results

As shown in Figure 4-14, the temperature limit corresponding to Category I (200°C) was exceeded by 11 transformers when Model 2 was used to compute the total hotspot temperature. Carrying out this same screening process for all transformer thermal models and GIC susceptibility categories results in the compilation of results shown in Table 4-3. Table 4-3 also includes results from simulations of winding hotspots (not shown in Figure 4-14).

Table 4-3
Number of transformers exceeding temperature limits

Transformer Thermal Model	Model Type	Assumed Condition-Based Geomagnetically Induced Current Susceptibility Category		
		I	II	III
1	Structural part	1	2	12
2	Structural part	11	17	33
3	Structural part	1	2	6
4	Winding	0	0	1

Step 4: Thermal Assessment

The numbers of transformers that were identified as exceeding the specified temperature limits in Table 4-3 were then combined with the probabilities of a given transformer being in one of the three GIC susceptibility categories. The result was the expected number of transformers, E(X), to be at potential risk of thermal damage [6]:

$$\begin{aligned}
 E(X) &= \sum_{j=1}^K p_j X_j \\
 &= p_1 X_1 + p_2 X_2 + p_3 X_3
 \end{aligned}
 \tag{Eq. 4-3}$$

Where:

p_1 is the probability that a given transformer is in Category I or 0.36

p_2 is the probability that a given transformer is in Category II or 0.25

p_3 is the probability that a given transformer is in Category III or 0.39

X_1 is the number of transformers exceeding the temperature limits assuming entire transformer fleet is in Category I

X_2 is the number of transformers exceeding the temperature limits assuming entire transformer fleet is in Category II

X_3 is the number of transformers exceeding the temperature limits assuming entire transformer fleet is in Category III

The results of these calculations for all 11 target locations are provided in Table 4-4.

**Table 4-4
Transformer thermal assessment results using the LANL E3 EMP environment**

Target Location	Total Number of Transformers Exceeding Temperature Limits Based on Assumed Condition-Based Geomagnetically Induced Current Susceptibility of Entire Transformer Fleet			Estimated Number of Transformers at Potential Risk of Damage, E(X)
	Category I	Category II	Category III	
1	11	17	33	21
2	7	18	26	17
3	3	13	36	18
4	2	3	8	5
5	6	7	18	11
6	2	8	14	8
7	0	3	7	3
8	5	13	19	12
9	4	4	7	5
10	4	7	17	10
11	4	15	30	17

The assessment results provided in Table 4-4 indicate that the number of transformers expected to be at potential risk of thermal damage ranged from 3 to 21, depending on target location evaluated. As with the initial assessment that was performed [6], transformer impacts were found to be geographically dispersed. *Because of the known limitations with the ORNL E3 EMP environment, the results shown in Table 4-4 are considered the definitive transformer thermal results from the EPRI E3 EMP assessments.*

4.3.2.2 Voltage Stability Assessment

The voltage stability assessment using the LANL E3 EMP environment was performed using the same transient stability (time-domain simulation) approach that is documented in the initial EPRI study [5]. A flow diagram of the process is shown in Figure 4-15.

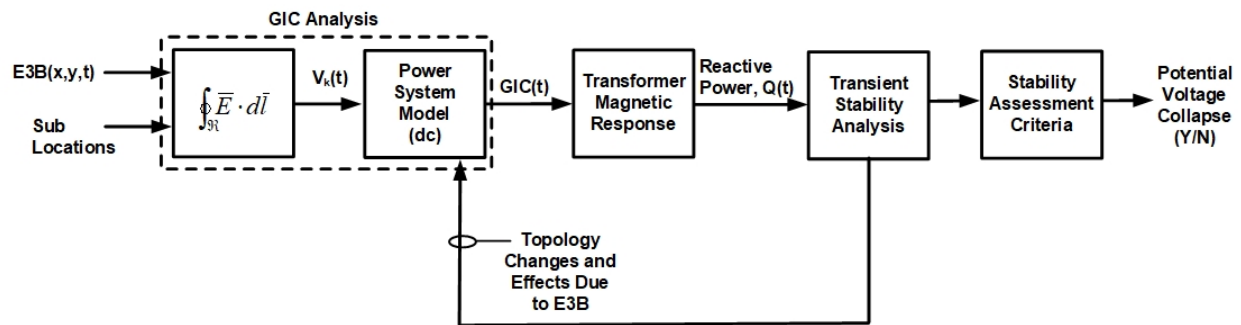


Figure 4-15
Procedure for voltage stability assessment evaluating impacts of E3 EMP only

Time-series GIC flows induced by the E3 EMP environment were used to determine reactive power demands at each transformer location within the interconnection model. Dynamic (transient stability) models for loads, rotating machinery, and protection systems as described in [5] were used to assess potential impacts. Additional modeling improvements, such as the addition of time-overcurrent relays for selected large power transformers and modifications to some generation controls, were also included in the updated study. As with the previous study, the effects of harmonics were not included. Lastly, as stated previously, due to time constraints, only a single target location in the Eastern Interconnection and a single target location in the Western Interconnection were evaluated in this voltage stability assessment.

Using the procedure illustrated in Figure 4-15, a voltage stability study was performed to evaluate the potential impacts of the LANL E3 EMP environment alone on the stability of the bulk power system. Figure 4-16 illustrates the effect that the environment can have on system voltage levels.

During the first 10 seconds of the environment, the E3 EMP field is quite weak and GIC flows are minimal. Thus, reactive power absorption of transformers is minimal (few transformers experience part-cycle saturation due to the low levels of GIC), and so system voltage levels remain essentially at pre-event levels. At approximately 10 seconds the E3 EMP environment begins to increase significantly, resulting in higher GIC flows and part-cycle saturation of large power transformers resulting in additional reactive power demand on the system and a corresponding decline in system operating voltage. As the environment evolves, the transmission voltages begin to sag further. Voltage sags begin to cause motor stalling at load buses throughout

the system, resulting in further decline in system voltage levels. As the E3 EMP environment continues to evolve and system voltage levels continue to decline there is progressive loss of generation and load. Ultimately, voltage levels continue to decrease until a point where voltage collapse occurs. In this particular simulation (refer to Figure 4-16 for an illustration of the per-unit magnitude of system voltage levels as a function of time), voltage collapse occurs at approximately 32 seconds after the E3 EMP environment begins.

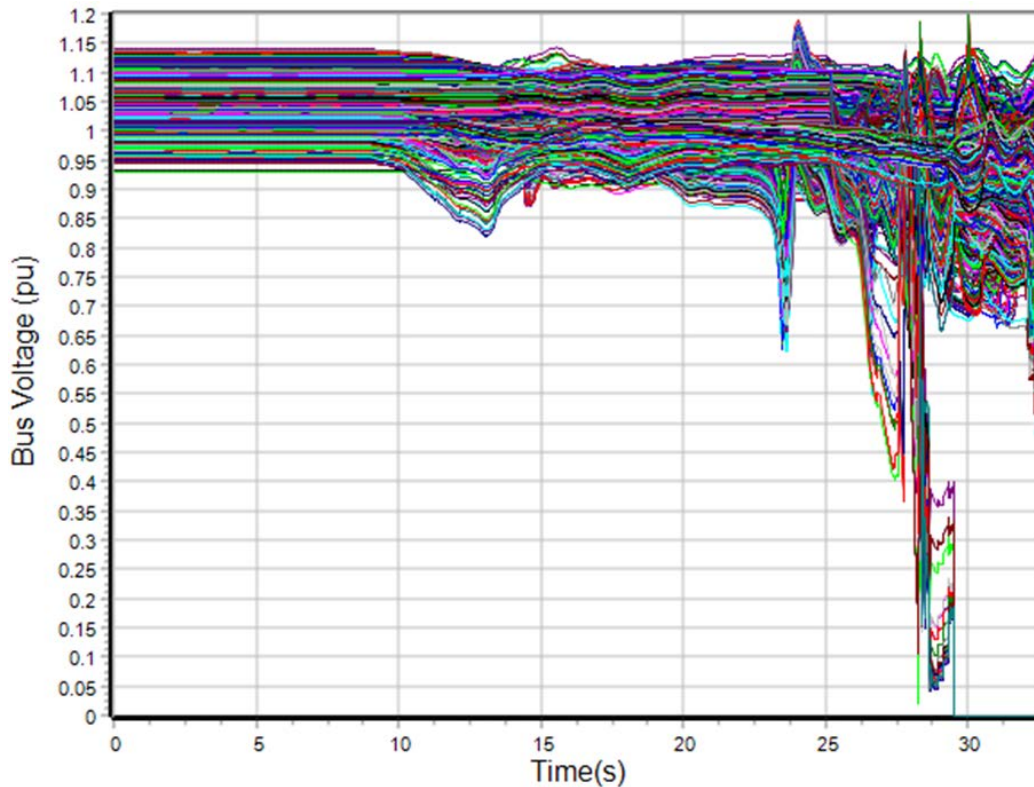


Figure 4-16
Example bus voltages during dynamic simulation of E3 EMP effects

Once simulation results show that voltage collapse has occurred, it is difficult to precisely determine the extent of the collapse. Simulation results prior to the collapse, and in particular time-varying contour maps of system voltages, can be evaluated to estimate the size of the affected region. Although it is difficult to predict the actual boundaries of collapse, the simulation results indicated that the region of blackout could include multiple states covering a geographic area on the order of 200,000–300,000 square miles. A comparison of the simulation results (total generation tripped during the event, total load tripped during the event and whether voltage collapse occurred) from the two target locations is provided in Table 4-5.

Table 4-5
Comparison of voltage stability assessment results

Target Location	Generation Tripped (MW)	Load Tripped (MW)	Voltage Collapse (Yes/No)
Eastern Interconnection	12,523	27,870	Yes, Regional
Western Interconnection	2,229	5,957	Yes, Regional

With the LANL E3 EMP environment as the driver of GIC flows, the updated voltage stability assessment yielded more severe results than the initial study [5] using the ORNL E3 EMP environment. In both scenarios (target locations) that were re-evaluated using the LANL E3 EMP environment, regional blackout was found to occur, whereas in the previous simulations using the ORNL E3 EMP environment the system remained stable. Although all 11 target locations were not re-evaluated using the LANL E3 EMP environment, it is plausible that voltage collapse would be experienced in each case, based on the results of the two scenarios that were evaluated.

4.4 Assessment of E1 EMP + E3 EMP Impacts

Prior HEMP assessments evaluated the potential impacts of E1 EMP alone or E3 EMP alone; however, during a HEMP attack a system could be exposed to both E1 EMP and E3 EMP. The impacts of E2 EMP are assumed to be inconsequential to the electric transmission system. Prior assessments including the one described previously have indicated the potential for E1 EMP to damage DPRs over large geographical areas. Prior assessments have also shown that regional voltage collapse is possible. E1 EMP impacts to DPRs and other control equipment could cause topology changes prior to the E3 EMP due to relay failure, or could challenge protection systems while the system is collapsing, potentially affecting how the system responds to E3 EMP. Thus, evaluating the potential effects of E1 EMP and E3 EMP in concert is important to assess the overall impact of HEMP on the bulk power system.

A block diagram describing the approach that was used to assess the combined effects of E1 EMP and E3 EMP on the bulk power system is described in Figure 4-17.

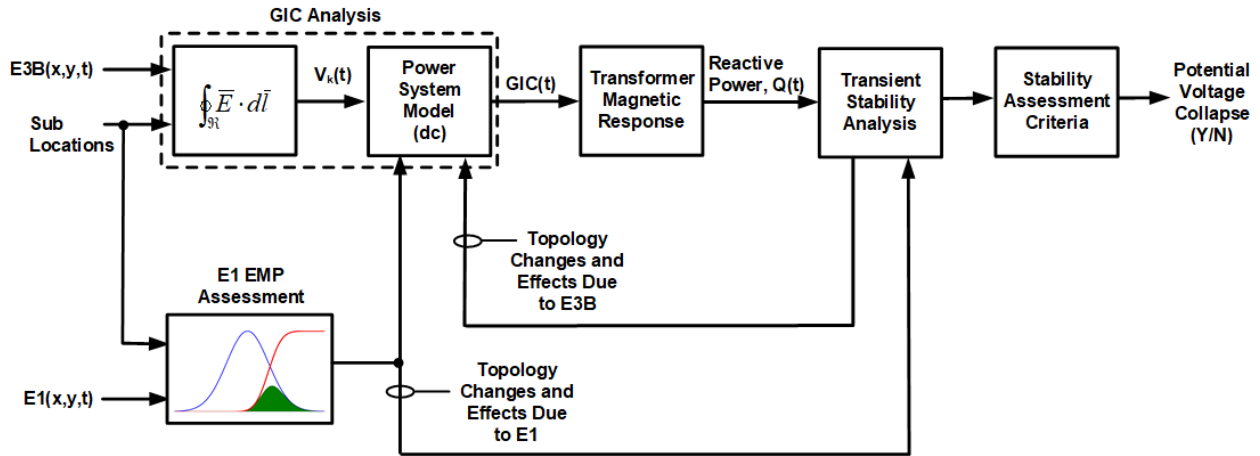


Figure 4-17
Combined E1 + E3 assessment process diagram

Referring to Figure 4-17, the bounding HEMP environments for the individual assessments (E1 EMP and E3 EMP) were based on the same target locations. The E1 EMP assessment was performed off-line using the approach described previously, and the impacts were used to inform the E3 EMP assessment. The scaled LANL environment (50 kV/m) and both Example 1 and Example 2 E1 EMP assessment results were used as the basis of the combined assessments. Testing of DPRs indicated that damage to a single voltage input would not cause the relays to immediately trip, so when the assessment predicted a particular DPR would be damaged by E1 EMP, the DPR was assumed non-functional in the transient stability model. In other words, the relay would not be able to trip if it was called upon to do so during the E3 EMP event. The E3 EMP portion of the study was performed in the same manner as the E3 EMP-only assessment described previously.

A comparison of the simulation results from the previous study using the E3 EMP environment alone and the new study assessing impacts of the both E1 EMP and E3 EMP is provided in Table 4-6.

Table 4-6
Comparison of voltage stability assessment results: E3 only and E1 + E3

Target Location	Assessment Type	Generation Tripped (MW)	Load Tripped (MW)	Simulation Time (Sec)	Voltage Collapse (Yes/No)
EI	E3 Only	12,523	27,870	32	Yes, Multiple States
	E1 + E3 (OH Line – Example 1)	12,813	28,035	32	Yes, Multiple States
	E1 + E3 (Cables – Example 2)	12,813	28,035	32	Yes, Multiple States
WECC	E3 Only	2,229	5,957	32	Yes, Multiple States
	E1 + E3 (OH Line – Example 1)	2,229	5,957	32	Yes, Multiple States
	E1 + E3 (Cables – Example 2)	2,229	5,957	32	Yes, Multiple States

The results shown in Table 4-6 indicate that E1 EMP impacts, as they were modeled, do not significantly affect the outcome of the E3 EMP assessment results. However, significant damage to DPRs would be expected to degrade recovery efforts.

4.4.1 Modeling Uncertainties Associated with Assessment of Combined E1 EMP + E3 EMP Effects

There are a number of uncertainties that could potentially affect the outcome of the combined E1 EMP + E3 EMP assessments. A few of these are described as follows:

- The potential effects of E1 EMP damage to generating facilities or loads were not included in the assessment. From a system load standpoint this assumption is pessimistic, as load loss due to E1 EMP effects would tend to aid voltage stability. From a generation perspective, the assumption may be optimistic, as the loss of generating units or generation controls could negatively affect voltage stability and/or longer-term frequency control. Future research is needed to better quantify these potential impacts.
- E1 EMP damage to control systems such as automatic generation control (AGC) were not included and could worsen the effects and make it difficult to maintain long-term frequency control. Such effects could potentially widen the area of impact.
- Impacts of E1 EMP on conventional generation controls or inverter-based generation (IBG) are largely unknown and were not included in the assessment. It is possible that E1 EMP impacts to those controls could affect the ability of such devices to provide reactive power support to the system during the E3 EMP event or frequency control post event. Additional E1 EMP testing of generator controls or wind and solar photovoltaic (PV) inverters could be useful in understanding such impacts.
- Inverter-based generation and shunt reactive power sources such as static var compensators (SVCs) and STATCOMs have lower reactive power overload capability relative to synchronous generators. Reactive current (and power) will be quickly limited by hard limits in the fast-acting controllers in these devices. This behavior is different from that of a synchronous machine, where reactive power overloads and higher field current are tolerable for brief periods. Therefore, as synchronous machines are replaced with power electronics based equipment it is important to evaluate their dynamic reactive power capability relative to their predecessors to maintain resilience to these types of events.
- The effects of harmonics were not included in the analysis. The potential effects of harmonics on the bulk power system resulting from geomagnetic disturbance (GMD) events are well-known, and it is expected that similar effects could occur as the result of E3 EMP. Future research and analysis could help quantify the potential bulk power system effects of harmonics that are generated as a result of an E3 EMP event. Additional modeling capability is needed to integrate harmonics assessments into the transient stability analysis presented in this report.

- As high-voltage circuit breakers begin to trip due to the effects of voltage collapse there is considerable uncertainty regarding their ability to interrupt the significant levels of GIC that can be generated by E3 EMP. This is of particular concern if circuit loading is low such that the combined waveform (fundamental frequency + harmonics + GIC) does not contain a zero crossing. Testing of high-voltage circuit breakers and additional modeling and simulation could help determine the potential for circuit breaker damage to occur.

4.5 Assessment of E1 EMP Impacts on Voltage Stability

Because of the uncertainty related to how DPRs might respond if they are disrupted or damaged by E1 EMP during a HEMP event, an additional voltage stability assessment was performed to determine if the effects of E1 EMP alone could potentially cause voltage instability or blackout. For this study, only the Eastern Interconnection target location was evaluated, and the effects of E3 EMP were ignored. In this study, 1% of the line terminals identified as having a damaged DPR in the Example 2 E1 EMP assessment (unshielded signal cable on the ground) were randomly selected and assumed to have caused trips immediately after the event. For the E1 EMP portion of the analysis, the 50 kV/m environment described in Section 2 was used. In total, it was found that approximately 21,500 line terminals were affected and 215 of those were randomly selected and assumed to have caused simultaneous tripping of their corresponding line terminals immediately after the initiating E1 EMP event. A transient stability simulation was then performed to determine how the system would respond to 215 line terminals randomly tripping across an interconnection. Automatic reclosing of the line terminals was not considered.

The results of dynamic simulations using the same transient stability model of the Eastern Interconnection used in the previous assessments showed that the system would experience perturbations due to the tripping of the 215 line terminals, but the system remained stable throughout the simulation period. Obviously, this result is dependent on the number of DPRs that are assumed to have tripped and their location as well as other factors and uncertainties. Although it cannot be concluded from a single dynamic simulation whether or not the effects from E1 EMP alone could cause voltage instability, the system did remain stable in this one case after being subjected to a 50 kV/m E1 EMP environment, which demonstrates the ability of the bulk power system to ride through an extreme event. That said, there are two principle uncertainties that could significantly affect this outcome. First, E1 EMP damage to control systems such as automatic generation control (AGC) could worsen the effects and make it difficult to maintain long-term frequency control, which could result in system instability. Second, impacts of E1 EMP on conventional generation controls such as excitation systems, governors and distributed control systems (DCS) or inverter-based generation (IBG) are largely unknown. Damage to these devices could also affect the ability of these systems to respond to the system perturbations that result from E1 EMP impacts. More research and analysis, potentially using Monte Carlo techniques, is needed to quantify the potential impacts of E1 EMP alone on voltage stability.

5

APPROACHES FOR MITIGATING THE EFFECTS OF HEMP

5.1 E1 EMP Mitigation

Hardening against the effects of E1 EMP requires mitigating the potential impacts of both conducted and radiated disturbances generated by the incident E1 EMP pulse. Referring to the substation control house illustrated in Figure 5-1, the incident E1 EMP pulse can couple to cables entering the building or the antenna that is used for communications such as SCADA, or it can propagate through the building skin and radiate equipment directly or couple to cables located inside the control house. Thus, when designing an E1 EMP hardening strategy for a substation, the design engineer must consider both of these threats.

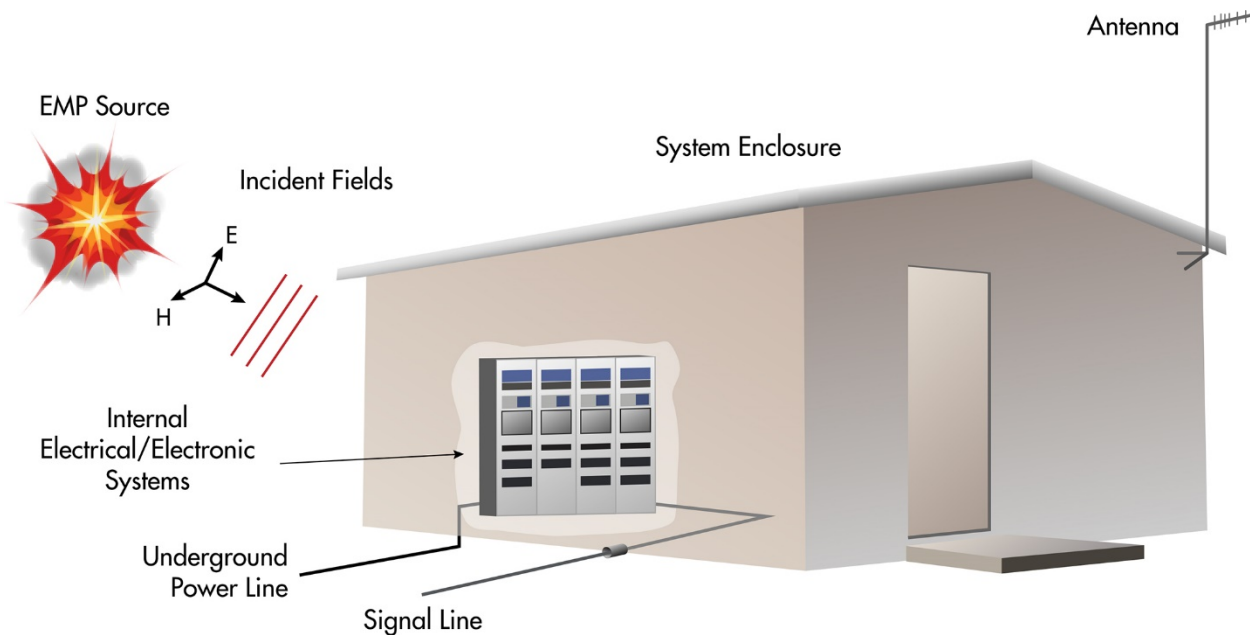


Figure 5-1
Example radiated and conducted disturbances through a single-barrier substation control house

The following hardening options are categorized as pertaining to transmission control centers or substations.

5.1.1 Transmission Control Centers

Transmission control centers (not to be confused with substation control houses) are an integral part of bulk power system control and operation. They perform a critical role not only during normal operation, but also during and after system events, as they are the central command center for blackstart operations. Because of these functions, they are considered a mission critical system.

If it is determined that the facility should be hardened against HEMP, it is suggested that the performance specifications in MIL-STD-188-125-1 [23] be followed. Following the stringent shielding requirements (80 dB from 10 MHz to 1 GHz) also provides significant protection against other electromagnetic threats such as intentional electromagnetic interference (IEMI). Cost is always a consideration, and the facility owner must determine how much of the facility to harden. A number of utilities have hardened their control centers to MIL-STD-188-125-1 specifications. Some have chosen to harden the entire facility, while others have hardened only the portions deemed critical to maintaining bulk power operations.

5.1.2 Substations

5.1.2.1 Mitigation of Radiated Threats

An important aspect of hardening against the potential impacts of E1 EMP is mitigation against free field illumination of the incident plane wave. Testing has demonstrated that some DPRs are resilient to free field illumination threats, but some DPRs do require that the enclosure, for example a substation control house where the devices are located, provide a modest level of attenuation. For example, Type 2 failures of some DPRs were observed at E-field levels as low as 15 kV/m. Designing structures to provide 20 dB or more of attenuation across all pertinent frequencies would reduce an incident field level of 50 kV/m to 5 kV/m or less and provide margin. To provide additional mitigation and margin, 30 dB across the frequency range defined in MIL-STD-188-125-1 (10 MHz to 1 GHz) may be more appropriate for critical substation applications.

In general, the following design features are required in substation control houses to meet a 30 dB shielding effectiveness requirement:

- Six-sided enclosure constructed of sheet steel or conductive concrete. Metal enclosures may be constructed from a combination of sheet steel with connections fastened together via welds or bolts. In the case of bolted connections, a gasket designed for radio frequency (RF) shielding may be required.
- Points of entry should be considered and designed such that they maintain the integrity of the facility shield.
 - The enclosure should be free of any windows.
 - Doors and other entryways should be minimized and designed such that they meet the required shielding performance specification while in the closed position. This may require the use of special RF doors.

- Electrical systems (power cables, control cables, signal cables, communications, etc.) should penetrate the facility shield through appropriately designed waveguides, or via cable seals or entry glands with suitable electromagnetic compatibility (EMC) properties.
- Mechanical systems associated with substation control houses, for example HVAC systems and piping, should penetrate the facility shield through appropriately designed waveguides. Hoses or pipes constructed of dielectric material should be converted to metal piping prior to penetrating the facility shield.

When the shielding design of a substation control house allows a significant portion of the incident wave to penetrate the shield or enter through an aperture, the transmitted wave can excite one or more resonances, which can result in amplification of the field inside the enclosure. It is important that a facility shield design consider such resonances to ensure that the equipment contained within the enclosure is not adversely affected. In general, it is best to avoid locating critical equipment near walls or corners.

As a final consideration in the design of substation control houses, the level of attenuation that is required should be based on the E-field levels that result in disruption or damage to the critical equipment contained within the enclosure. Because of the complexities associated with designing facility shields, it is not possible to prescribe specific design options that will guarantee a specific shielding level. It is recommended that the shielding design criteria be performance-based and defined at each frequency of interest. Lastly, shielding effectiveness testing using MIL-STD-188-125-1 compliant testing methods should be used to assess the performance of the final shielding design.

If critical assets are located in areas of the substation that are external to the substation control house (e.g., circuit breaker cabinets), the design of these enclosures may require the same performance requirements as the control house. The original equipment manufacturer (OEM) should be consulted whenever such requirements are identified.

5.1.2.2 Mitigation of Conducted Threats

Protection and control (P&C) equipment items such as DPRs in a substation control house rely on analog controls and signals from instrument transformers located in the substation yard to perform their function. These voltage and current signals are provided to DPRs via signal cables. During a HEMP event, unshielded signal cables can act as antennae and bring significant voltage and current surges into the substation control house if the transients are not properly mitigated. Metallic control cables that are connected to the DPRs to facilitate analog controls also provide a means of exposing DPRs and other equipment to conducted transients.

5.1.2.2.1 Low-Voltage Surge Protection Devices and Filters

Mitigation designs must always include the potential for conducted surges, originating outside of the enclosure, to propagate inside the enclosure through electrical conductors. The level of protection that is required should be based on the voltage and current surge levels that result in disruption or damage of the equipment being protected, but in general will include the use of low-voltage surge suppression devices and/or filters. These devices either divert a significant portion of the incident surge to ground as in the case of a low-voltage SPD or shunt-connected

filters, or they impede the propagation of the surge beyond the device, as in the case of a series RFI filter. An example of a prototype low-voltage surge protection device designed to protect the analog inputs and control outputs of a DPR using a hybrid technology (combination of TVS diodes and MOVs) is shown in Figure 5-2.

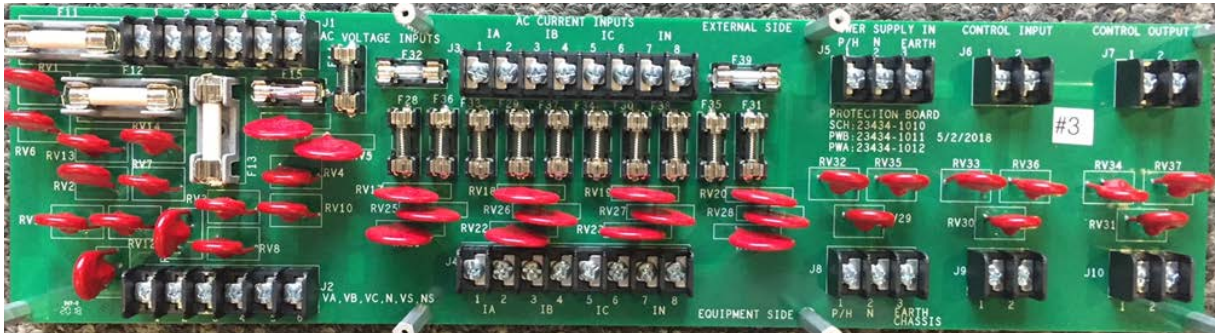


Figure 5-2
Example of a prototype low-voltage surge protection device designed to protect the analog inputs and control outputs of a DPR

If possible, SPDs should be located externally to the facility shield inside a shielded marshalling enclosure or cabinet so that the incident voltage/current surges are reduced prior to entering the facility shield. Depending on the application, additional surge protection/filtering may also be required near the equipment being protected. In all cases, it is important to keep wired connections from the SPD or filter to the protected equipment as short as possible. Ground leads of devices external to the facility shield should be connected to the grounded external enclosure. Proper grounding design is critical.

5.1.2.2.2 Control/Signal Cables

All control and signal cables entering the substation control house should be of the shielded type with the shield grounded at both ends of the cable. Longitudinal corrugated copper tape (LCT) or helical copper tape shielded cables generally provide the best performance. Control cable shielding conductors should be grounded on both ends and prior to entering the facility shield. When cable shields are grounded at both ends, the shielding conductor can be subjected to large fundamental frequency currents during power system faults or switching events. Protection of the shielding conductor can be achieved by the use of one or more appropriately sized parallel grounding conductors located in the same cable trough [28, 29]. IEEE Std. 525 [28] and IEC Std. 61000-5-2 can be referred to for best practices regarding grounding to eliminate fundamental frequency effects in control cables.

To maximize performance of the facility shield, all cable shields should have their shields terminated and grounded using an EMC cable seal or EMC entry gland. The EMC cable seal or EMC entry gland acts as an integrated part of the facility shield and electrically bonds the cable shield to the facility shield. An example of an EMC cable seal is shown in Figure 5-3.



Figure 5-3
Example of an EMC entry shield

With the cable shield electrically bonded to the facility shield, conducted transients on the cable shield are diverted to ground through the facility shield and do not penetrate the control house.

5.1.2.2.3 Fiber Optics (IEC 61850)

A possible method of minimizing the impact of conducted transients on metallic conductors is to convert all analog quantities to digital signals that can be transmitted over fiber optic cables. Protection and control systems based on this method are available. These protection and control systems are broadly characterized as IEC 61850 systems. An example architecture of such a system is shown in Figure 5-4.

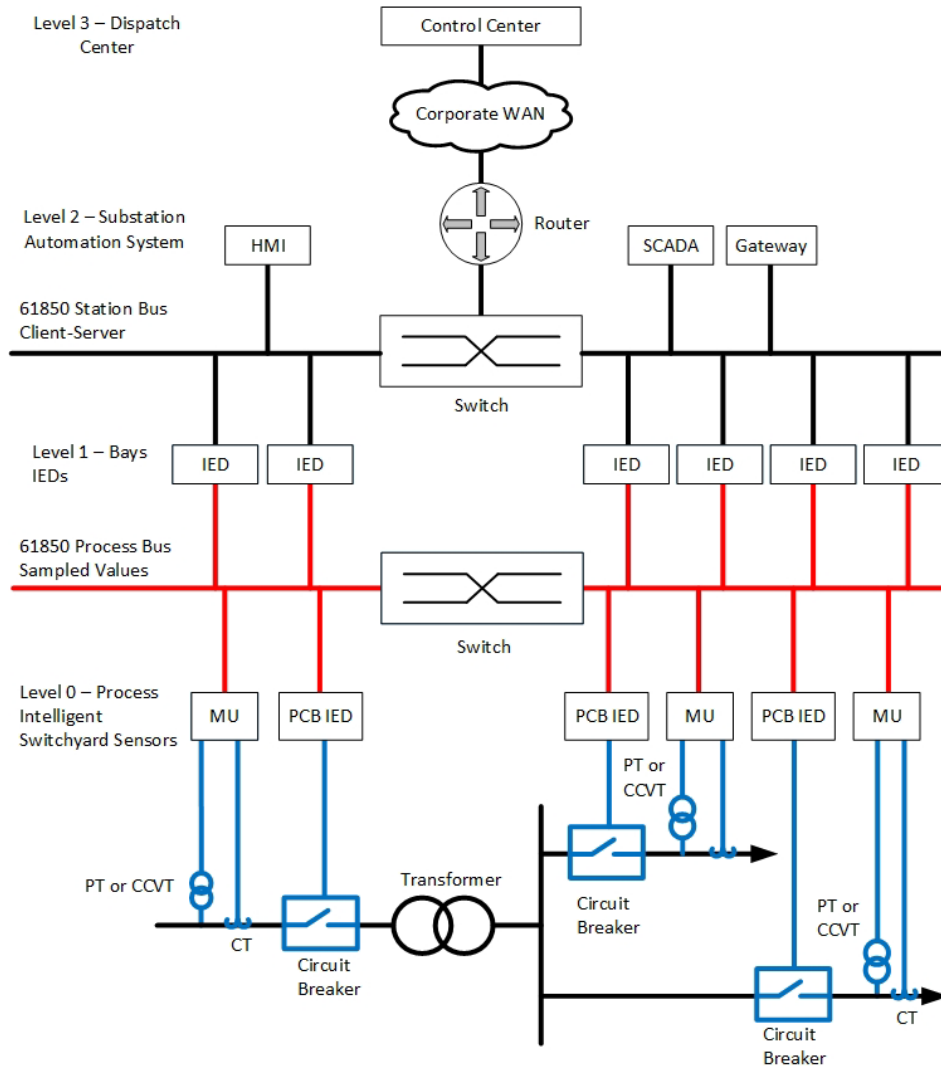


Figure 5-4
Example architecture of an IEC 61850 based protection and control system

Referring to Figure 5-4, the blue lines illustrate analog circuits from CTs, PTs, CCVTs, breaker controls, and so on that are located externally to the substation control house. These circuits are connected to intelligent electric devices (IEDs) or merging units (MUs), where the analog signals are converted to digital quantities that are then transmitted over fiber optic cables to the main control unit located within the substation control house. Direct injection testing of MUs has indicated that the analog inputs of the devices are susceptible to conducted transients and should be properly protected in the same manner as analog inputs of DPRs.

When fiber optic cables are used, points of entry should be appropriately designed to bring the optical fiber inside the facility shield. Waveguide below cutoff⁸ penetrations may be considered. These devices, which can accommodate multiple fiber optic cables with linked connectors, allow

⁸ A waveguide-below-cutoff is a device that is designed to attenuate signals that are below the cutoff frequency and acts as a wave guide (or propagates) signals above the cut-off frequency. The term waveguide-below-cutoff is somewhat of a misnomer since the devices act as a waveguide *above* the cutoff frequency.

the fiber optic cables to be brought inside the facility shield while maintaining the shielding integrity of the enclosure. Figure 5-5 is an example of a waveguide below cutoff penetration for fiber optic cable. Fiber optic cables containing metallic conductors for power delivery require shielding similar to the shielding for other metallic cables.



Figure 5-5
Fiber optic penetration waveguide

5.1.2.2.4 Cable Trenches and Marshalling Cabinets

A common method of routing control and signal cables is in concrete troughs. These troughs can be installed flush with the ground or slightly above the ground as illustrated in Figure 5-6.



Figure 5-6
Example of a cable trough located within a substation

These troughs provide minimal attenuation of the incident E1 EMP field; however, their shielding performance is not important if shielded cables or fiber optic cables are used. In situations where it is not feasible to use shielded cables, an alternative (but not equivalent) approach is to install the cable trough such that the top is flush with the ground and then use a conductive lid to cover it. However, 3D simulations have shown that the conductive lid alone may not be adequate in all cases.

The control cables entering and exiting the building out to the substation yard, through the trenches, should enter the control house through a shielded marshaling cabinet located at the entrance of the control house (refer to Figure 5-10).

5.1.2.2.5 Grounding and Bonding

The two primary goals of a proper grounding system are the following:

- To provide protection to personnel inside and outside of the facility
- To protect equipment from damage

The grounding design necessary for HEMP hardening can be different than what is typically used in substation applications. The following sections provide an overview of the grounding design practices used to mitigate the effects of E1 EMP on equipment.

When feasible, the grounding system should include an equipotential ground plane as described in MIL-HDBK-419A [30], where the six-sided facility shield comprises a large portion of the equipotential ground plane. An earth electrode system or external ground grid is designed to provide a low-impedance path for diverting fundamental frequency and radio frequency (RF) currents to ground. Additional roles of the earth electrode system include, but are not limited to, reducing step and touch potentials (personnel safety) as well as minimizing potential differences between interconnected systems located in the substation yard. Because of their lower impulse impedance, horizontal wires located below grade are the best choice for HEMP grounding [30]. Vertical ground rods may be added to the horizontal wires to achieve the stability necessary for fundamental frequency grounding applications. An example of a ground grid external to the facility shield that utilizes both horizontal conductors and ground rods is illustrated in Figure 5-7. Note that only the ground ring external to the facility shield (substation control house) is shown. In a practical substation application, the grounding system shown in Figure 5-7 would be encapsulated within the ground grid of the entire substation.

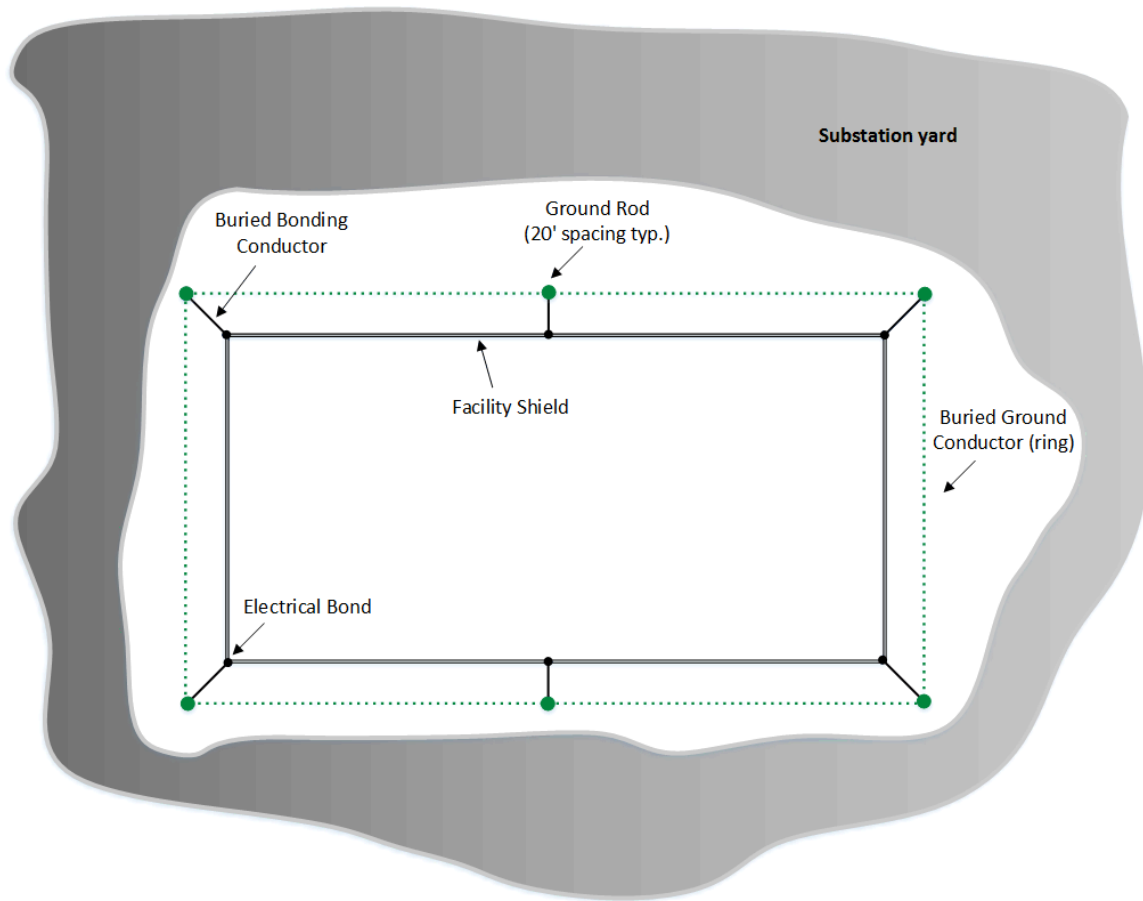


Figure 5-7
Example ground ring external to the facility shield

Additional design details regarding the design of grounding systems used in HEMP hardening applications can be found in MIL-HDBK-419A [30]. The designer should always refer to IEEE Std. 80 and other relevant industry standards to ensure that the final grounding design meets local code and personnel safety requirements.

Bonding of metallic parts and connecting them to a low-impedance grounding system is necessary for personnel safety, but it is also necessary to meet EMC performance requirements. Bonding conductors may be either wires or flat bonding straps such as the one illustrated in Figure 5-8.



Figure 5-8
Example of a flat bonding strap

In general, emphasis is placed on using bonding straps as opposed to wires for bonding in EMC applications, but the impedance difference between the two is not as significant as one might think. In general, a flat metallic bonding strap has approximately 80% of the impedance of a single wire, but the parallel connection of two wires offers a 50% reduction in overall impedance. Thus, the use of parallel wires may be appropriate in some applications.

Grounding conductors that originate outside of the substation control house, for example the parallel grounding conductors that are located in a cable trough, should not penetrate the facility shield. External grounding conductors should be connected externally, and then a separate ground conductor should be established internally to the facility shield, as shown in Figure 5-9 (refer to proper connection). If this connection is not possible, the least compromising arrangement (immediate right of proper connection) may be considered.

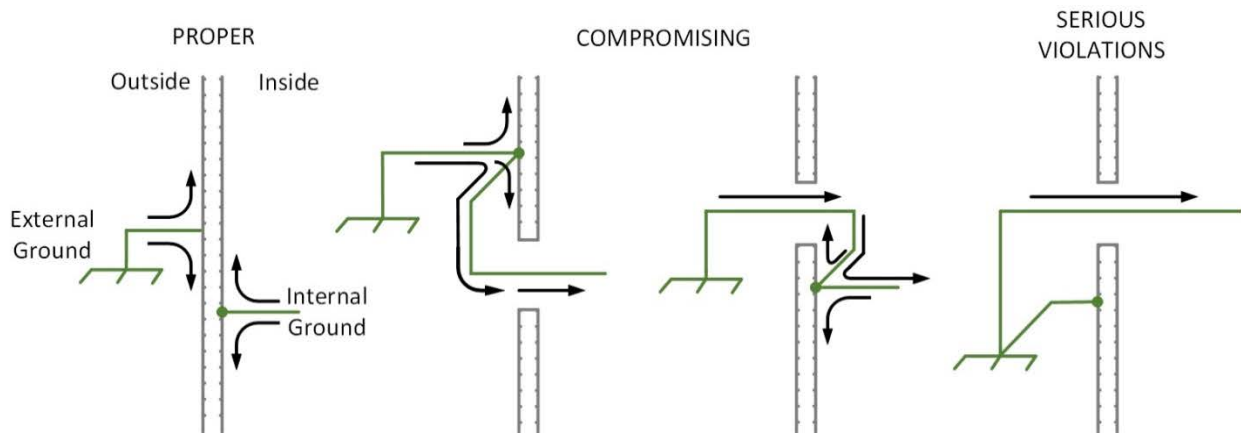


Figure 5-9
Examples of various connection methods of grounding conductors that originate externally to the facility shield [30]

5.1.2.3 Example Application

A generic design illustrating some of the mitigation options described previously is provided in Figure 5-10. For reasons of clarity, the grounding system is not shown.

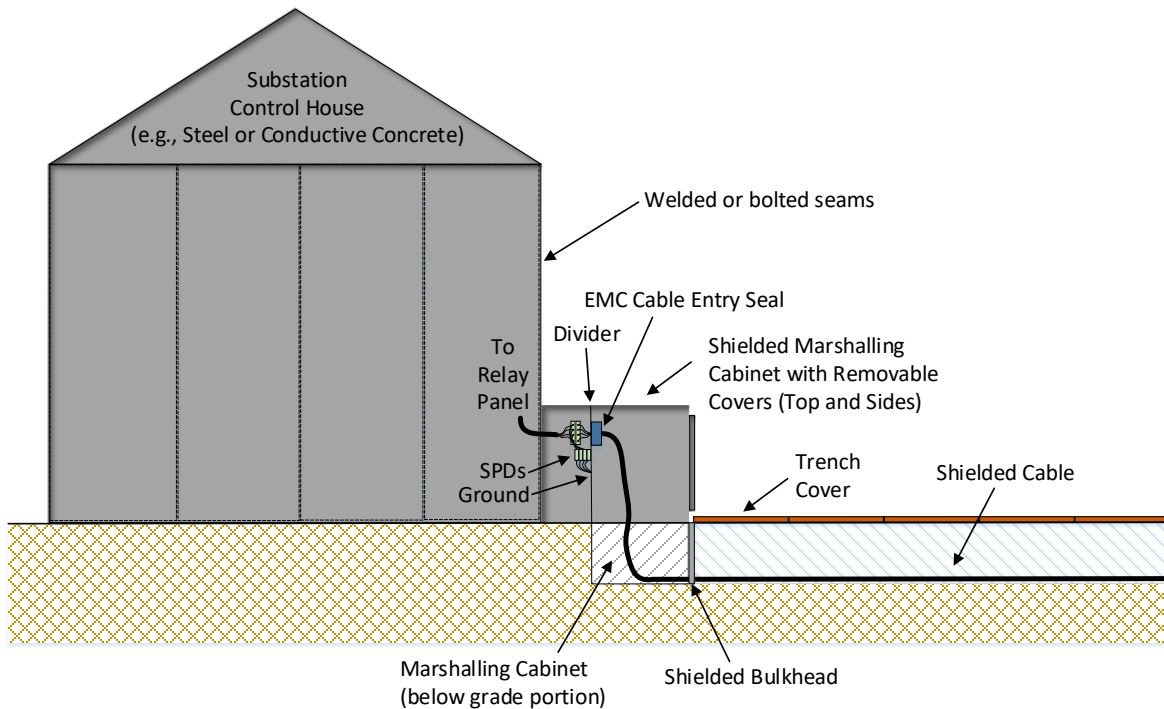


Figure 5-10
Illustration of an E1 EMP hardened substation control house

5.1.2.4 Equipment Sparing

Sparing of critical assets such as DPRs may be considered as part of the E1 EMP mitigation strategy. In general, if the DPRs are powered off and not connected to any external wires they are resilient to the full threat level of 50 kV/m. If additional protection is necessary or desired, the DPRs or other critical assets can be stored in shielded bags or shielded enclosures until needed. It is important that these assets be maintained and periodically tested to ensure functionality if ever needed.

5.2 E2 EMP Mitigation

Research findings indicate that E2 EMP will not impact transmission system assets; thus, no specific mitigation options are provided. Existing lightning protection and insulation design performance should provide adequate protection.

5.3 E3 EMP Mitigation

The following subsections provide a listing of options for mitigating the potential impacts of E3 EMP.

5.3.1 Avoiding Protection System Misoperations

Based on past experience with GMD events, it is recognized that system harmonics generated by part-cycle saturated transformers can cause some protection systems to misoperate [31], [32], and it is expected that the same effects could occur during an E3 EMP event. In general, the protection systems of grounded shunt capacitor banks and SVCs are the most susceptible to potential impacts. Mitigation of protection system misoperations can be achieved by doing the following:

- Replacing electromechanical or solid-state relays with DPRs that employ low-pass digital and analog filters to filter out harmonic content of analog voltage and current signals. (Note that DPRs may be more susceptible to E1 EMP effects and should be hardened appropriately.)
- Modifying the protection settings of existing protective relays to allow reactive power resources to “ride through” an E3 EMP event.⁹
- Modifying protection schemes such that they inherently filter out network imbalances.

5.3.2 Blocking or Reducing the Flow of Geomagnetically Induced Currents

Completely blocking or reducing the flow of GIC in system transformers is an effective means of reducing the potential impacts of E3 EMP, since the flow of GIC in large power transformers is the root cause of part-cycle saturation and its associated impacts on the electric power grid. There are several ways in which this can be achieved:

- Neutral blocking devices (NBDs)
- GIC reduction devices (GRDs) such as neutral resistors
- Series capacitors

Because there is currently no warning associated with HEMP events, operational procedures that may mitigate potential impacts of GMD events by opening lines or de-energizing transformers are not expected to be available to protect against E3 EMP. Additional information regarding the options that are expected to provide benefit during a HEMP attack are provided below.

⁹ It is important to note that modifying protection settings and/or schemes requires an understanding of the equipment withstand levels and the expected harmonic levels resulting from an E3 EMP event.

5.3.2.1 Neutral Blocking Devices (NBDs)

The use of capacitors in the neutral of grounded-wye transformer windings is an effective means of blocking the flow of GIC in transformer windings. An NBD inserts a capacitance between the transformer neutral and its ground connection when a predefined GIC level is detected. The capacitance of the device presents a very large impedance ($\sim 1/\omega C$) to the low-frequency GIC such that the flow of GIC in the transformer is negligible. This mitigation method can essentially block the flow of GIC in generator step-up units (GSUs), but because of the direct connection of the primary and secondary terminals of an autotransformer through the series winding, inserting an NBD in the neutral of an autotransformer does not completely block the flow of GIC. Based on system topology and the number and location of NBDs employed, GIC flows in the system can be displaced to other transmission paths or reduced overall.

Figure 5-11 shows a schematic of a prototype NBD developed by EPRI in the 1980s [33], and Figure 5-12 provides a physical representation of a commercially available NBD.

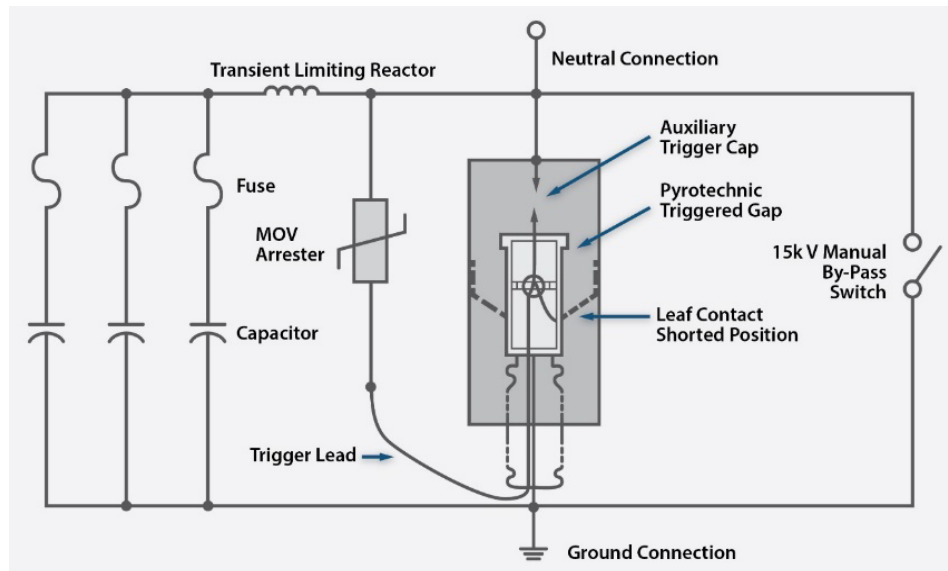


Figure 5-11
Generic circuit diagram of a neutral blocking device



Figure 5-12
Physical representation of a neutral blocking device deployed in the field
Courtesy of EMPRIMUS, LLC

Various capacitor ratings can be used in NBDs. Depending on the rating of the capacitor, the transient voltage developed across the NBD during fault conditions or other system conditions may stress the device and the neutral bushing of the transformer that it is connected to. To minimize impacts on the transformer neutral bushing and the NBD itself, surge protection should be used to limit the voltage stress during system events.

5.3.2.2 GIC Reduction Devices (GRDs)

Unlike NBDs, which utilize a capacitor to block the flow of GIC, a GRD inserts a resistance between the transformer neutral and ground to reduce the flow of GIC. A GRD reduces the GIC magnitude by increasing the total dc resistance of the transformer. Due to system imbalance and zero sequence harmonic current flows during normal power system operation, neutral resistive GRDs dissipate energy while in use. Specifications and design of neutral GRDs should consider the maximum expected fundamental and harmonic current levels so that the resistive GRD can perform reliably.

5.3.2.3 Series Capacitors

Series capacitors are used in transmission systems to reduce the inductive reactance of transmission lines to enhance system stability. The industry has extensive operating experience with these devices.

Like NBDs, the inclusion of a capacitor in series with a transmission line will modify the dc network topology, and thus the GIC flows. In some cases, series capacitors may increase the levels of GIC flow in other parts of the system including transformers [34].

5.3.2.4 Engineering Studies

When employing GIC blocking or reduction technologies, it is necessary to perform detailed engineering assessments to determine the effectiveness of the mitigation approach and to assess the potential for unintended consequences to system protection, system operation, or insulation coordination. Engineering studies that may be considered when deploying GIC reduction technologies are provided in Table 5-1 [35].

Table 5-1
Summary of recommended engineering design studies to perform when utilizing GIC mitigation technologies

		Series Capacitors	Neutral Blocking Devices	GIC Reduction Devices
Insulation Coordination	Switching Surges	✓	✓	✓
	Lightning Surges	✓	✓	✓
Protection and Coordination		✓	✓	✓
Continuous RMS Rating of Device, with Consideration of Part-Cycle Saturation Harmonics		✓	✓	✓
Subsynchronous Resonance (SSR)		✓		
Circuit Breaker Transient Recovery Voltage (TRV)		✓		
Ferroresonance		✓	✓	
GIC and Voltage Stability Analysis		✓	✓	✓

5.3.3 Automatic Switching and Load Shedding

One of the principal effects of part-cycle saturation is the increase in reactive power absorption of transformers. This effect makes the transformers appear as large reactive loads. To compensate for this additional reactive load, automatic removal of some shunt reactive power compensation devices, for example shunt reactors, and employing under-voltage load shedding (UVLS) may help reduce the risk of voltage collapse during an event.

5.3.4 Equipment Sparing

Although research findings indicate that widespread damage to large power transformers due to additional hotspot heating from part-cycle saturation is not expected to occur, additional sparing could also be considered as part of a mitigation strategy. When sparing single-phase large power transformers that could potentially be damaged by GIC it is important to understand the differences in how the transformers could be damaged relative to more traditional causes. In many cases where a three-phase transformer bank is comprised of three single-phase transformers, a spare for only one of the three phases is available on site for replacement.

This is because, in general, it can be assumed that the probability of multiple phases being damaged is very small. However, in the case of GIC-induced failure, all three phases of the transformer bank could be exposed to potentially damaging levels of GIC, and it is expected that the thermal behavior of all three phases is identical. Thus, in the case of GIC-induced damage the likelihood of multiple phases being damaged is much higher than with more traditional damage mechanisms. Transformer sparing philosophies used to mitigate the potential impacts of E3 EMP should consider these differences.

Because of the uncertainty regarding the ability of high-voltage circuit breakers to interrupt current waveforms that do not contain zero crossings due to high levels of GIC flows that could be generated due to E3 EMP, including these devices in equipment sparing programs may be considered.

6

SYSTEM RECOVERY FOLLOWING A HEMP ATTACK

6.1 Power System Restoration Process

Power systems are designed to operate reliably under a variety of operating scenarios and credible contingency conditions. Occasionally, an unexpected contributing factor is present, resulting in cascading outages across the grid, leading to a widespread blackout. Power system restoration is the process of returning generators and transmission system elements to service and restoring load following an outage of the electric system [36]. Around the world, restoration is treated as a critical aspect of power system operations and planning. Regulatory bodies in the United States and around the world have put in place mandatory reliability standards and grid codes that range in scope from the development of restoration plans to periodic review/testing/revision of these plans to implementation of these plans following a blackout event [25], [37], [38], [39].

A typical restoration process consists of 4 steps:

1. Assess system status
2. Determine and implement restoration strategy
3. Implement step-by-step facility energization procedure
4. Synchronize islands and interconnect with neighboring systems

An illustrative step-by-step facility energization procedure is shown in Figure 6-1. An integral part of this procedure is the development of cranking paths starting from the blackstart generators to the non-blackstart generators by energizing various transmission facilities such as transmission lines, transformers, and reactive compensation devices, and by restoring loads along the cranking paths as necessary.

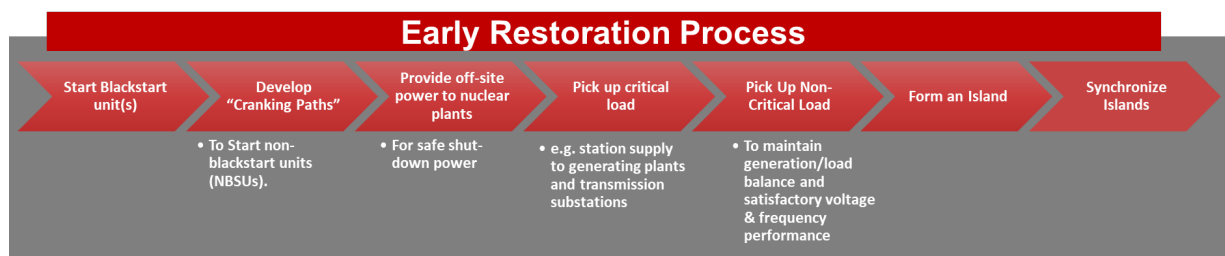


Figure 6-1
Overview of a step-by-step facility energization procedure

A key aspect of the step-by-step procedure illustrated in Figure 6-1 is that each Transmission Operator is responsible for restoring its own system. Aid from external systems, in general, is to be minimized or avoided altogether. The exception is in the case of pre-arranged external blackstart resources. However, when implementing a plan during an actual restoration process, seeking help from, or providing help to, a neighboring system is encouraged when feasible.

6.2 Potential Impacts of a HEMP-Induced Blackout on Restoration Process

A HEMP-induced blackout could pose challenges to the restoration process due to the following issues:

- Unavailable/inoperable/damaged equipment along the cranking paths
- Impaired situational awareness capability
- Inability or difficulty with notifying and/or communicating with response personnel

Thus, recovering from a HEMP-induced blackout can pose unique challenges relative to blackouts resulting from more traditional causes. Table 6-1 provides a summary of potential impacts of a HEMP-induced blackout on the restoration process.

Table 6-1
Potential impacts of a HEMP-induced blackout on restoration process

Restoration Step		Potential Impacts of a HEMP Event
1	Assess System Status	Damage to communication equipment, DPRs, and/or metering equipment may cause partial to total loss of SCADA/ICCP/EMS data, resulting in impaired situational awareness capability.
2	Determine and Implement Restoration Strategy	Identifying a practical restoration strategy could be challenging due to impaired situational awareness and the possibility of widespread inoperable/unavailable/damaged equipment. The restoration strategy may need to be revised by focusing on other less damaged portions of the system.
3	Implement Step-By-Step Facility Energization Procedure	Predefined step-by-step facility energization procedures may not be practical to implement due to the possibility of widespread inoperable/unavailable/damaged equipment and/or loss of SCADA. If a revised strategy (Step 2) calls for alternative cranking paths based on available generation, transmission, distribution, and load resources, analytical tools and simulation studies could be helpful to establish technical feasibility of alternative paths.
4	Synchronize Islands and Interconnect with Neighboring Systems	Impacts will be similar to those mentioned in Step 3.

6.3 Suggestions for Enhancing Preparedness

Suggestions for helping the industry improve preparedness for restoring the bulk power system following a HEMP-induced blackout are provided in Table 6-2. Industry efforts are already underway to address many of these suggestions.

Table 6-2
Suggestions for preparedness

Suggestions		Summary
1	Equipment Redundancy/Sparing	Deploy additional backup/sparing for critical protection and control and communication equipment at key transmission and generating stations.
2	Reduction in Magnitude/Duration of HEMP Impact Through Mitigation and Hardening	Employ E1 EMP mitigation measures to reduce HEMP impact on transmission system assets.
3	Dispatching Field Personnel (including notification of personnel to respond)	During restoration, dispatch field personnel to check damage to key and vulnerable equipment along the cranking paths.
4	Equipment Repair	Make personnel available to repair damaged equipment along the cranking paths.
5	Communication Equipment	Assess HEMP impact on communication equipment and data transmission and identify alternative communication measures that can be used.
6	Transmission-Distribution Coordination	Improve coordination between transmission and distribution operators.
7	Manual Monitoring	During restoration, dispatch field personnel for manual monitoring of key electrical quantities along the cranking paths and other locations as required.
8	Simulation Studies and Tools	During restoration, perform simulations to support operations (e.g., to evaluate technical feasibility of alternative cranking paths).
9	Loss of SCADA/ICCP/EMS Data	Employ investigative efforts to assess impact of loss of data on operational (EMS) tools and processes to identify and employ mitigation measures.
10	Restoration Plan: Assumptions	Revise assumptions to account for potential unavailability of critical equipment along the established cranking paths. Also, identify natural points of synchronization of islands for placement of synchrosopes.
11	Restoration Plan: Restoration Strategy	Devise an alternative strategy, assuming unavailability of vulnerable equipment along the currently established cranking paths.
12	Restoration Plan: Step-by-Step Facility Energization Procedure	Devise alternative cranking paths, assuming unavailability of vulnerable equipment along the currently established cranking paths.
13	Training	Revise training programs to account for potential HEMP impacts and above-mentioned revisions in restoration plans and restoration processes.

Additional information regarding these thirteen items can be found in Reference [40].

7

SUMMARY AND CONCLUSIONS

This report has summarized the work and findings of a three-year research effort to determine the potential impacts of a high-altitude electromagnetic pulse (HEMP) on the electric transmission system and to identify potential options for mitigating these impacts. A brief summary of findings is provided below.

7.1 E1 EMP

Because digital protective relays (DPRs) are arguably the most critical electronics-based asset in a substation, testing primarily focused on these devices. Over 60 DPRs were tested as a part of this research. Testing included:

- Free field illumination testing based on MIL-STD-461G/RS105 to determine the magnitude of the incident E-field that could cause damage or disruption of a device under test (DUT)
- Direct injection testing using a voltage impulse with waveform defined in MIL-STD-188-125-1 [23] to determine:
 1. the voltage surge magnitude that could cause damage or disruption of a device under test (DUT), and
 2. the performance of potential surge protection devices
- Shielding effectiveness testing of substation control houses based on the MIL-STD-188-125-1 [23] approach to assess the ability of these structures to shield internal components from incident electromagnetic waves.

Testing of DPRs showed that these devices are susceptible to conducted transients, but were found to be mostly resilient to free field illumination of E1 EMP. Limited testing of other devices such as SCADA and communications systems indicated that they could be susceptible to both radiated and conducted threats.

An interconnection-scale E1 EMP assessment was performed to provide a first-order approximation of the potential impacts of E1 EMP on DPRs located within an electrical interconnection. Potential disruption or damage to DPRs assuming exposure to the nominal E1 EMP environment provided by Los Alamos National Laboratory (LANL; up to 25 kV/m at the most severe location on the ground) and baseline soil conditions was found to be moderate, whereas damage from the same environment but scaled so that the maximum peak field at the most severe location on the ground was 50 kV/m was found to be more of a concern. Based on the assumptions made in the assessments, it was estimated that approximately 5% of the transmission line terminals in a given interconnection could potentially have a DPR that is damaged or disrupted by the nominal E1 EMP environment, whereas approximately 15% could potentially be affected by the scaled E1 EMP environment.

Because of the uncertainty related to how DPRs might respond to E1 EMP during a HEMP event, an additional voltage stability assessment was also performed to determine if the effects of E1 EMP alone could potentially cause voltage instability or blackout. The limited assessment indicated that E1 EMP impacts alone were not found to cause immediate, interconnection-scale disruption or blackout of the power grid, but this finding is not conclusive since it is unknown how damaged DPRs might respond during an actual event or how potential E1 EMP damage to generator controls and other systems such as automatic generation control (AGC), not included as a part of this study, might affect the long-term operation of the grid. Additional research is needed to quantify and understand these uncertainties and how they might, in combination, affect the stability of the electric power grid.

A number of options for mitigating the potential impact of conducted transients on DPRs were tested and/or evaluated. Devices that were tested included the following:

- Low-voltage surge protection devices (SPDs) including MOV and hybrid technologies (TVS diode + MOV or TVS diode + gas tube)
- Radio frequency interference (RFI) filters
- Individual surge protection components such as transient voltage suppressing (TVS) diodes
- HEMP power line filter
- Auxiliary current transformer (CT)

Testing results were mixed. Some devices performed well, while others failed to provide an acceptable level of protection. Hybrid SPDs, those employing multiple surge protection technologies such as TVS diodes and metal oxide varistors (MOVs), performed best. Other mitigation options that appeared promising when used in combination with low-voltage SPDs included the following:

- Shielded control/signal cables with proper grounding
- Use of fiber optics based communications and protection and control systems
- Modifications to substation control houses to enhance electromagnetic shielding properties
- Grounding/bonding enhancements
- Additional sparing of critical assets such as DPRs, SCADA, and communications equipment

7.2 E2 EMP

First order assessments using the maximum threat level of 100 V/m defined in IEC 61000-2-9 indicated that the induced voltages would not exceed the lightning performance level of equipment or the assumed capability of DPRs. Thus, impacts to the transmission system are not expected to occur.

7.3 E3 EMP

Interconnection-scale E3 EMP assessments (transformer thermal and voltage stability) were performed using two different E3 EMP environments. The initial assessments were performed using the Oak Ridge National Laboratory (ORNL) E3 EMP environment, while later assessments were performed using a much higher fidelity environment provided by LANL.

The results of the assessments indicated that E3 EMP alone could result in a regional blackout encompassing multiple states, but immediate, widespread transformer damage due to hotspot heating from part-cycle saturation is not expected to occur.

Options for mitigating E3 EMP impacts were found to be like those that can be employed to protect against the effects of GMD events and include the following:

- Avoiding protection system misoperations by modifying protection and control schemes to be resilient to harmonics and system imbalance
- Blocking or reducing the flow of geomagnetically induced currents (GICs)
- Automatic removal of some shunt reactive power compensation devices, for example shunt reactors, and/or employing under-voltage load shedding (UVLS)
- Sparing of large power transformers and high-voltage circuit breakers

7.4 Combined Effects of E1 EMP and E3 EMP

The combined effects of E1 EMP and E3 EMP were simulated to assess the potential threat that the full HEMP environment may present to the bulk power system. E2 EMP effects were not included since they were shown to be of minimal consequence to the transmission system.

E1 EMP impacts, as they were modeled, did not significantly affect the outcome of the E3 EMP assessment results. However, significant damage to DPRs, SCADA, and communications equipment would be expected to degrade recovery efforts and viability of controlling frequency post-event due to potential damage to AGC and other control measures.

7.5 System Recovery

The impacts of HEMP on system recovery efforts were evaluated. Potential impacts of HEMP, and in particular E1 EMP, on system recovery were found to include the following:

- Unavailable/inoperable/damaged equipment along the cranking paths
- Impaired levels of situational awareness (including observability and controllability)
- Inability to notify, or difficulty in notifying, key response personnel

Until the transmission system is appropriately hardened against the potential impacts of E1 EMP, recovering from a HEMP-induced blackout may present challenges that have not been experienced following blackouts from more traditional causes. Identifying a practical restoration strategy *in situ* could be challenging due to impaired situational awareness and because of the possibility of widespread inoperable/unavailable/damaged equipment. Restoration strategies may need to be revised by focusing on other, less-damaged portions of the system. The predefined Transmission Operator step-by-step facility energization procedures may not be practical to

implement following a HEMP event, due to the possibility of widespread inoperable/unavailable/damaged equipment. If a revised strategy calls for alternative cranking paths based on available generation, transmission, distribution, and load resources, analytical tools and simulation studies may be helpful to establish technical feasibility of these paths. Lastly, training on the differences between recovery following a HEMP-induced blackout and recovery following a blackout from a more traditional cause may prove to be beneficial for the industry.

8

RECOMMENDATIONS FOR FUTURE RESEARCH

There were a number of research gaps that were identified during this three-year effort. Many of them were evaluated during the course of the research, but some could not be acted upon due to lack of resources or scope limitations. Several areas where additional EMP research is warranted are described below.

8.1 Integrated Energy Network Assets

The use of microgrids and an integrated energy network (IEN) is often described as a potential approach for increasing the resiliency of electric power networks. Additionally, because of socio-economic reasons, the existing bulk power system will likely morph into a hybrid system that consists of traditional assets and newer technologies. Because these newer systems consist of assets with considerable electronics-based protection, controls and communication systems (e.g., microgrids, utility-scale inverter-based generation, demand response, smart meters) it is important to understand the potential impact that E1 EMP may have on these devices and system operation. Although E2 EMP is not considered a threat for transmission assets, it may be a threat for assets that operate at lower voltages (e.g., low-voltage inverters connected to rooftop PV). Additionally, some types of technologies (e.g., inverters and uninterruptible power supply systems) could be susceptible to the high levels of harmonic voltage distortion that could propagate from the high-voltage system as a result of E3 EMP impacts.

Additional research in this area could identify classes of technologies within the IEN framework that may be at risk of potential damage from E1 EMP and/or E3 EMP, and that if damaged could significantly degrade the resiliency of the electric grid. Research following a similar framework as the project described in this report could be performed to assess potential impacts and establish hardening and mitigation options for these systems.

8.2 Generation Facilities and End-Use Equipment

This research project focused on the potential impacts of HEMP on the electric transmission system, which included substations at generation facilities (i.e., switchyards). Additional research is needed to evaluate the potential impacts of HEMP on generation facilities themselves and on the end-use equipment that makes up the electric demand of the system. Research following a similar framework to that described in this report could be performed to assess potential impacts and establish hardening and mitigation options for these systems.

8.3 Software Tools and Methods for Performing HEMP Assessments

The assessments that were performed as a part of this research required the development of “in house” software tools. Many of the calculations, for example E1 EMP coupling, are very complex and require expertise that is not common among electric utility engineers. Performing complex studies such as the interconnection-scale E1 EMP + E3 EMP assessment requires

significant investment resources to first gain the knowledge and experience necessary to develop the simulation capability that is required and then to develop the capability to perform these kinds of studies. Traditionally, these types of studies have been performed by the government and other research entities; however, electric utilities have the most knowledge of their systems and would be in the best position to perform the studies, if resources such as commercially available software tools and training were available. Additional research and development could be used to enhance the capability and methods for performing HEMP assessments so that they can be more easily translated into commercial software tools that are used by utility engineers. Additional training is also warranted to provide additional technical background to those performing the studies.

8.4 Equipment Testing

Significant direct voltage surge injection testing of equipment was performed as a part of this research. When evaluating the waveform of the simulated overvoltages obtained from the E1 EMP coupling calculations, it was discovered that the pulse shape of the overvoltage was much wider than the MIL-STD-188-125-1 pulse. In many cases the resulting overvoltage had a rise time that was orders of magnitude slower than the rise time defined in the standard. Future research could investigate how these differences manifest themselves in terms of damage thresholds in equipment.

When the direct injection testing and free field illumination tests were performed, they were performed in isolation. Additional research and development is needed to test equipment such as DPRs when they are simultaneously exposed to threat-level radiated and conducted transients, to determine if developing damage thresholds based on testing that decouples these threats is providing an acceptable level of immunity.

8.5 HEMP Environments

Additional unclassified E1 EMP and E3 EMP environments that included high-fidelity spatio-temporal characteristics necessary for interconnection-scale assessments were made available to this research project. However, these environments are not publicly available. Work should continue by U.S. government agencies to develop and distribute E1 EMP and E3 EMP environments with proper spatio-temporal characteristics that are suitable for civilian use. Knowledge gained as a part of this research could inform utility requirements in this space.

8.6 Field Trials of E1 EMP Hardening of Substations

Because of the risk of unintended consequences with implementing E1 EMP mitigations in a substation environment, a deliberate approach to hardening substations is recommended.

Evaluating field deployments of these mitigation technologies and approaches could provide a unique opportunity for identifying potential unintended consequences and associated engineering solutions, identifying/developing maintenance processes and procedures, and providing realistic cost data to inform future decision making. EPRI launched a follow-on research effort in 2019 to further evaluate the E1 EMP mitigation options that were identified through this initial research project.

9

REFERENCES

1. IEC 61000-2-9, “Electromagnetic Compatibility (EMC) - Part 2: Environment, Section 9: Description of HEMP Environment - Radiated Disturbance,” International Electrotechnical Commission, Geneva, Switzerland, 1996.
2. Bell Telephone Laboratories, EMP Engineering and Design Principles, Whippany, NJ, 1975.
3. Los Alamos National Laboratory, “EMP/GMD Phase 0 Report, A Review of EMP Hazard Environments and Impacts,” Los Alamos, NM, 2016.
4. Oak Ridge National Laboratory, “Study to Assess the Effects of Magnetohydrodynamic Electromagnetic Pulse on Electric Power Systems—Phase I—Final Report,” 1985.
5. EPRI, “Magnetohydrodynamic Electromagnetic Pulse Assessment of the Continental U.S. Electric Grid: Voltage Stability Analysis,” Palo Alto, CA, 2017, 3002011969.
6. EPRI, “Magnetohydrodynamic Electromagnetic Pulse Assessment of the Continental U.S. Electric Grid: Geomagnetically Induced Current and Transformer Thermal Analysis,” Palo Alto, CA, 2017, 3002009001.
7. S. Glasstone and P. Dolan, The Effects of Nuclear Weapons, 3rd Edition, U.S. Department of Defense and the Energy Research Development Administration, 1977.
8. E. Vance, Electromagnetic-Pulse Handbook for Electric Power Systems, Stanford Research Institute, 1975.
9. Oak Ridge National Laboratory, “Electromagnetic Pulse Research on Electric Power Systems: Program Summary and Recommendations,” 1993.
10. EMP Commission, “Report of the Commission to Assess the Threat to the United States from Electromagnetic Pulse (EMP) Attack: Volume 1 - Executive Report,” 2004.
11. EMP Commission, “Report of the Commission to Assess the Threat to the United States from Electromagnetic Pulse (EMP) Attack: Critical National Infrastructures,” 2008.
12. “Hearing before the Subcommittee on Cybersecurity, Infrastructure Protection and Security Technologies of the Committee on Homeland Security, House of Representatives, 113th Congress of the United States,” 2014.
13. Commission to Assess the Threat to the United States from Electromagnetic Pulse Attack, “Nuclear EMP Attack Scenarios and Combined-Arms Cyber Warfare,” 2017.
14. DOE and EPRI, “Joint Electromagnetic Pulse Resilience Strategy,” 2016.
15. EPRI, “High-Altitude Electromagnetic Pulse Effects on Bulk-Power Systems: State of Knowledge and Research Needs,” Palo Alto, CA, 2016, 3002008999.
16. EPRI, “Analysis of Early-Time High-Altitude Electromagnetic Pulse (E1) Coupling of Three-Dimensional Substation Structures,” Palo Alto, CA, 2018, 3002013960.

17. EPRI, “Coupling of Early-Time High-Altitude Electromagnetic Pulse (E1) into Technological Infrastructure,” Palo Alto, CA, 2018, 3002013934.
18. M. Ianoz, B. Nicoara, and W. Radasky, “Modeling of an EMP Conducted Environment,” *IEEE Transactions on Electromagnetic Compatibility*, vol. 38, no. 3, pp. 400–414, August 1996.
19. Metatech, Meta-R-321, “The Late-Time (E3) High-Altitude Electromagnetic Pulse (HEMP) and Its Impact on the U.S. Power Grid,” 2010.
20. Commission to Assess the Threat to the United States from Electromagnetic Pulse Attack, “Recommended E3 HEMP Heave Electric Field Waveform for the Critical Infrastructures,” July 2017.
21. F. Tesche, M. Ianoz, and T. Karlsson, *EMC Analysis Methods and Computational Models*, Wiley Interscience, 1997.
22. MIL-STD-461G, “Requirements for the Control of Electromagnetic Interference Characteristics of Subsystems and Equipment.”
23. MIL-STD-188-125-1, “High-Altitude Electromagnetic Pulse (HEMP) Protection for Ground-Based C4I Facilities Performing Critical, Time-Urgent Missions.”
24. EPRI, “Assessment of E1 EMP Impacts on Substations,” Palo Alto, CA, 2019, 3002015002.
25. North American Electric Reliability Corporation, “Reliability Standards for the Bulk Electric Systems of North America,” February 2018.
26. North American Electric Reliability Corporation, “Screening Criterion for Transformer Thermal Impact Assessment White Paper,” Atlanta, GA, 2017.
27. EPRI, “PTX Transformer Fleet Management Software, Version 3.0,” EPRI, Palo Alto, 2016, 3002007833.
28. IEEE Std. 525-2016, *IEEE Guide for the Design and Installation of Cable Systems in Substations*
29. EPRI, “HEMP Protection of Substation Control Houses: Hardening Per MIL-STD 188-125-1 and IEC SC-77c Standards,” Palo Alto, CA, 2017, 3002010841.
30. Department of Defense, MIL-HDBK-419A, “Grounding, Bonding and Shielding for Electronic Equipments and Facilities (Vol. 1 of 2),” 1987.
31. North American Electric Reliability Council (NERC), “March 13, 1989 Geomagnetic Disturbance,” Princeton, NJ, 1990.
32. B. Bozoki, et al., “The Effects of GIC on Protective Relaying,” *IEEE Transactions on Power Delivery*, Vol. 11, No. 2, April 1996, pp. 725-739.
33. EPRI, “Mitigation of Geomagnetically Induced and DC Stray Currents,” Palo Alto, CA, 1983, EL-3295.
34. L. Marti, “Effects of Series Compensation Capacitors on Geomagnetically Induced Currents,” *IEEE Transactions on Power Delivery*, vol. 29, no. 4, pp. 2032–2033, 2014.

35. EPRI, “Guidelines for Hardening Bulk Power Systems Against the Effects of Magnetohydrodynamic Electromagnetic Pulse (MHD-EMP) (E3),” Palo Alto, CA, 2017, 3002012166.
36. Federal Energy Regulatory Commission, “FERC-NERC Regional Entity Joint Review of Restoration and Recovery Plans,” January 2016.
37. European Union, “Establishing a Network Code on Electricity Emergency and Restoration,” November 2017.
38. Australian Energy Market Operator, “Power System Security Guidelines,” January 2018.
39. National Grid - Saudi Arabia, “The Saudi Arabian Grid Code,” October 2016.
40. EPRI, “Power System Restoration Following a High-Altitude Electromagnetic Pulse (HEMP) Induced Blackout,” Palo Alto, CA, 2018, 3002014579.
41. L. Marti, A. Rezaei-Zare, and A. Narang, “Simulation of Transformer Hotspot Heating Due to Geomagnetically Induced Currents,” *IEEE Transactions on Power Delivery*, vol. 28, no. 1, pp. 320–327, 2013.
42. M. Lahtinen and J. Elovaara, “GIC Occurrences and GIC Test for 400 kV System Transformer,” *IEEE Transactions on Power Delivery*, vol. 17, no. 2, pp. 555–561, 2002.

A

TRANSFORMER THERMAL MODEL PARAMETERS

This appendix describes the modeling parameters for each of the four transformer thermal models that were used in the thermal assessment.

Model 1 (Structural Part)

The first model was based on simulations performed by the transformer manufacturer using a finite element method (FEM) model that was validated using laboratory tests. The transformer is an autotransformer with nameplate rating of 133.3 megavolt ampere (MVA) 230kV:115kV:13.2kV autotransformers (400 MVA three-phase bank rating). The asymptotic behavior of the model is provided in Table A-1. Note that asymptotic values beyond 50 amps/phase are based on the slope of a straight-line segment describing the last two entries in the table.

Table A-1
Asymptotic behavior of Model 1 (structural part)

Geomagnetically Induced Current (amps/phase)	Steady-State Temperature Rise (°C)
10	62
20	90
30	103
40	115
50	126
5000	5571

The heating time constant was 600 seconds, and the cooling time constant was 650 seconds.

Model 2 (Structural Part)

Model 2 is based on a single-phase 133 MVA 500kV:16.5kV transformer (400 MVA three-phase bank rating) [41]. During a factory acceptance test, the transformer was energized at nominal voltage and injected with 5 amps of dc current. The corresponding hotspot temperature rise of the core tie plate was measured. Winding hotspot temperature data were not provided.

The thermal time constant for the Model 2 was found to be 780 seconds for the heating phase. No information regarding the thermal time constant during the cooling phase was provided in [41]; therefore, the cooling time constant was also assumed to be 780 seconds. Additional information necessary to derive the asymptotic behavior was not provided; therefore, a linear asymptotic behavior with slope of 2.76°C/amp was assumed.

Model 3 (Structural Part)

Model 3 is based on a field test of a transformer. The transformer is described in [42] as a three-phase 410 kV:120kV:21 kV GY-GY-D 400 MVA three-winding transformer. During the field test, the transformer was energized at nominal voltage and injected with various levels of dc current, and the corresponding hotspot temperatures were measured at various locations within the transformer. See Figure 8 in [42] for further details regarding the hotspot temperature measurements.

The thermal model associated with this study was based on the highest measured temperature. The asymptotic behavior is provided in Table A-2. The asymptotic behavior beyond 67 amps/phase was assumed linear.

Table A-2
Asymptotic behavior of Model 3 (structural part)

Geomagnetically Induced Current (amps/phase)	Steady-State Temperature Rise (°C)
17	36
27	54
33	65
42	78
50	90
59	100
67	114
5000	5403

The heating time constant was chosen to be 800 seconds, and the cooling time constant was chosen to be 500 seconds.

Model 4 (Winding)

Model 4 is based on a transformer described in [41] as a single-phase 250 MVA 345kV:24.5kV conventional transformer (750 MVA three-phase bank rating). The simulated data were fitted with a single exponential with thermal time constant of 150 seconds. No information regarding the thermal time constant during the cooling phase was provided; therefore, the cooling time constant was assumed to be 150 seconds. The asymptotic behavior was based on the temperature rise associated with a GIC level of 20 amps/phase and was assumed linear with a slope of 0.3°C/amp.

B

DIRECT INJECTION TESTING OF HIGH-VOLTAGE INSTRUMENT TRANSFORMERS

Direct injection voltage surge testing using the methods described in Section 3 was performed to determine how much of the incident voltage surge would propagate through the instrument transformers. Figure B-1 shows the measured input and output waveforms and calculated frequency response of a 123 kV CCVT (600:1) when it was subjected to a fast-front voltage impulse (E1 EMP induced surge) meeting the waveform specification of MIL-STD-188-125-1. The frequency response shown in Figure B-1 was obtained by performing a fast Fourier transform of the output and input waveforms and computing the ratio, $H(\omega) = V_{\text{sec}}(\omega)/V_{\text{pri}}(\omega)$, at each discrete frequency, ω . The gain in dB at each discrete frequency was then computed as $20\log_{10}(H(\omega))$.

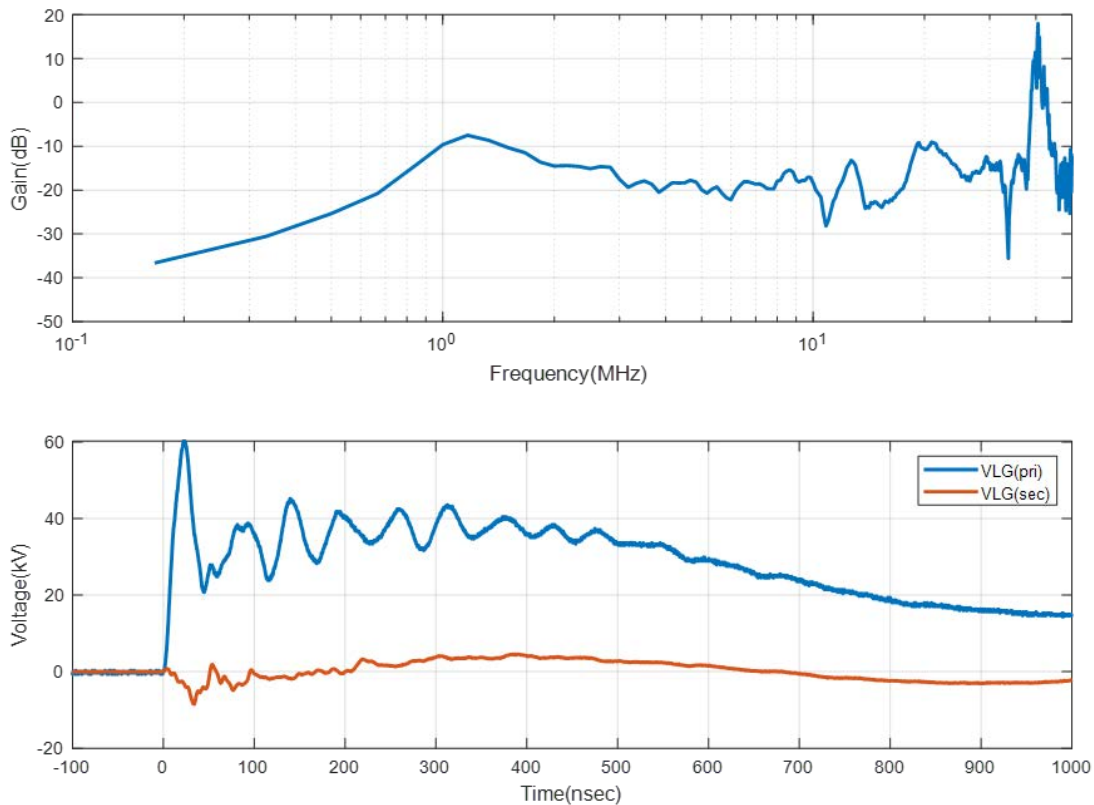


Figure B-1
Calculated frequency response and measured direct voltage surge injection response of a CCVT

The CCVT that was tested had a nominal turns ratio of 600:1 (gain of -55.6 dB) at 60 Hz. However, as shown in Figure B-1, the gain of the CCVT is frequency dependent, and exhibits an average gain of approximately -16.5 dB or 0.15 over the frequency range of 0.5–30 MHz.

Results from a similar impulse test of a 14.4 kV to 120 V (120:1) wound magnetic potential transformer (PT) are illustrated in Figure B-2.

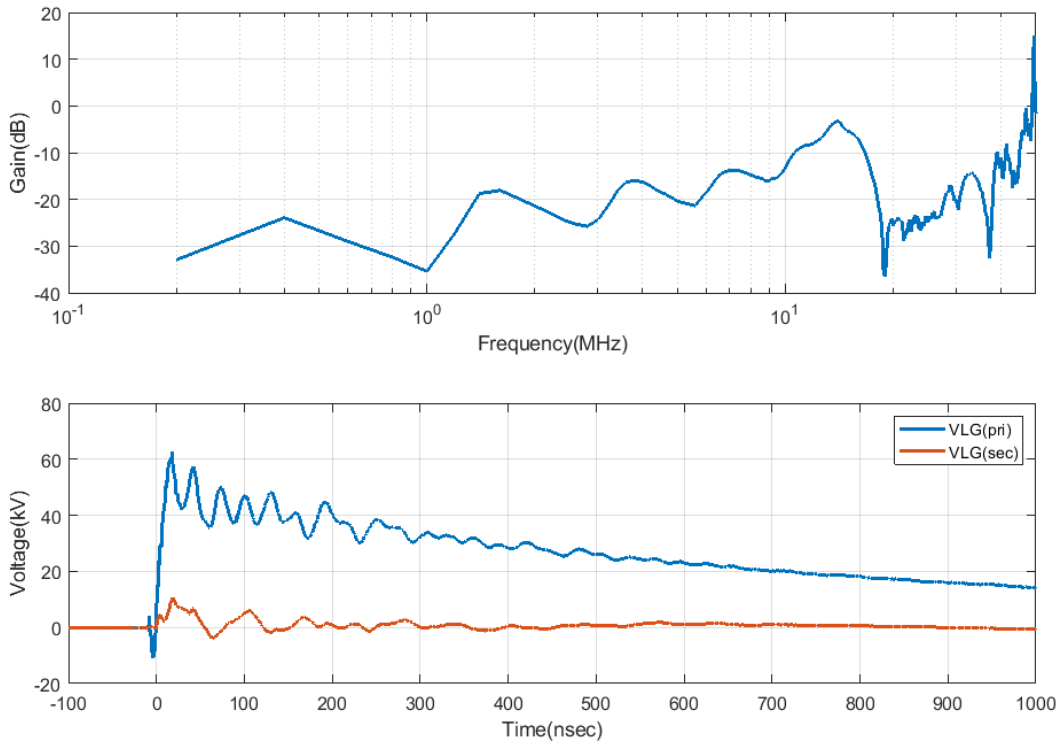


Figure B-2
Calculated frequency response and measured direct voltage surge injection response of a distribution-class PT

The peak magnitude of the measured secondary voltage is approximately 25% of the peak magnitude of the voltage applied to the primary. Similar to the CCVT response, the gain of the PT is frequency dependent, and has an average value of approximately -18 dB or 0.13 over the frequency range of interest (0.5–30 MHz).

Results from both tests indicate that a considerable portion of the incident wave can propagate through the instrument transformer at the frequencies of interest. Thus, equipment connected to the instrument transformers through shielded cables could experience significant stress due to this effect.

The Electric Power Research Institute, Inc. (EPRI, www.epri.com) conducts research and development relating to the generation, delivery and use of electricity for the benefit of the public. An independent, nonprofit organization, EPRI brings together its scientists and engineers as well as experts from academia and industry to help address challenges in electricity, including reliability, efficiency, affordability, health, safety and the environment. EPRI also provides technology, policy and economic analyses to drive long-range research and development planning, and supports research in emerging technologies. EPRI members represent 90% of the electricity generated and delivered in the United States with international participation extending to 40 countries. EPRI's principal offices and laboratories are located in Palo Alto, Calif.; Charlotte, N.C.; Knoxville, Tenn.; and Lenox, Mass.

Together...Shaping the Future of Electricity

Program:

Substations

© 2019 Electric Power Research Institute (EPRI), Inc. All rights reserved. Electric Power Research Institute, EPRI, and TOGETHER...SHAPING THE FUTURE OF ELECTRICITY are registered service marks of the Electric Power Research Institute, Inc.

3002014979